HYBRID ORGANIC-INORGANIC PERVAPORATION MEMBRANES FOR DESALINATION

Zongli Xie

Bachelor of Chemical Engineering
Master of Engineering Science

Institute for Sustainability and Innovation,
School of Engineering & Science,
Victoria University

Submitted in fulfilment of the requirements of the degree of Doctor of Philosophy

(2012)

Abstract

Membrane desalination using reverse osmosis (RO) has been the leading candidate technology for supplying fresh water in recent years. However, there is a strong motivation for improving the established membrane process and/or developing alternative membrane technologies to overcome the limitations of high energy cost and brine discharge problems of RO technology. In the later context, pervaporation is a potential membrane technology as it has the advantage that the energy need is essentially independent of the concentration of the salt feed water. The pervaporation process combines the evaporation of volatile components of a mixture with their permeation through a nonporous polymeric membrane under reduced pressure conditions. In desalination applications, pervaporation has the advantage of near 100% of salt rejection. The pervaporation of an aqueous salt solution can be regarded as separation of a pseudo-liquid mixture containing free water molecules and bulkier hydrated ions formed in solution upon dissociation of the salt in water. Previous studies have demonstrated the possibility of applying pervaporation to produce distilled water from aqueous salt solutions. However, the water flux reported in the literature so far is generally quite low (<6 kg/m^2·hr). It is believed that one of the main limitations for desalination using pervaporation is the lack of the high performance membranes with both high permeate flux and good salt rejection.

Poly(vinyl alcohol) (PVA), a water soluble hydrophilic polymer, has been studied intensively for membrane applications because of its good chemical stability, film-forming ability and high hydrophilicity. High hydrophilicity is critical for desalination membranes to minimise membrane fouling by natural organic matter. However, PVA has poor stability in water. Therefore, it must be insolubilised by modification reactions such as grafting or crosslinking to form a stable membrane with good mechanical properties and selective permeability to water. Among various insolubilisation techniques, hybridisation between PVA and inorganic particles has received significant interest as it not only restricts the swelling of PVA but also provides the inherent advantages of the organic and inorganic compounds. However, there is little published result on application of this type of membranes for pervaporation desalination.

This project reports the development of a new type of hybrid polymer-inorganic membrane based on PVA/maleic acid/silica for desalination by pervaporation. The hybrid membrane was synthesised via a sol-gel route by using tetraethoxy-silane (TEOS) as the silica precursor with

maleic acid (MA) as an additional crosslinking agent. The resulting hybrid membranes with varying silica and MA contents were characterised with a range of techniques including FTIR, SEM, TEM, WAXD, TGA, DSC, PALS and contact angle. It was found that crosslinking among PVA, MA and TEOS led to a more compact structure with increasing amorphous membrane character with improved thermal properties and suppressed swelling. Pervaporation testing results on separating aqueous NaCl solution demonstrated a potential application of this type of hybrid membrane for desalination with improved water flux and high salt rejection. By adjusting MA and silica content, both water flux and salt rejection could be improved.

The optimised hybrid PVA/MA/silica membrane was examined in relation to the diffusion coefficient, mass transfer coefficients and free volume of membrane. Heat treatment favoured the completion of the crosslinking reaction among PVA, MA and TEOS, and also favoured the polycondensation reaction of TEOS. This resulted in a less hydrophilic membrane with reduced fractional free volume (FFV), consequently reducing the water flux. The hydrophilic nature of hybrid membranes provides high water affinity and water sorption, and incorporation of silica particles into the polymer matrix at the nano-scale enhanced the free volume of the membrane and diffusion of water molecule through the membrane. The close correlation among pervaporation properties (e.g., global mass transfer coefficients, water flux and salt rejection), transport properties (e.g., NaCl/water diffusivity and permability) and FFV of the membrane confirmed that the diffusion through membrane was the controlling step of pervaporation separation of aqueous salt solution for this unsupported hybrid membrane.

Other key factors studied in this project include the thickness of the membrane and the process operating conditions. In the studied laminar flow region, feed velocity had little or negligible effect on the water flux and diffusion coefficients of water. This result indicates that the membrane transport properties are rate limiting, as changing the hydrodynamics made no effect to the flux so the flux was not limited by mass transfer properties through the boundary layer. High feed temperature and high vacuum had a significant enhancing effect on the water flux and diffusivity coefficients of water due to the increased driving force. A high water flux of 11.7 kg/m^2·hr could be achieved at a feed temperature of 65°C and a vacuum of 6 Torr, which is a significant improvement compared to currently available membranes with fluxes of less than 6 kg/m^2·hr.

Declaration

"I, Zongli Xie, declare that the PhD thesis entitled hybrid organic-inorganic pervaporation membranes for desalination is no more than 100,000 words in length including quotes and exclusive of tables, figures, appendices, bibliography, references and footnotes. This thesis contains no material that has been submitted previously, in whole or in part, for the award of any other academic degree or diploma. Except where otherwise indicated, this thesis is my own work".
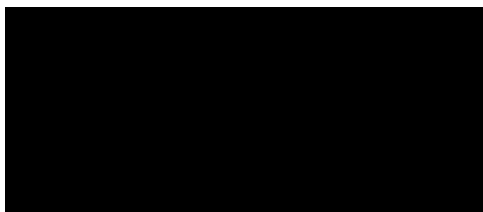
Signature: Date: 16/12/2012

Acknowledgement

This thesis marks the end of my PhD journey and has been seen through to completion with the support and encouragement of numerous people including my supervisors, my families, my friends, colleagues and various universities. I would like to thank all those people who made this thesis possible and an unforgettable experience for me.

First, I would like to express my sincere gratitude to my supervisors Professor Stephen Gray (VU) and Dr Manh Hoang (CSIRO) for their continuous guidance and support throughout my PhD study. I would like to thank for their motivation, enthusiasm and patience throughout my journey. They have always been source of knowledge and inspiration for providing encouragement and suggestions to solve the encountered problems throughout my study. I will always be indebted to them for the training and development I received as well as the skills and preparation necessary to be successful in future research endeavours.

I would like to thank fellow colleagues in my research group for their great support, patience and generosity I received over the years, for providing a stimulating and fun filled environment. Special thanks to Derrick Ng for his continuous help and great patience in helping me with the laboratory work. My sincere thanks also go to Buu Dao, Dr Cuong Nguyen for helping me to start my research work smoothly. Buu Dao has helped me to understand the polymer chemistry and helped me in many ways from membrane fabrication to characterisation. I am very grateful to Dr Brian Bolto, Dr Tuan Duong, Dr Anita Hill, Dr Ludo Dumee for their kind help and stimulating discussion to enlighten me in solving problems.

During this work I have collaborated with many colleagues for whom I have great regard, and I wish to extend my warmest thanks to all those who have helped me with my work in CSIRO, Deakin University and Victoria University. In particular, I would like to thank A/Prof Lingxue Kong, Dr Mary She, Juan Zhang from Deakin Univeristy for their help in TEM work, Ms. Liz Goodall, Mr. Mark Greaves from CMSE for SEM and XRD. Bebeto Lay, Peipei Huang, Ying He for their assistance on membrane characterisation.

I also like to extend huge, warm thanks to my fellow students Juan Zhang, Sharmiza Adan and Jianhua Zhang for their help and friendship. I am indebted to my friends for their encouragement and spiritual support I received from my friends over the years.

Last but not the least, I wish to thank my family, especially my sons Jerry and Kevin, for their love and encouragement during these years. Their support helped me go through the challenge times along this journey. Without their support and understanding, I could not have completed my PhD study. To them, I dedicate this thesis.

List of Publication and Awards

Journal Papers:

[1] Z. Xie, M. Hoang, T. Duong, D. Ng, B. Dao, S. Gray, "Sol-gel Derived Poly(vinyl alcohol)/Maleic Acid/Silica Hybrid Membrane for Desalination by Pervaporation", Journal of Membrane Science, 2011, 383, 96-103, DOI:http://dx.doi.org/10.1016/j.memsci.2011.08.036.

[2] Z. Xie, D. Ng, M. Hoang, T. Duong and S. Gray, "Separation of aqueous salt solution by pervaporation through hybrid organic-inorganic membrane: effect of operating conditions", Desalination, 2011, 273(1), 220-225.

[3] Z Xie, B Dao, J Hodgkin, M Hoang, A Hill, and S. Gray, "Synthesis and characterization of hybrid organic-inorganic materials based on sulphonated polyamideimide and silica", Journal of Polymer Research, 2011,18, 965-973.

[4] B.Bolto, M.Hoang and Z. Xie, "A review of membrane selection for the dehydration of aqueous ethanol by pervaporation", Chemical Engineering and Processing: Process Intensification, 2011, 50(3), 227-235, doi:10.1016/j.cep.2011.01.003.

[5] B. Bolto, T. Tran, M. Hoang, Z. Xie, "Crosslinked poly(vinyl alcohol) membranes", Progress in Polymer Science, 2009, 34, 969-981.

[6] Z. Xie, M. Hoang, D. Ng, C. Doherty, A. Hill, S. Gray, "Effect of heat treatment on pervaporation separation of aqueous salt solution through hybrid organic-inorganic membrane", Journal of Membrane Science (submitted).

Conference proceedings:

[1] Z. Xie, M. Hoang, D. Ng, T. Duong, B. Dao, and S. Gray, "Poly(vinyl alcohol) based hybrid organic-inorganic membrane for desalination by pervaporation", AMS7 conference, 3-6 June 2012, Busan, Korea.

[2] Z. Xie, M. Hoang, D. Ng and S. Gray, "Strucutre and performance relationship of Poly(vinyl alcohol) based nanocomposite membrane", SINCS2011 conference, 31 Oct-2 Nov, 2011, Shanghai, China.

[3] Z. Xie, M. Hoang, D. Ng, T. Duong, B. Dao and S. Gray, "Study of hybrid PVA/Maleic Acid/TEOS membrane for pervaporation separation of aqueous salt solution", CAM 2011 conference, May 23-25th, Melbourne, Australia.

[4] Z. Xie, M. Hoang, D. Ng, T. Duong, B. Dao and S. Gray, "Sol-gel derived hybrid polymer-inorganic membrane for pervaporation desalination process", IMSTEC10/AMS6 Conference, 22-26 November 2010, Sydney, Australia.

[5] Z. Xie, M. Hoang, S. Gray, "Hybrid Organic-inorganic Membrane for Pervaporation Desalination", 2010 AWA - CSIRO Membrane Cluster Workshop, Jun. 9th, 2010, Sydney, Australia.

[6] Z. Xie, M. Hoang, B. Dao, T. Duong, D. Ng and S. Gray, "Sol-gel Derived Poly(vinyl alcohol)/Silica Hybrid Membrane- Synthesis and Characterisation", 5th IWA specialised membrane technology conference for water & wastewater treatment, 1-3 September 2009, Beijing, China.

[7] Z. Xie, M. Hoang, T. Duong, S. Gray, "Sol-gel derived poly(vinyl alcohol)/silica hybrid membrane- synthesis and characterisation", Proceeding of the Singapore International Water Week 2009, 22-26 Jun, 2009, Singapore.

Awards:

[1] 2012 Travel award from Australian Nanotechnology Network (ANN) to attend the 5th Asia Nano Camp and won the Best poster award.

[2] 2012 Travel award from MSA to attend the AMS7 conference.

[2] 2011 Travel award to attend the ANSTO/AINSE Neutron School.

[3] 2010 Travel award to attend EU NanoMemCourse.

[4] Best poster award in 2010 EU NanoMemCourse workshop.

Table of Contents

List of Figures

List of Tables

Chapter 1

Introduction

1.1 Background

The long history of desalting in Australia ranges from the wood-fired stills of the Coolgardie goldfileds over 100 years ago, to distillation in the North West, solar ponds at Coober Pedy and electrodialysis for the first plant at Yulara. The plants installed ranged from multistage flash distillation, vapour compression distillation, electrodialysis and reverse osmosis (RO) (Hoang *et al.* 2009). In recent years, there has been an increased emphasis on desalination and membrane desalination using reverse osmosis (RO) has been the leading technology for supplying fresh water via desalination and industrial water reuse. Among various desalination technologies used in the world, RO accounts for >65% of total world desalination capacity and distillation accounts about 30% (Korngold *et al.* 1996). In Australia, installed RO seawater desalintion capacity will increase from 45 GL/year in 2006 to over 450 GL/year by 2030 (Hoang *et al.* 2009). The main advantages of membrane technology as compared with other unit operations in chemical engineering are related to its unique separation principle, i.e. the transport selectivity of the membrane. Separations with membranes do not require additives, and they can be performed isothermally at low temperatures.

Although RO membranes have good overall performance and water fluxes when using transmembrane pressures up to 100 bar, the main limitations of RO technology are the overall high energy cost and the sensitivity of RO membrane elements to fouling. Figure 1-1 shows the breakdown of production costs for a 100 ML/day seawater RO plant (Adham, 2007). As can be seen, the energy requirement of RO operation is very high, with as much as 23% of total water cost for seawaer desalination attributed to energy cost. In general, according to the size of the unit and the type of process used, the energy requirement vary between 6 and 10 kWh/m^3 and investment costs vary between 600 and 2000 US\$/m^3/d (Korngold *et al.* 1996). The product water cost is mostly in the range of less than \$1.25/m^3 for potable water and \$1.25-\$2.00/m^3 for industrial water (Hoang *et al.* 2009). Despite much progress being made in lowering the energy requirements and cost of RO, challenges remain to be overcome. The high energy requirement of RO operation and the complexity in the management of RO brine concentrate are major

obstacles to more widespread applications of this technology. Therefore, there is a strong motivation for improving established membrane materials and developing alternative low energy membrane technology.
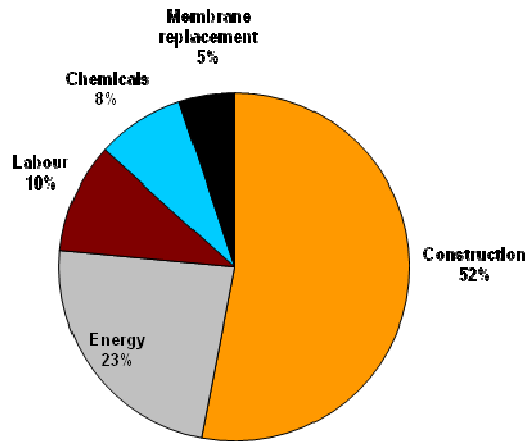
Figure 1-1: Costs of water production, 100 ML/day seawater desalination plant (Adham, 2007)

Pervaporation is a combination of diffusion of a liquid through a membrane and then its evaporation into the vapour phase on the other side of the membrane. The mechanism of mass transfer (or diffusion) of liquid across the membrane includes successive stages of sorption of a liquid and its diffusion through the free volume of the polymeric material. Transport through the membrane is driven by the vapour pressure difference between the feed solution and the permeate vapour. In desalination applications, pervaporation has the advantage of nearly 100% salt rejection and potentially low energy consumption if waste heat is used, and unlike RO the energy needed is independent of the concentration of salt in the feed water. Compared with RO, pervaporation might have advantages in brine treatment or in hot application as RO membranes are restricted to <40°C. To date there is little published information on the application of pervaporation for desalination and wastewater treatment. It is believed one of the main limitations is the lack of high water flux with current commercial membranes, generally being <6 kg/m^2.hr.

Previous studies have demonstrated the concept the desalination by pervaporation and identified the need for new membrane materials with enhanced water flux to broaden the scope of future membrane applications. This study reports the development of a new type of hybrid polymer-inorganic membrane based on poly(vinyl alcohol) (PVA)/maleic acid/silica for desalination by

pervaporation. The hybrid membrane was synthesised via a sol-gel route by using tetraethoxy-silane (TEOS) as the silica precursor with maleic acid (MA) as an additional crosslinking agent. The resulting hybrid membranes with varying silica and MA contents were characterised with a range of techniques to establish the structure-property relationship. Pervaporation separation of aqueous salt solution of hybrid PVA/MA/silica membranes was examined with respect to the diffusion coefficient, mass transfer coefficients and free volume of membrane. Other key factors studied in this project include the thickness of the membrane, effect of the heat treatment and the process operating conditions such as feed flowrate, feed temperature and permeate pressure. A process engineering model was also developed to estimate the specific energy required for pervaporation.

1.2 Objectives

The objective of this study was to develop scaleable energy efficient hybrid organic-inorganic membrane materials with properties that exceed the performance limits of current commercial polymer membranes for desalination by pervaporation. The research program included:

- To develop a method to synthesise PVA based hybrid organic-inorganic membrane materials with inorganic silica particles uniformly dispersed in the polymer matrix at the nanoscale and with improved stability.

- To characterise the membrane structure and properties, and test membrane performance with respect to water flux and salt rejection in order to establish the structure-performance relationship.

- To study the transport properties of developed hybrid membranes for desalination by pervaporation and identify the rate-limiting step(s) in mass transport.

- To study the effect of process operating conditions on pervaporation performance of synthesised hybrid organic-inorganic membranes for scale-up consideration.

- To establish a process engineering model to estimate the specific energy and membrane requirement for desalination by pervaporation.

3

1.3 Thesis outline

This thesis consists of the following chapters which are briefly summarised below:

Chapter 2 provides a literature review of pervaporation processes, membrane material selection and development for desalination by pervaporation, the mass transport mechanism through pervaporation membranes and previous studies on hybrid organic-inorganic membranes.

Chapter 3 describes the synthesis methods and characterisation techniques used for PVA based hybrid organic-inorganic membranes. It also details the experimental set-up and analytical methods for membrane performance testing.

Chapter 4 describes in more details the development of hybrid organic-inorganic membranes based on PVA, maleic acid (MA) and tetraethoxy-silane (TEOS). This chapter focuses on characterising the sol-gel derived hybrid PVA/MA/silica membranes. The role of MA and TEOS on pervaporation performance are discussed with correlation to physical properties of hybrid membranes such as water uptake, hydrophilicity, thermal properties, morphology and crystallinity, and free volume analysis.

Based on results from previous chapters, a selected hybrid PVA/MA/silica membrane optimum water transport properties was chosen for further studies. Chapter 5 details the effect of heat treatment such as heating temperature and heating time on pervaporation performance of the hybrid PVA/MA/silica membrane. Chapter 6 details the effect of operating conditions including feed flowrate, temperature, permeate pressure on pervaporation performance of the hybrid PVA/MA/silica membrane.

Chapter 7 details the development of a process engineering model to evaluate the specific energy requirement of the desalination by pervaporation. A breakdown of thermal and electrical energy requirements for pervaporation in recirculation mode is outlined. Effects of feed temperature and permeate pressure on specific energy and membrane requirements are also discussed. The energy requirements by pervaporation were compared with other desalination technologies such as multi stage flash (MSF), multi evaporation distillation (MED) and RO.

Chapter 8 summarises the main findings and conclusions from this research work and recommendations for future research.

Chapter 2

Literature Review

2.1   Introduction

Pervaporation, considered as a clean technology, is a potential low energy membrane technology which has been extensively used for separation of mixtures of aqueous-organic or organic liquids. For its application in desalination, it has the advantages of near 100% salt rejection and the energy need is independent of salt concentration of the feed water. This chapter presents a literature review of membrane material selection and development for desalination by pervaporation and the mass transport mechanism through pervaporation membranes. The advantages and approaches of hybrid organic-inorganic membranes through sol-gel reactions are discussed with a focus on poly(vinyl alcohol) (PVA) based membranes. Key factors affecting the pervaporation process including membrane thickness and various operating parameters such as feed temperature and permeate pressure, are reviewed. Some insights into the membrane morphology and engineering aspects for commercialisation of pervaporation are also included.

2.2   Desalination by pervaporation

2.2.1   Pervaporation overview

Pervaporation, aimed at the separation of liquid mixtures, involves a dense membrane that is in contact with the feed solution on one side, while permeate is removed as a vapour from the other side (downstream). The permeate side is usually kept under vacuum to enhance the rate of permeation (Baker 2004). At least one of the components is transported preferentially through the membrane. Usually the permeating vapour is condensed at reduced pressure, the presence of non-condensable gases would hinder the transport of permeating vapour from the membrane to the condenser. The necessary heat for the evaporation of the permeate is taken from the sensible heat of the feed mixture which is cooled down accordingly. In contrast to all other membrane separation processes employing non-porous membranes, a phase change for the permeating substance occurs from feed to permeate (Bruschke 1995).

Figure 2-1 shows a schematic drawing of the pervaporation process to separate liquid mixtures. Transport through the membrane is driven by the vapour pressure difference between the feed solution and the permeate vapour. The vapour pressure difference can be created in several ways. In the laboratory, a vacuum pump was usually used to draw a vacuum on the permeate side of the system. Industrially, the permeate vacuum is most economically generated by cooling the permeate vapour, causing it to condense and, spontaneously creating a partial vacuum (Baker 2004). The driving force is characterised in practice by the difference in partial pressure or activities of the permeating component in the liquid feed and in the vapour-phase permeate, removed from the back side of the membrane under vacuum (Sander and Soukup 1988).
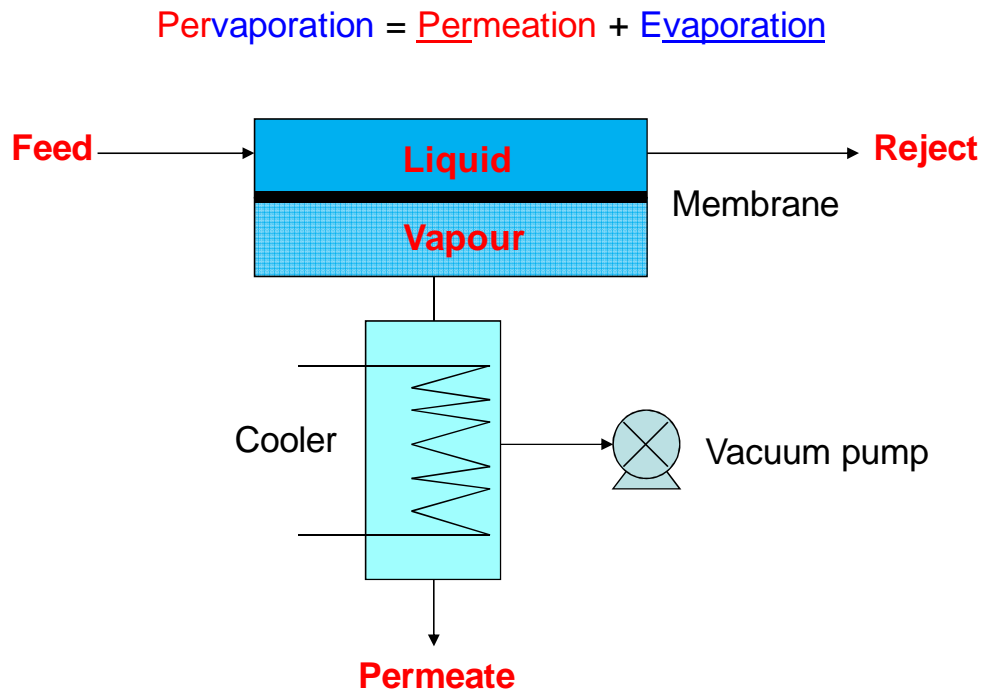
Figure 2- 1: The concept of pervaporation process.

Pervaporation is considered as a clean technology. The separation of compounds using pervaporation processes can be generally classified into three major fields viz. (i) dehydration of aqueous–organic mixtures, (ii) removal of trace volatile organic compounds from aqueous solution and (iii) separation of organic–organic solvent mixtures (Baker 2004, Smitha *et al.* 2004). The process was first studied systematically to separate organic mixtures by Binning and co-workers at American Oil in the 1950s (Binning *et al.* 1961) and

picked up in the 1970s by Aptel, Neel and others (Aptel *et al.* 1974). By the 1980s, advances in membrane technology made it possible to prepare economically viable pervaporation systems. The first commercial system for the dehydration of azeotropic ethanol/water mixtures was installed by GFT in 1982. Since then, more than 100 plants have been installed for this application, with the largest processing 5000 kg/h of ethanol at Bethenville, France (Baker 2004). The second commercial application of pervaporation was the removal of small amounts of volatile organic compounds (VOCs) from contaminated water. This technology was developed by Membrane Technology and Research with the first commercial plant installed in 1996 (Cox and Baker 1998). The third commercial application was the separation of organic/organic mixtures. The first commercial pilot plant was reported by Separex for the separation of methanol from methyl *tert*-butyl ether/isobutene mixtures in 1988 (Chen *et al.* 1988). A timeline illustrating some of the key milestones in the development of pervaporation is shown in Figure 2-2.
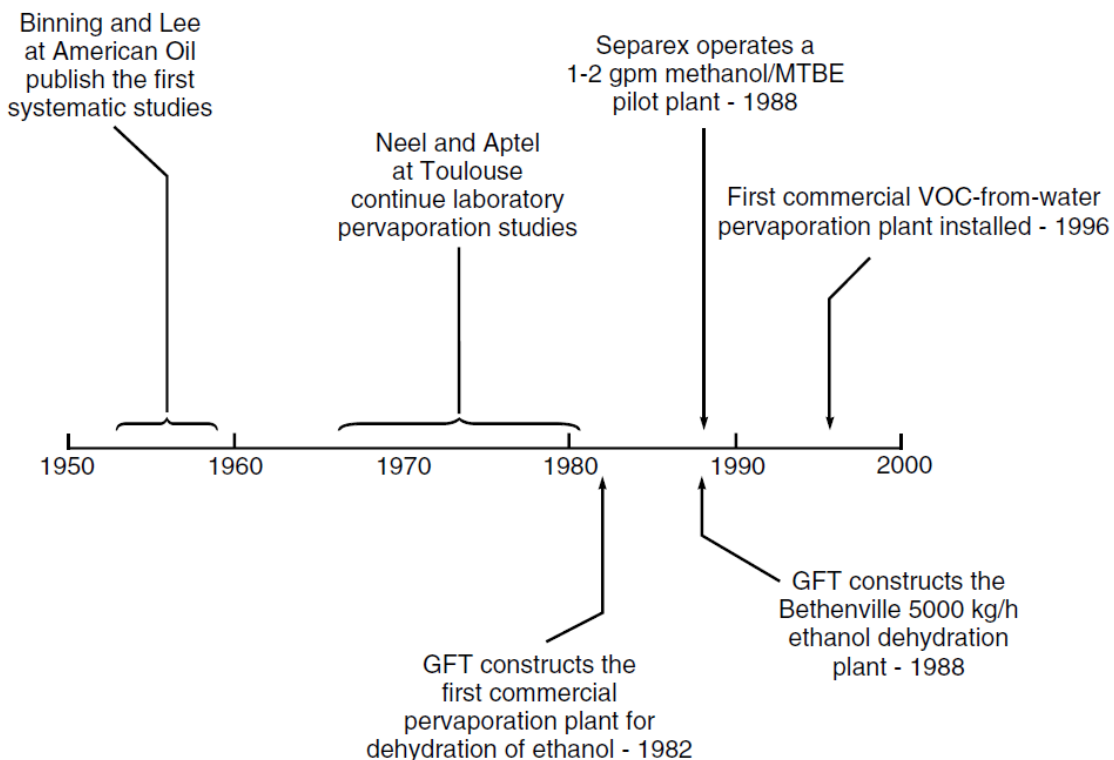
Figure 2- 2: Milestones in the development of pervaporation (Baker 2004).

In general, separation by pervaporation is based on the solution-diffusion mechanism of transport through non-porous membranes (Bruschke 1995, Smitha *et al.* 2004). The

mechanism of mass transfer for liquids across diffusion-type (nonporous) polymeric membranes includes successive stages of sorption of a liquid, its diffusion through the free volume of the polymeric material and then desorption of a vapour phase on the permeate side (Bruschke 1995). In this process, the phase state changes from the liquid on the feed side to the vapour on the permeate side. The physicochemical properties of membrane-forming polymers and of components of liquid mixtures exert a decisive influence on the selectivity of membranes and intensity of mass transfer (Kuznetsov *et al.* 2007).

The selectivity and permeation rates of pervaporation membranes are governed by the solubility and diffusivity of each component of the feed mixture to be separated (Kulkarni *et al.* 2006), which are intrinsic permeability properties of the membrane material. Similar to non-porous membranes used for gas separation, the permeability of a component is the product of the membrane sorption coefficient (K) and the diffusion coefficient (D). The membrane selectivity of component i and j is the product of the diffusion selectivity (D_i/D_j) of the membrane material and the solubility selectivity (K_i/K_j), generally governed by the chemistry of the membrane material (Baker 2004, Freeman 1999). Therefore, membrane materials are generally tailored for particular separation applications (Baker 2004).

2.2.2 Desalination by pervaporation

As applied to desalination, pervaporation involves the transport of water through non-porous membranes via the solution-diffusion mechanism. As shown in Figure 2- 3, desalination by pervaporation is a combination of diffusion of water through a membrane and then its evaporation into the vapour phase on the other side of the membrane. The selectivity in the process is governed by the partial pressure differences of the feed components and intrinsic selectivity of the membrane (Korngold *et al.* 1996). As a potential low energy process, it has the advantage of near 100% salt rejection. In contrast with other membrane technologies, such as reverse osmosis and electrodialysis, it also has the advantage that the energy need is essentially independent of the salt concentration in feed water. Using a partial water vapour pressure gradient as a driving force for the transport of water across the membrane, pervaporation can handle high salt concentrations without losing much of its driving force. For instance, the partial vapour pressure of a 2 M NaCl solution at 75°C is only 8% lower of that of pure water at the same temperature (Zwijnenberg *et al.* 2005). It is, hence, capable of concentrating salt solutions up to supersaturated levels, which allows for the recovery of salt by crystallisation. When compared with porous membrane distillation membranes, a

8

potential advantage for pervaporation membranes is the greater physical integrity of their dense membrane structure (Bolto *et al.* 2010). The main advantages of pervaporation over conventional separation processes are:

- Complete separation (in theory) of ions, macromolecules, colloids, cells etc., to produce a high-quality permeate.

- Water can be recovered at relatively low temperatures.

- Low-grade heat (solar, industrial waste heat) may be used.

- Does not require extensive pretreatment as required for pressure-based membrane treatment processes such as RO.

- Hydrophilic pervaporation membranes are potentially low fouling.
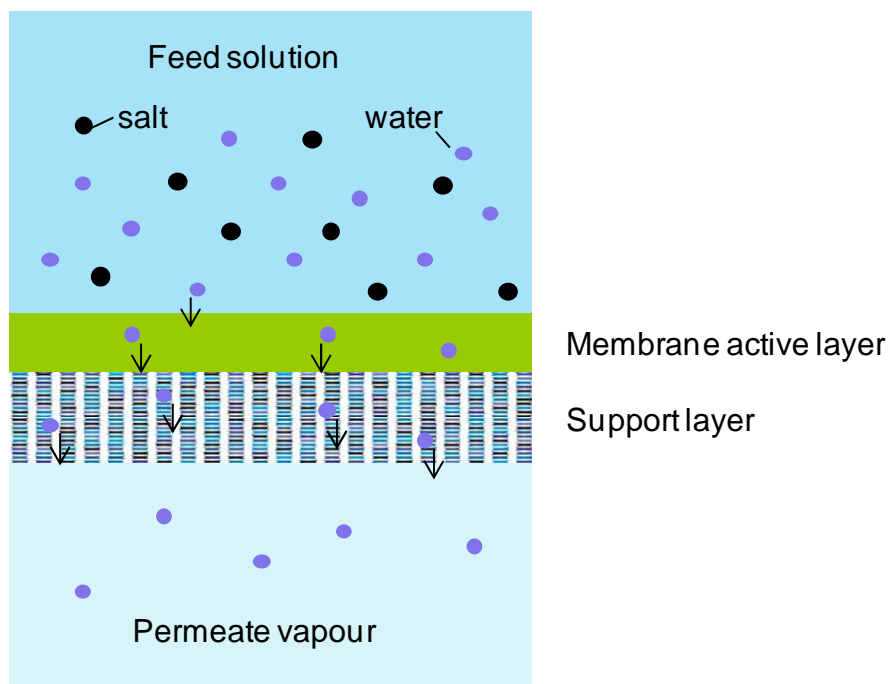
Figure 2- 3: Desalination by pervaporation process where water passes through a dense pervaporation membrane.

Desalination by pervaporation involves a succession of stages of sorption of liquid water on the membrane and the diffusion of the water vapour through the free volume of a hydrophilic membrane. The pervaporation of an aqueous salt solution can be regarded as

separation of a pseudo-liquid mixture containing free water molecules and bulk hydrated ions formed in solution upon dissociation of the salt in water (Kuznetsov *et al.* 2007). The separation selectivity of such a mixture depends on the competitive diffusion of its constituent components through unit elements of the free volume. For highly selective separation, the size of these elements should be small and similar to the van der Waals diameter of water molecules (~2.8Å) (Franks 2000). For this reason, it is preferable that the membrane structure should be highly structurally ordered on the super-molecular level. For example, in the case of cellulose, this is favoured due to its hydrophilic nature and the dense packing of polymer chains, provided by the network of intermolecular hydrogen bonds (Kuznetsov *et al.* 2007). It should also be noted that the transport of bacteria, viruses, and other pathogenic species across diffusion membranes is completely eliminated by the very small size of free-volume elements compared to the size of the pathogens (>20nm, about 100 times larger than the size of free volume elements).

An overall view of reported desalination by pervaporation results is listed in Table 2-1. By far the best outcome in open literature is with cellulose membranes, followed by silica, ionic polyethylene and the various polyether membranes. The highest flux of 6.1 kg/m^{2}h was reported for a cotton cellulose membrane at 40°C with membrane thickness of 30µm. The low flux of current polymeric membranes is believed to be the main limiting factor for commercial application of the pervaporation process for desalination.

Previous works showed that feed temperature is a crucial parameter, the benefit of which is attributed to an increase in diffusivity and reduction in flow viscosity that occurs on heating. Hence expenditure on thermal energy will improve water flux. Alternative thermal sources that could be exploited are solar, geothermal and industrial waste heat. Mechanical energy in the form of extra applied pressure or vacuum can likewise be called upon to enhance the flux. The main parameters for higher water flux are:

- Higher feed water temperature

- Increased vacuum

- Lower membrane thickness

- Improved membrane permeability

Table 2- 1: Summary of desalination by pervaporation data available (Bolto *et al.* 2010)

Membrane Polymer	Feed Conc., g/L	Temp., °C	Membrane Thickness, μm	Flux, kg/m²h	Reference
Cotton cellulose	40	40	30	6.1	Kutznetsov *et al.*, 2(
Cellulose diacetate on MD membrane	40	40	0.5-1.5	4.1-5.1	
Sulphonated polyethylene, cation exchanger	0-176	25-65	100	0.8-3.3	Korin *et al.*, 1996
Quaternised polyethylene, anion exchanger	0-176	45-65	50-18	1.5-3.0	Korngold *et al.*, 199
	35	60	70	2.3	
	35	60	170	0.5	
Polyether amide	35	Solar, 60-80	40	0.25	Van Andel, 2001
Polyether amide	35	Solar, 46-82	40	0.2	Zwijnenberg, *et al.*,
Polyether ester	3.2-5.2	Solar, 22-29	160	0.15	Quiňones-Bolaňos *ϵ*
	9.9-18			0.13	2005
	20-30			0.12	
Silica	35	20	1-10	3.7	Ladewig *et al.*, 201(

2.3 Commercial and engineering aspects of pervaporation

The pervaporation process was first commercialised for ethanol dehydration in 1980s based on the crosslinked PVA/PAN composite membrane. Since then, both the scope of application and the types of pervaporation membranes have been extensively enlarged (J.Jonquieres *et al.* 2002). A wide range of solvents have been covered in the dehydration market, which includes various alcohols, ethers, ketones, acid and some polymer solvents like THF, dioxane. The SULTZER PERVAP® membranes also succeeded in methanol/MTBT, and ethanol/ETBE separation (Shao and Huang 2007).

The performance of pervaporation mainly depends on:

- The membrane properties

- The operating conditions

- The module design

Module design plays an important role in the overall performance of any membrane plant. Key parameters to be taken in to consideration for the module design include packing density, cost-effective manufacture, easy access for cleaning, reduction in boundary layer effects and cost-effective membrane replacement. Based on above, modules can be distinguished into tubular, capillary, hollow fibre, plate-and-frame type, and spiral wound modules (Smitha *et al.* 2004). The module configuration has to be carefully optimised in order to reduce the temperature change of the solutions along the membrane module (reduction of the heating and cooling costs). One particular issue affecting pervaporation module design is that the permeate side the membrane often operates at a vacuum of less than 100 Torr. The pressure drop required to draw the permeate vapour to the permeate condenser may then be a significant fraction of the permeate pressure. Efficient pervaporation modules must have short, porous permeate channels to minimise this permeate pressure drop (Baker 2004).

For pervaporation, the plate-and-frame type is the dominating module configuration employed in pervaporation since this configuration can provide low resistance channels in both the permeate and feed sides. It also has the advantages in ease of manufacturing and high temperature operation with efficient interstage heating between stages (Smitha *et al.*

2004, Shao and Huang 2007). In plate and frame systems, the feed solution flows through flat, rectangular channels. Packing densities of about 100-400 m^2/m^3 are achievable.

Pervaporation requires volatilisation of a portion of liquid feed. In pervaporation, the enthalpy of vaporisation must be supplied by the feed. Due to this, a large thermal gradient is established across the membrane with continual heat loss to the permeate resulting in a reduction in flux. To compensate for this heat loss, interstage heaters within the membrane module are required to reheat the feed. In the case of hollow fibre modules, where surface area/volume ratios are high, hollow fibres may have problems with longitudinal temperature drops and inefficient use of downstream surface area (Smitha *et al.* 2004). In addition, it should be noted that ensuring low transport resistance in the permeate side is a critical consideration in pervaporation module design. This is because the efficient evaporation of the permeate molecules at the downstream face of the membrane needs an extremely low absolute pressure. The presence of a resistance in the permeate channel can greatly affect the pervaporation separation process. Because of this characteristic, the compactness of the membrane module is no longer a preferential consideration for pervaporation modules. It is difficult for a hollow fibre module to be employed in pervaporation unless the fibre length is short, or the fibre diameter is big enough to provide a small temperature gradient along the fibre, e.g. 5-25mm (Bowen *et al.* 2003). As a result, tubular membranes seem to be a feasible module configuration for pervaporation, such as tubular zeolite membranes developed by Mitsui Engineering & Shipbuilding Co. However, the manufacturing cost of these modules is high. Capillary modules are generally not used in pervaporation due to its high mass transport resistance when compared to the other modules due to increased boundary layer thickness.

Spiral wound modules have the advantages of high packing density (>900 m^2/m^3) and a simple design. It is generally considered difficult to develop for pervaporation because of the chemical susceptibility of the adhesive required (Smitha *et al.* 2004). However, this may not be the case for desalination applications as there is no solvent in the feed. Therefore, there is a potential to develop the spiral wound module for desalination by pervaporation.

2.4   Mass Transport in Pervaporation Membranes

2.4.1 *Solution-diffusion model*

The solution-diffusion mechanism is widely accepted to describe the mass transport through non-porous membranes (Shao and Huang 2007). It was first proposed by Sir Thomas Graham (1866) based on his extensive research on gas permeation through homogeneous membranes. Following this model, the overall mass transfer can be separated into three consecutive steps (Bruschke 1995, Graham 1866):

(i) sorption of a component out of the feed mixture and solution in to the upstream surface of the membrane material;

(ii) diffusion of the dissolved species across the membrane matrix along a potential gradient;

(iii) desorption of dissolved species from the downstream side of the membrane.

These three fundamental processes also govern the mass transport across pervaporation membranes (Binning *et al.* 1961). When a pervaporation membrane is in contact with a liquid feed mixture, it is generally believed that the thermodynamic equilibrium reaches instantly at the membrane–feed interface (Binning *et al.* 1961, Lonsdale 1982), therefore:

$$\frac{C_m}{C_{feed}} = K \tag{2-1}$$

where C_m and C_{feed} represent the concentrations of a species at the membrane surface and the feed, respectively, and K is thus the partition coefficient of a species between the membrane and the feed phase. Therefore, K is a characteristic parameter dependent upon the interaction of the species with the membrane. Mass transport through the membrane is a diffusion-controlling process, which is generally governed by Fick's first law (Lonsdale 1982, Crank and Park 1968):

$$J = -D\frac{dC}{d\delta} \tag{2-2}$$

where J is the permeation flux of a species through the membrane, D is the diffusion coefficient of the species in the membrane, and δ is the thickness of the membrane. By introducing the partition coefficient K of the species at the membrane/feed, and membrane/permeate interface, the concentrations of a species at the faces of the membrane can be expressed in terms of the feed and permeate concentrations, respectively. Fick's first law thus becomes:

$$J = DK\frac{\Delta C}{\delta} = \frac{DK}{\delta}\Delta C \tag{2-3}$$

where both the diffusion, and the partition coefficients are treated as constants. If the transmembrane concentration (ΔC) is taken as the driving force for the mass transport, the permeability (P) of the species in the membrane can be defined as:

$$P = DK \tag{2-4}$$

Clearly, the permeability is an index measuring the intrinsic mass transport capability of a membrane for a species. The ideal separation factor of a membrane for species i and j can be defined as (Baker 2004, Freeman 1999):

$$\alpha_j^i = \frac{P_i}{P_j} = \frac{D_i}{D_j}\frac{K_i}{K_j} = \left(\alpha_j^i\right)_D\left(\alpha_j^i\right)_K \tag{2-5}$$

In pervaporation the membrane is in contact with the feed liquid, and typical sorption is 2–20 wt%. Sorption of one of the components of the feed can then change the sorption and diffusion of the second component. As a rule of thumb, the total sorption of the feed liquid by the membrane material should be in the range 3–15 wt%. Below 3 wt% sorption, the membrane selectivity may be good, but the flux through the material will be too low. Above 15 wt% sorption, fluxes will be high, but the membrane selectivity will generally be low because the diffusion selectivity will decrease as the material becomes more swollen and plasticized. The sorption selectivity will also tend towards unity (Baker 2004).

Research efforts in pervaporation were thus devoted to seeking the right membrane materials to maximize the differences in these parameters (diffusion coefficient D, partition coefficient K, and thus permeability P) so that the desired separation can be carried out in an efficient manner (Baker 2004). By manipulating the chemistry of membrane materials, either sorption- or diffusion-selectivity-controlled membranes can be made. For example,

for the separation of acetone from water it is preferred to use silicone rubber membranes. Silicone rubber membrane is made from a hydrophobic rubbery material and preferentially sorb acetone, the more hydrophobic organic compound. For rubbery materials the diffusion selectivity term, which would favour permeation of the smaller component (water), is small. Therefore, silicone rubber membrane is sorption-selectivity-controlled and preferentially permeates acetone. On the other hand, the crosslinked PVA membrane is made from a hydrophilic rigid material and because PVA is hydrophilic, the sorption selectivity favours permeation of water, the more hydrophilic polar component. Also because PVA is glassy and crosslinked, the diffusion selectivity favouring the smaller water molecules over the larger acetone molecules is substantial. As a result, PVA membranes permeates water several hundred times faster than acetone (Hollein *et al.* 1993)

Experimentally, the permeation flux, and the separation factor can be obtained, respectively by:

$$J = \frac{Q}{A \cdot \Delta t} \tag{2-6}$$

$$\left(\alpha_j^i\right)_{permselectivity} = \frac{\left(Y_i / Y_j\right)}{\left(X_i / X_j\right)} \tag{2-7}$$

where Q is the quantity (in gram or mole) of the permeate collected in a time interval Δt, A is the effective membrane area used for the test, and X, and Y represent the fractions of the components in the feed and the permeate, respectively. Permeation a function of vapour pressure of each species. Since the downstream pressure in pervaporation operation is negligibly small when operated under vacuum conditions, the permeation flux of each species through the membrane is essentially proportional to its intrinsic permeability as well as its activity in the feed. As such, the separation factor defined in Equation (2-7) is equivalent to the ideal permselectivity as defined in Equation (2-5).

2.4.2 *Free volume theory of diffusion*

The mobility of polymer segments is closely related to the free volume of the system. The free volume can be qualitatively visualised as the volume which is not occupied by the polymer molecules but constitutes a part of the bulk volume of the overall polymer solid or polymer/diluents system. The free volume may be closely related to the void volume in

semicrystalline polymers, and more generally one may visualise it as a "hole" opened by thermal fluctuation of molecules or present because of geometrical requirements of random chain packing. However, in the free volume theory, the "hole" or free volume which serves as the passage for diffusing penetrating molecules does not designate any fixed pore and its size and location fluctuate with time (Yasuda *et al.* 1968a). It is generally true that in a given membrane, increased free volumes corresponds to increased diffusion coefficients of the penetrants (Shao and Huang 2007).

In the free volume theory, the diffusion coefficient can be generally expressed by (Cohen and Turnbull 1959):

$$D = B \exp\left[-\frac{\gamma \cdot v^*}{v_f} \right] \tag{2-8}$$

where D is the diffusion coefficient of permeant molecules, B is constant, γ is a numerical factor introduced to the equation to correct for overlap of the free volume which should lie between 0.5 and 1. v^* is a characteristic volume required to accommodate the diffusion permeant molecules in the sample, v_f is the free volume in the sample.

Yasuda *et al.* (1968a) have proposed that water and salt diffusion through hydrogels can be interpreted with the free volume theory of diffusion. In the pervaporation process, based on the free volume theory, the water or salt diffusion coefficient is expected to change exponentially with the reciprocal free volume (Ju *et al.* 2010). When a membrane is swollen or plasticised by transport species, the interaction between polymer chains tend to be diminished, and the membrane matrix will therefore experience an increase in the free volume. The fractional fee volume (FFV) of polymers is defined as follows (Shao and Huang 2007):

$$FFV = \frac{\text{specific free volume}}{\text{polymer specific volume}} \tag{2-9}$$

Positron annihilation lifetime spectroscopy (PALS) is a modern tool to investigate the size and size distribution of free volume elements in polymers (Tung *et al.* 2009, Dong *et al.* 2008). This method is based on the measurement of positron lifetime and lifetime intensity in a material. The annihilation of positrons in a polymer occurs via several pathways. One of the pathways, based on o-Ps in the triplet spin state, is typically sensitive to free volume

elements in a polymer, including their size (characterised by o-Ps lifetime τ_3) and concentration (characterised by intensity I_3), respectively (Dong *et al.* 2008). PALS has been used to study the microstructure of various polymers, such as glassy and partially crystalline polymers, thermally stable polymers, gas separation polymers and polymer hydrogels (Ju *et al.* 2010). Desalination (Tung *et al.* 2009) and pervaporation membrane (Peng *et al.* 2006a) materials were also investigated using PALS. Based upon these studies, the PALS technique can probe free volume, which is important in determining penetrant selectivity in dense desalination membranes (Ju *et al.* 2010).

2.5   Membrane selection for pervaporation

2.5.1   Membrane morphology

The design of suitable membranes for pervaporation is of great importance for its further development. Generally, the membranes used for laboratory scale trials are always homogeneous and symmetric (Figure 2- 4a) because they are easy to cast and possess the intrinsic separation properties of the polymer. However, to attain commercial viability, the membranes successful on the laboratory scale are prepared in an asymmetric or composite form. These two morphologies offer a possibility of making a barrier with a thin effective separation layer, which enables high flux while maintaining desirable mechanical strength (Smitha *et al.* 2004).

Asymmetric membranes consist of a thin dense layer on top of a porous support layer of the same material (Figure 2- 4b). These membranes are prepared by the phase inversion technique where a homogeneous polymer solution is cast as a thin film or spun as a hollow fibre and immersed in a non-solvent bath after giving it a brief time in air to allow partial evaporation of the solvent. The membrane is formed by the replacement of solvent by non-solvent and precipitation of the polymer (Smitha *et al.* 2004).

Composite membranes consist of a porous support layer with a thin dense skin layer coated on top of it (Figure 2- 4c). The top layer is of a material different from the support layer. Utilization of composite structures offers a means of minimizing membrane cost by reducing the quantity of expensive high performance material used. Composite membranes allow the properties of the dense separating layer and the porous support layer to be optimised individually (Smitha *et al.* 2004), e.g., the membranes for water permeation utilise a supporting layer such as a nonwoven porous polyester on which is cast either a

polyacrylonitrile (PAN) or polysulfone (PS) ultrafiltration membrane, and finally a 0.1 µm thick layer of crosslinked PVA which provides separation (Chang *et al.* 1998).

Dense film

(a)

Dense top layer

Porous support made of same polymer

(b)

Coated top layer

Porous support made of different polymer

Membrane support fabric

(c)
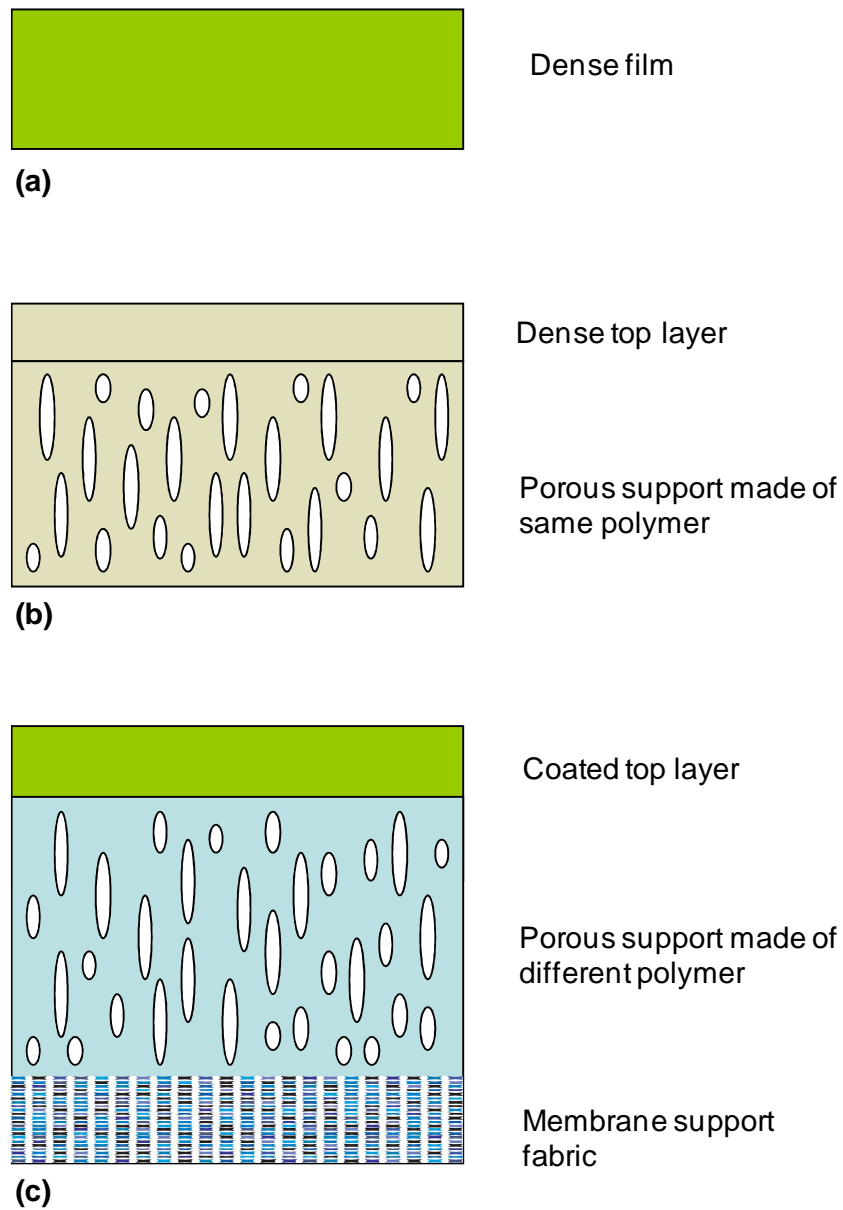
Figure 2- 4: Schematic representation of three different types of membrane structure (modified from Smitha *et al.* 2004).

2.5.2   *Membrane materials selection overview*

In pervaporation, a wide range of materials including dense metals, zeolites, polymers, ceramics and biological materials have been used for the manufacturing of membranes. However, polymers form the most widely used material for membrane manufacturing at present (Smitha *et al.* 2004). Shao and Huang (2007) have reviewed polymeric membrane

19

pervaporation with an emphasis on the fundamental understanding of the membranes in the areas of alcohol and solvent dehydration. This review provided an analytical overview on the potential of pervaporation for separating liquid mixtures in terms of the solubility parameter and the kinetic parameter of solvents. They also reported the importance of solvent coupling in diffusion transport and how this coupling can be accounted for. Chapman *et al.* (2008) complemented the work of Shao and Huang by reviewing hydrophilic polymeric and inorganic membranes for dehydrating solvents such as ethanol and isopropyl alcohol. They also reported the hybrid organic-inorganic membranes for alcohol dehydration. As virtually all pervaporation membranes are non-porous polymeric systems, and membrane selection is focussed on polymer design and modification. The development of an optimum polymer for pervaporation application is a challenge for polymer chemists and may need entirely new concepts and ideas. Some of the polymer modifications suggested are the incorporation of inorganic additives, crosslinking the polymers, blending a mixture of polymers, and the use of copolymers and polymer graft systems.

Membranes with both high permeability and selectivity are desirable. Higher permeability decreases the amount of membrane area requirement, thereby decreasing the capital cost of membrane units. Higher selectivity results in higher purity product. A trial and error approach in the past has revealed that, for the dehydration of organic liquids, hydrophilic polymers are preferred as hydrophilic membranes have a higher sorption capacity for water than solvents. On the other hand, for the removal of organics from aqueous solutions, hydrophobic elastomers are the most suitable as hydrophobic membranes have a higher sorption capacity for organics. The selection of the membrane polymer is usually made on the basis of solubility and diffusivity data for the various components of the mixtures in a membrane polymer.

Table 2-2 summarises some key factors important for mass transport through a pervaporation membrane. Solubility and diffusivity of low molecular mass solutes in polymers strongly depend on the molecular size and shape of the solute, the polymer solute interactions, and the chemical and physical properties of the polymer. Diffusivity not only depends on molecular interactions, but also on the solute size and the state of aggregation of the membrane polymer. It differs significantly for glassy and rubbery polymers (Staudt-Bickel and Lichtenthaler 1994). A general trade-off has been recognised between

permeability and selectivity (Freeman 1999). The improvement in diffusivity necessary for good fluxes usually means a decrease in selectivity and vice versa.

Table 2- 2: Factors affecting overall mass transport (Staudt-Bickel and Lichtenthaler 1994).

Intermolecular interactions	Molecular size and shape
	Polarity and polarisability
	Hydrogen bonding
	Intermolecular donor-acceptor interactions
State of aggregation of the polymer	Glass transition temperature
	Ratio of amorphous to crystalline domain
Physical properties	Thickness of selective nonporous layer
	Porosity and thickness of support
Operating conditions	Feed composition
	Feed temperature
	Thickness of boundary layers
	Permeate pressure

Hydrophilic polyvinyl alcohol (PVA) based pervaporation membranes were the first membranes successfully used for organic solvent dehydration at industrial scale. Dehydration of organic liquids using this type of membrane still remains the main industrial application of pervaporation (Baker 2004). Owing to their hydrophilic character, these membranes enable the extraction of water with fluxes and selectivity depending upon the chemical structure of the active layer and its mode of crosslinking. Most of the hydrophilic membranes commercially available are made of PVA, thermally crosslinked or crosslinked by special agents to provide chemical resistance in acid or in strong solvating media (Smitha

et al. 2004). In desalination by pervaporation, polymer selection would appear to be related to that for dehydration of organic liquids, so that hydrophilic polymers are still preferred.

2.5.3   Membranes for desalination by pervaporation

Although pervaporation has been extensively used in separation of organic compounds, there is no commercial application of pervaporation for desalination mainly due to the low water flux of current available membranes. This section will focus on reviewing previous studies on membrane selection for desalination by pervaporation.

o   *Cellulosic Membranes*

Membranes have been made from plant cellulose of thickness 30 ± 5 µm, and also bacterial cellulose obtained from *Acetobacter xylinum*, which had thicknesses of 40 and 240 µm (Kutznetsov *et al.*, 2007). Composite membranes were made by depositing a thin layer (3-5 µm) of cellulose diacetate on a microporous polytetrafluoroethylene membrane with the subsequent saponification of the coating layer in a 1:1 $NaOH$-CH_3COONa buffer solution at 50°C. Pervaporation at 40°C of a 4% salt solution gave complete salt rejection at fluxes of 0.9 to 6.1 kg/m^2h, as detailed in Table 2-3.

Table 2- 3: Fluxes for desalination by pervaporation of 4% NaCl at 40°C and 0.2 mbar (Kutznetsov *et al.*, 2007).

Membrane Material	Water flux, kg/m^2h
Cellulose diacetate (wood)	0.91
Wood cellulose	1.7
Cotton cellulose	4.6
Cotton cellulose, wetted before use	6.1
Bacterial cellulose	1.9
Cellulose diacetate composite on microporous membrane*	4.1, 5.1

[*] After saponification of the cellulose diacetate in a 1:1 $NaOH$-CH_3COONa buffer solution at 50°C.

Wood based membranes exhibited lower permeabilities, the lowest being for the less hydrophilic cellulose diacetate. Cotton derived cellulose swelled more and had a higher flux, especially when swollen in water before use. Composite membranes had a flux of 4.1 to 5.1 kg/m^2h. All membranes demonstrated 100% salt rejection at significant differences in their water permeability. A possible reason for the difference in permeability between these membranes may be due to differences in hydrophilicity and structure features (Kuznetsov *et al.* 2007). For example, the content of -OH groups in the cotton derived cellulose membrane is higher and the positions of -OH groups are not strictly fixed and easily change in interaction with water or water vapour.

o *Sulphonated Polyethylene Membranes*

Pervaporation performance in desalination with hollow fibre cation exchanger membranes based on sulphonated polyethylene (PE) was reported (Korin *et al.* 1996). The fibres had diameters of 400-1800 µm, a wall thickness of 50-180 µm and a charge density of 0.6-1.2 meq/g. The salt content in the feed was 0-176 g/L, and the flux obtained was 0.8-3.3 kg/m^2h when the inlet brine temperature was 25-65°C. The optimal specifications were fibres of diameter 1200 µm and wall thickness 100 µm, with a charge density of ~1.0 meq/g. The highest flux of 3.3 kg/m^2h was achieved when the feed temperature was 60°C. There was a 15% decrease in water flux when the salt concentration in feed was increased from 0 to 176 g/L (Korngold and Korin 1993). This was ascribed to a reduction in the swelling of the membrane at the higher salt level.

Anion exchange versions of the hollow fibre polyethylene membranes have been made by sulphochlorination, amination, followed by quaternisation of the amino groups (Korngold *et al.* 1996). Using them in a recycled air sweep pervaporation system, the water flux was 1.5-3.0 kg/m^2h when the water temperature was 45-65°C. There was a significant decrease in flux when thicker-walled fibres were used, from 2.3 kg/m^2h for 70 µm thickness to 0.5 kg/m^2h for 170 µm thickness. This flux reduction was due to the increase in membrane thickness. Diffusion of liquid water through the continuous pathway of water shells around charged groups is claimed to be faster than diffusion through clusters of free water in the membrane (Cabasso *et al.*, 1985).

o *Polyether Amide Membranes*

Akzo patented a polyether amide membrane made from ε-caprolactam and a mixture of poly(ethylene oxide) and poly(propylene oxide) (van Andel 2001). The membrane was reported to be effective in solar powered desalination for irrigation purposes. The membrane was in the form of a 40 µm thin film extruded onto a supporting layer that formed an irrigation mat. Raising the feed water temperature to 60-80°C by simulated solar heating for 12 h per day yielded an average flux of 0.25 kg/m^{2}h. In dry areas with many sunny days (> 300 days per year) this should produce 1000-1300 kg/m^{2}y. It is generally thought that effective irrigation requires ~500 kg/m^{2}y. The membrane was claimed to be exceptionally resistant to the aggressive combination of sea water and heat in the long-term.

A tubular configuration of a non-porous polyether amide membrane of 40 µm thickness has been used in a solar driven pervaporation process to desalinate untreated seawater and wastewater from oil production (Zwijnenberg *et al.* 2005). Along with high salt rejection, high level rejection of boron, arsine and fluoride was also reported. The water flux was low at ~0.2 kg/m^{2}h, but was independent of the feed concentration and was not affected by severe fouling resulting from the concentration process. This was explained by the dynamic characteristic of the solar process. The transport resistance resulted from increased salinity and fouling was compensated by a higher feed temperature from the solar process.

o *Polyether Ester Membranes*

Polyether ester membranes made by DuPont have been tested in hollow fibre and corrugated sheet modes for PV reclamation of contaminated water for the purpose of crop irrigation (Quiñones-Bolaños *et al.* 2005). The membrane polymer was a hydrophilic thermoplastic elastomer that was claimed to have good chemical resistance and high mechanical strength. A DuPont patent reported polyether ester elastomers made up of a poly(trimethylene-ethylene ether) ester soft segment and an alkylene ester hard segment (Sunkara 2005). The model contaminants present in the test water included borate, selenates, and 0.3-30 g/L sodium chloride. The hollow fibre configuration gave the best results compared to the corrugated flat sheet. The highest flux of 0.15 kg/m^{2}h was for a 3.2-5.2 g/L salt feed at 29°C. This decreased to 0.10 kg/m^{2}h at 22°C. This was attributed to the increase in molecular diffusivity and the reduction in flow viscosity at the higher temperature. Increasing the salt concentration also decreased the flux slightly. The water flux increased

linearly from 0.08 to 0.15 kg/m^{2}h when the feed pressure varied from 20 to 100 kPa. The solute rejection was independent of the feed concentration and membrane configuration. The removal of borate, selenate and sodium chloride was over 80% from highly contaminated waters (Quiñones-Bolaños *et al.* 2005).

o *Silica Membranes*

Silica membranes have been made on α-alumina substrates using tetraethylorthosilicate and various amounts of a triblock copolymer made from poly(ethylene glycol) and poly(propylene glycol), which was used as a template (Ladewig *et al.* 2010). Calcining under vacuum carbonised the template and trapped it within the membrane matrix. Synthetic seawater was desalinated at a flux of 3.7 kg/m^{2}h with 98.5% salt rejection at room temperature and a driving force of 100 kPa.

Previous studies have demonstrated the concept of desalination by pervaporation with the high salt rejection, but the water fluxes were generally low. The highest reported water flux was only 6.1 kg/m^{2}h for a cellulose membrane (Kutznetsov *et al.*, 2007). Selection of the membrane polymer material is critical as it related to the inherent permeability. In addition, the thickness of the membrane is another vital factor. The active layer should be as thin as possible in order to reduce the membrane resistance. To make pervaporation as a viable alternative desalination process, it is therefore important to develop a thin pervaporation membrane which can achieve both high water flux and salt rejection.

2.6 Hybrid Organic-inorganic Membranes

2.6.1 Background and classification of hybrid organic-inorganic materials

One of the conditions for successful development of new membrane processes in recent years is the utilization of well-adapted membranes. The ability of a membrane to accomplish a desired separation depends on the relative permeability of the membrane for the feed phase components. The rate at which any compound permeates a membrane depends upon two factors — an equilibrium effect (partitioning of components between feed phase and membrane phase) and a kinetic effect (for example, diffusion in a dense membrane). Hence, the choice of a given membrane material is not arbitrary but based on very specific physical and chemical properties (Guizard *et al.* 2001). The most important class of membrane materials are organic polymers due to a number of advantages. In general, polymer

membranes have good film forming ability and can be processed into very compact systems. They are not expensive and can be applied indifferently to large or small fluid volume treatment.

Membranes with both high permeability and selectivity are desirable for practical separation. In general, polymer membranes have disadvantages of limited mechanical, chemical and thermal resistance compared to inorganic membranes (Guizard *et al.* 2001). Despite concentrated efforts to innovate polymer type and tailor polymer structure to improve separation properties, current polymeric membrane materials commonly suffer from the inherent trade-off effect between permeability and selectivity (Freeman 1999), which means that membranes of high permeablility are generally less selective and vice-versa. On the other hand, although some inorganic membrane materials have shown good separation properties above the upper-bound trade-off curve (Walcarius 2001), which was constructed on an empirical basis for many gas or liquid pairs using published permeability and selectivity data (Robeson *et al.* 1994), their large-scale application is still restricted due to the poor processability and high capital and membrane replacement costs. Therefore, it can be envisaged that elaboration of hybrid membrane materials by bridging organic and inorganic components will be an efficient approach to overcome the trade-off hurdle (Peng *et al.* 2005a). This approach is also adopted in this study with the aim to enhance the water flux through the membrane.

Hybrid organic-inorganic composite materials are promising systems for many applications due to their extraordinary properties, which arise from the synergism between the properties of the components. They have attracted considerable attention as potential "next generation" membrane materials (Peng *et al.* 2005a, Merkel *et al.* 2002, Uragami *et al.* 2002). There are several routes for fabricating these materials, but probably the most prominent one is the incorporation of inorganic building blocks in organic polymers. These materials have gained much interest due to remarkable changes in properties, such as increases in mechanical strength and thermal stability compared to pure organic polymers. A general classification of hybrid organic-inorganic materials was proposed (Guizard *et al.* 2001, Wen and Wilkes 1996, Eckert and Ward 2001) distinguishing "class I" materials, in which the inorganic and organic components interact through weak hydrogen bonding, van der Waals contacts, or electrostatic forces, from "class II" materials, in which the inorganic and organic components are linked through strong ionic/covalent bonding (Figure 2- 5).
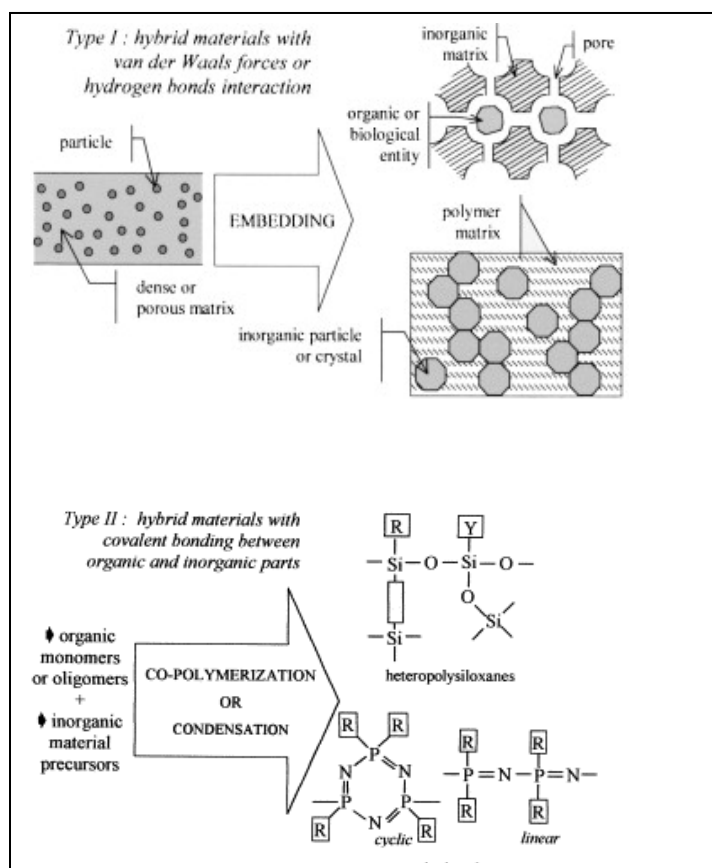
Figure 2- 5: Hybrid organic-inorganic materials (type I with van der Waals forces or hydrogen bonds; type II with covalent bonding) (Guizard *et al.* 2001).

The "class I" organic-inorganic membranes are prepared by simply incorporating inorganic particles, such as zeolite, carbon molecular sieve, and silica into dense polymeric membranes to improve molecular separation properties (Peng *et al.* 2005a, Merkel *et al.* 2002). Peng *et al.* prepared crystalline graphite flake filled poly(vinyl alcohol) membrane (Peng *et al.* 2005b). They introduced graphite to interfere with polymer chain packing and augmented free volume and, thus, obtained higher permeability membranes. However, most "class I" organic-inorganic membranes failed to cross the upper-bound trade-off curve due to the following main disadvantages: agglomeration of inorganic particles and formation of nonselective voids, which usually exist at the interface of these two phases since the interaction between inorganic particles and polymer is of physical origin. Moore and Koros have summarized the relationship between organic-inorganic membrane morphologies and transport properties (Moore and Koros 2005). They identified that the trade-off phenomenon was mainly derived from the non-ideal effects such as varying degrees of rigidification in the surrounding polymer, undesirable voids at the interfaces, and partial or total clogging of

the dispersed phase. Therefore, it is possible that "class II" hybrid organic-inorganic membranes will become membranes of choice.

The dominant processing method of the "class II" organic-inorganic membranes, which can efficiently avoid formation of nonselective voids at the organic-inorganic interface and the agglomeration of inorganic particles, is based on the convenient and mild sol-gel process (Peng *et al.* 2005a, Wen and Wilkes 1996). Kusakabe *et al.* (1998) prepared polyurethane (PU) membranes containing tetraethyl orthosilicate (PU/TEOS) and applied them to benzene/cyclohexane fractionation. They found that benzene/cyclohexane selectivity in the hybrid membrane was higher than that in the PU counterpart. However, the permeation flux was lower in the hybrid membrane. Uragami *et al.* (2002) prepared PVA/TEOS hybrid membranes for pervaporation separation of aqueous ethanol solution, which also showed decreased permeability and increased selectivity. In a latter study, Peng *et al.* (2005a) prepared PVA- γ-(glycidyloxypropyl)trimethoxysilane (GPTMS) hybrid membrane for pervaporation separation of benzene/cyclohexane with the aim to improve the trade-off between permeability and selectivity were prepared by an in situ sol-gel approach. The permeation flux of benzene increased from 20.3 g/m^2h for pure PVA membrane to 137.1 g/m^2h for PVA-GPTMS membrane with 28 wt % GPTMS content, while the separation factor increased from 9.6 to 46.9, simultaneously. Based on the free volume analysis, the enhanced and unusual pervaporation properties were attributed to the increase in the size and number of both network pores and aggregate pores, and the elongation of the length of the diffusion path in PVA-GPTMS hybrid membranes. In a separate study by Zhang *et al.* (2007), hybrid organic-inorganic membranes were prepared through sol–gel reaction of poly(vinyl alcohol) (PVA) with γ-aminopropyl-triethoxysilane (APTEOS) for pervaporation separation of ethanol/water mixtures. Both the free volume and the hydrophilicity of the hybrid membranes increased when APTEOS content was less than 5 wt%. Permeation flux increased remarkably with APTEOS content increasing, and water permselectivity increased at the same time, thus improving the trade-off between the permeation flux and water permselectivity of the hybrid membranes.

These results have shown that "class II" hybrid organic-inorganic membranes could provide a solution to improve the trade-off between flux and selectivity.

2.6.2   Sol-gel process in presence of polymer

The formation of interpenetrating networks between organic and inorganic moieties ("class II" materials) is carried out either by a sequential two-step process, wherein a secondary network is formed in a primary one (generally when inorganic is the host matrix), or by the simultaneous formation of the two networks. The resulting materials are microscopically phase separated, but macroscopically uniform (Sperling 1994). When organic polymer is the host matrix, an inorganic (crosslinked) moiety is formed by a polycondensation reaction, and interpenetrates during the process into an organic polymer. Difficulties of such an approach are potential incompatibilities between the moieties, leading to phase separation, and the challenge to find reactions for the formation of the second network which can be carried out in the presence the first one. A major problem arises from the different stabilities of the materials. While inorganic systems are thermally stable and are often formed at high temperatures, most organic polymers have an upper temperature limit ($< 250°C$). Therefore, the synthesis of hybrid systems requires the use of low temperature formation procedures (Kickelbick 2003). The most commonly employed preparation for hybrid organic-inorganic materials is the use of the sol-gel process for the formation of the inorganic network in the presence of organic species such as polymer, which are capable of interacting or chemically bonding with the metal alkoxides under mild conditions (Kickelbick 2003).

The sol-gel process is a widely researched field and primarily employed in the production of multicomponent systems, such as powders, fibres and coatings in optical and sensor applications (Bandyopadhyay *et al.* 2005). The sol-gel reaction starts with molecular precursors at ambient temperatures and consists of hydroxylation and condensation reactions involving a metal alkoxide, which lead to the formation of a three-dimensional inorganic network. The morphologies and properties of the resulting materials are controlled by the reaction conditions and the precursors used. Various metal (Si, Al, Ti, Zr…) alkoxide precursors can be used in the sol-gel reaction to give the corresponding metal oxide inorganic matrix, whereas the organic part is chemically linked to the metal atoms (Guizard *et al.* 2001). The most prominent inorganic material formed by the sol-gel method is SiO_2. Contrary to other metal alkoxides, the C-Si bond is stable with respect to hydrolysis, and therefore a variety of modifications can be directly incorporated into the SiO_2 network. The organic groups introduced into the sol-gel precursor can fulfil two functions: (i) modification of the inorganic network, resulting in improved compatibility between the two phases,

and/or (ii) the formation of a strong linkage between the organic and the inorganic phases via covalent bonds (Kickelbick 2003). Due to the interactions between the polymer and silanol groups generated during the sol-gel process, a macrophase separation is avoided, and the resulting materials have a high degree of homogeneity and optical transparency.

Tetraalkoxysilianes were the most commonly precursors for the inorganic SiO_2 network in hybrid organic-inorganic materials. Figure 2-6 shows the process of the polycondensation reaction of TEOS (Uragami *et al.* 2002). In the first step, TEOS was hydrolysed in the presence of an acid catalyst (A), and silanol groups were formed. These resulting silanol groups yielded siloxane bonds due to the dehydration or de-alcoholysis reaction (B) with other silanol groups or ethoxy groups during membrane drying. These reactions led to cohesive bodies between siloxane in the membrane.

(hydrolysis)
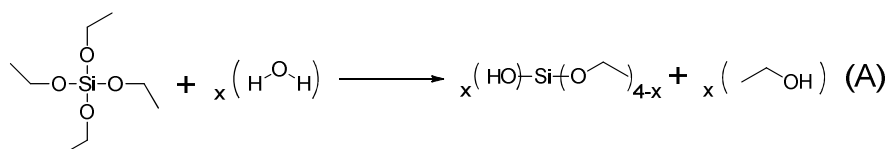
(condensation)
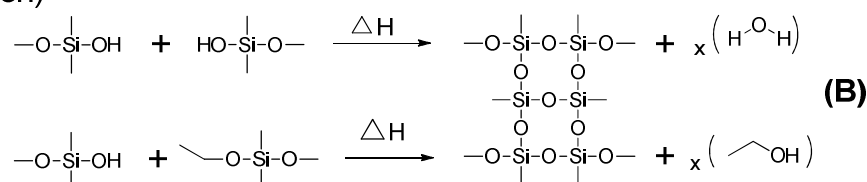
Figure 2- 6: Hydrolysis and condensation reaction for TEOS (Uragami *et al.* 2002)

During the preparation of PVA/TEOS hybrid membranes, the siloxane is dispersed in the PVA, and the silanol groups in the siloxane and the hydroxyl groups in the PVA form hydrogen and covalent bonds. These bonds are the crosslinking points between polymer chains, as illustrated in Figure 2-7. It was speculated that the formation of these hydrogen and covalent bonds contributed to the increase in membrane density and the decrease in the degree of swelling of the membrane with increasing TEOS content (Uragami *et al.* 2002).
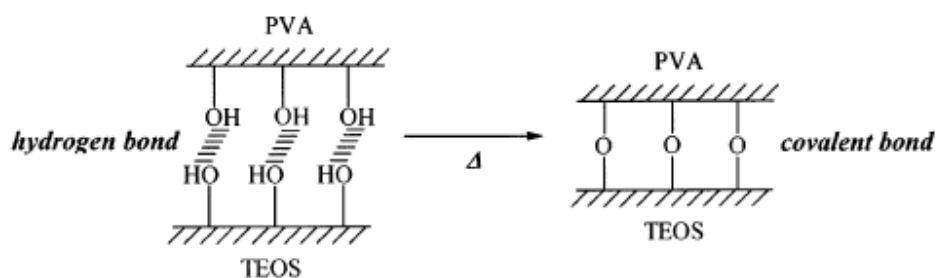
Figure 2-7: A proposed interaction between PVA and TEOS (Uragami *et al.* 2002).

In addition to commonly used tetraalkoxysilanes, trialkoxysilanes with an organic functionality have also been employed. In the case of tetraalkoxysilane, depending on the reaction conditions, a highly crosslinked silica network can be formed, while in the case of trialkoxysilanes a lower degree of crosslinking is usually observed. In addition, the functionality of the trialkoxysliane can be used for the formation of a covalent linkage between the polymer and the silica species (Kickelbick 2003). For example, aminophenyltrimethoxysliane was used as a bridging agent which reacts with the phthaloyl chloride end-capped polyamide to link the inorganic and organic phases (Ahmad *et al.* 1997).

The parameters employed for the sol-gel process have a crucial influence on the morphology of inorganic species in the resulting material which directly influences its properties (Kickelbick 2003). The morphology of materials depends on several factors including the type of metal alkoxide precursor, the nature of the solvent, type of catalyst, and the hydrolysis and pH conditions (Kickelbick 2003, Cornelius *et al.* 2001).

2.7   PVA based membranes

Poly(vinyl alcohol) (PVA) is hydrophilic in nature and contains pendant hydroxyl groups. Its aqueous solution can form transparent films. The inherent hydrophilicity of PVA makes it an attractive polymer for water treatment membranes (Bolto *et al.* 2009, Bolto *et al.* 2011). Table 2-4 lists the main characteristics of PVA membranes. PVA membranes have many advantages: thermal and chemical resistance and a high anti-fouling potential are accompanied by high water permeability. However, because of its unstable and large swelling nature in water, PVA must be adequately crosslinked to minimise swelling in water when fabricated for aqueous applications to ensure that the contaminants in water can be

31

retained, and that compaction under pressure can be minimised. There is a challenge to achieve this and still obtain economic permeate fluxes.

Table 2- 4: Attributes of PVA membranes (Bolto *et al.* 2009).

Positive	*Negative*
Excellent hydrophilicity	High degree of swelling
Permeability to water	Permeability to ions
Good mechanical properties	Compaction under pressure
Thermal resistance	Low flux when highly crosslinked
Resistance to chemicals	
Anti-fouling potential	
Low operating pressure	
Film forming ability	

2.7.1   Crosslinking of PVA

In the choice of appropriate membranes for pervaporation, crosslinked PVA is pertinent because of its very hydrophilic nature (Bolto *et al.* 2009). In membrane technology, there are two reasons to crosslink a polymer. The first reason is to make the polymer insoluble in the feed mixture and the second reason is to decrease the degree of swelling of the polymer in order to derive good selectivity(Smitha *et al.* 2004). This is also the case for PVA membranes. Extensive literature exists on crosslinking of PVA. PVA and crosslinked PVA membranes have been used extensively for pervaporation dehydration of aqueous ethanol. While the literature on applications as membranes or support material in water treatment is spasmodic, there has been a continuing effort in the biotechnology area to use PVA membranes for protein recovery (Li and Barbari 1995). As well, PVA gels have been studied extensively as biomaterials for artificial kidneys and pancreases, glucose sensors,

immuno-isolation membranes, artificial cartilage, contact lenses and drug delivery systems (Bolto *et al.* 2009). Methods of improving the mechanical integrity of PVA include freezing, heat treatment, irradiation, and chemical crosslinking.

Crosslinked PVA has good chemical, thermal and mechanical stability. It is appropriate for pressure-driven membranes designed for a variety of water treatment applications, such as microfiltration (MF) for removing particulate material, microbial cell residues and turbidity, ultrafiltration (UF) for taking out large organic molecules, nanofiltration (NF) for small organic molecule removal and softening, and reverse osmosis (RO) for desalination (Chapman *et al.* 2008). The highly polar nature of PVA minimises fouling in such applications. PVA membranes are also widely used for product recovery and for the separation of organic compounds from one another. Additionally they are also used for pervaporation of organic-aqueous feeds, where one component is selectively transferred through the membrane on the basis of the polarity, not volatility difference (Bolto *et al.* 2009).

Crosslinking can be performed in three ways. One is via chemical reaction using a compound to connect two polymer chains, the second by irradiation and the third is a physical crosslinking. A good example of this is the chemically crosslinked PVA composite membrane which shows excellent resistance to many solvents (Smitha *et al.* 2004). For chemical crosslinking, all multifunctional compounds capable of reacting with the hydroxyl group of PVA may be used as a crosslinker of PVA, e.g. maleic acid (Burshe *et al.* 1997), glutaraldehyde (McKenna and Horkay 1994,Yeom and Lee 1996), dicarboxylic acid (Huang and Rhim 1993). Crosslinked membranes exhibited less swelling, had a higher water permselectivity, but lower water permeability. It should be noted that excessive crosslinking has to be avoided, as it renders the polymer membrane brittle with a loss in stability thereby making it unsuitable for pervaporation applications.

PVA membranes were especially suited to dehydration procedures. A wide range of crosslinking agents such as dialdehydes (McKenna and Horkay 1994, Macho *et al.* 1994), dicarboxylic acids (Huang and Rhim 1993), and dianhydrides (Giménez *et al.* 1996) have been employed in the fabrication of PVA membranes. Among various crosslinking reagents, dicarboxylic acid crosslinked PVA have received the most attention. In addition to the network structure resulting from crosslinking of PVA, the resulting matrix may also

have un-reacted carboxylic groups which impart specific selectivity for membrane applications (Gohil *et al.* 2006).

Amic acid has been used as a crosslinker for PVA (Huang and Yeom 1990). Imidisation at 150°C gave an improved membrane for the pervaporation of aqueous ethanol when there was 12 wt% crosslinker present. More crosslinker showed the reverse effect because of the dispersion of unreacted crosslinker within the membrane. Separation factors ranged from 70-380 and permeation rates from 30-1,600 g/m^2h at 30-75°C, depending on the operating temperature and feed mixture composition. As the water concentration increased, the separation factor decreased and the permeation rate increased. This was explained by the plasticising effect of water, swelling of the amorphous regions of the PVA membrane, and allowing the polymer chains to become more flexible.

Crosslinking of PVA with maleic acid or citric acid has been used to prepare membranes for permeation studies of water and lower aliphatic alcohol mixtures (Burshe *et al.* 1997). Citric acid gave more selective behaviour than maleic acid, with the selectivity being highest for water-isopropanol and water-isobutanol systems. This was explained by the lower crystallility of citric acid crosslinked PVA membranes. It was believed that higher crosslinking degree would result in lower crystallility and more compact structure. As a result, selectivity increased. For the water-ethanol system the selectivity was 80 and the flux 495 g/m^2h for a 30% aqueous solution at 30°C.

PVA (MW 50 kDa) was crosslinked with poly(acrylic acid) or PAA (MW 2 kDa) by heat treatment at 150°C for 1 h. The products have been used for the PV of methanol/methyl tert-butyl ether mixtures, and later ethanol-water mixtures (Lee *et al.* 2003). For 50 wt% water ethanol solutions, the separation factor was 60 at 75°C and the flux 2,800 g/m^2h.

Fumaric acid, trans-$HO_2C-CH=CH-CO_2H$, has been employed as the crosslinking agent at 0.05 mole per mole of PVA in multilayer membranes formed on a polyacrylonitrile support membrane (Huang *et al.* 2006). In the pervaporation of 20 wt% water in ethanol, the separation factors varied from 779 to 211 over the feed temperature range 60 to 100°C, and fluxes from 217 to 1,511 g/m^2h. The increase in polymer matrix free volume, the difference in penetrate mobility and the strong water swelling effect at high temperature were attributed as the reasons for the increase of the flux and the decrease of the separation factor.

The dehydration of ethanol and other alcohol/water mixtures has been explored with PVA membranes crosslinked with glutaraldehyde (Yeom and Lee 1996). At 30°C the flux was 50 g/m^{2}h for ethanol of 10 wt% water content, and 130 g/m^{2}h when the water content was 20 wt%. The corresponding separation factors were 180 and 150. The flux increased with increasing water content, while the reverse was the case with the separation factor. The flux also increased with the feed temperature, but the separation factor was lowered. Similarly, glutaraldehyde crosslinked PVA membranes have been reported and their swelling properties explored (Praptowidodo 2005). The more crosslinked, less swollen membranes had lower fluxes but higher selectivities in the pervaporation of 10 wt% water in ethanol at 40°C, the fluxes ranging from 249 to 313 g/m^{2}h and the separation factors from 69 to 108. The details are given in Table 2-5. The more crosslinked membranes were less hydrophilic as -OH groups were consumed in the crosslinking reaction and the membranes were more rigid due to reduced chain movement explored (Praptowidodo 2005).

Table 2-5 summarises the types of chemical crosslinking agents that have been used for PVA. In general, glutaraldehyde was reported to be a more effective crosslinking agent than formaldehyde or glycidyl acrylate, which in turn gives a less swollen product than that obtained by increasing the crystallinity by heating. Toluene diisocyanate and acrolein gave similar results in the preparation of reverse osmosis membranes, but at an extremely high applied pressure. Crosslinking with maleic anhydride/vinyl methyl ether copolymers gave a good result, but at even higher pressure.

In general, the high degree of swelling of PVA can be overcome by crosslinking reactions, but with the consumption of some of the -OH groups responsible for the hydrophilicity. What is really needed is the formation of a network that provides a tight restraining without serious loss of hydrophilic behaviour. To achieve this, it is best to establish inorganic crosslinks between the linear polymer chains, since inorganic bonds are known to improve the toughness of the membrane (Kim *et al.* 2001). In doing so, with a minimum degree of crosslinking density, one can retain a higher number of hydrophilic groups in the polymer chains, so as to improve the overall pervaporation performance (Kulkarni *et al.* 2006). In addition, hybrid organic-inorganic materials have been recognised in various studies as functional materials that have the merits of lightness, pliability, and molding of organic materials, plus the heat resistance and strength of inorganic materials (Huang *et al.* 2006).

Table 2- 5: Crosslinking agents and crosslinking techniques used for PVA (Bolto *et al.* 2009).

Freeze-thaw treatment	Malic acid
Heat treatment	Malonic acid
Acid-catalysed dehydration	Fumaric acid
γ-Irradiation	Poly(acrylic acid)
Persulphate treatment	Trimesic acid
Formaldehyde	Trimesoyl chloride
Glutaraldehyde	Toluene diisocyanate
Glyoxal	Glycidyl acrylate
Terephthaldehyde	Divinyl sulphone
Acrolein & methacrolein	Boric acid
Urea formaldehyde/H_2SO_4	1,2-Dibromoethane
Citric acid	Tetraethoxysilane
Maleic acid & anhydride	γ-Glycidoxypropyltrimethoxysilane
Maleic anhydride copolymers/vinyl methyl ether	γ-Mercaptopropyltrimethoxysilane

2.7.2   *PVA/inorganic hybrid membranes*

PVA/silica hybrid membranes with TEOS as the silica precursor are the most studied PVA/inorganic hybrid membranes. For PVA/silica hybrid membranes, the hydroxyl groups in the repeating units of the polymer are expected to produce strong secondary interaction with the residual silanol groups generated from acid catalysed hydrolysis and polycondensations of TEOS (Bandyopadhyay *et al.* 2005). Table 2-6 summarises the pervaporation dehydration of ethanol using PVA/inorganic hybrid membranes.

Table 2- 6: Pervaporation dehydration of ethanol using PVA/inorganic hybrid membranes (Bolto *et al.* 2011)

Crosslinker	Feed, wt% water	Temp., °C	Separation Factor	Flux, g/m²h	Reference
TEOS (160°C)	15	40	329	50	Uragami *et al.*, 2002
TEOS (130°C)	15	40	893	40	
PEG blend & TEOS	15	50	300	46	Ye *et al.*, 2007
Poly(acrylic acid) copolymer & TEOS	15	40	250	18	Uragami *et al.*, 2005
γ-aminopropyl-triethoxysilane	5	50	537	36	Zhang *et al.*, 2007
Sulphated zirconia	5	50	263	10	Kim *et al.*, 2001
	10	50	142	105	
	20	50	86	183	
	30	50	61	1,036	

Membranes made from PVA crosslinked with 25 wt% of tetraethoxysilane (TEOS) were prepared for the pervaporation of aqueous ethanol, with the aim of minimising the swelling of the PVA (Uragami *et al.* 2002). The primary reaction was through the hydroxyl group in PVA, crosslinking with silanol groups occurring via hydrolysis and condensation of TEOS, to produce O–Si–O bridges. The hybrids showed better thermal stability and a low degree of swelling in water. The crosslinking limited the swelling of the polymer. It was claimed that there were strong hydrogen bonds as well as covalent bonds formed, along with a lowering of crystallinity. FTIR spectrum showed an intense absorption band at ~1072 cm^{-1}, indicating that a reaction took place between the OH groups in the polymer and the silanol groups in the crosslinker, to form C–O–Si bonds. Crosslinking makes the polymer chains in the amorphous regions more compact, resulting in less space for species to permeate through the membrane and making the resistance higher for the larger species. Annealing of the membranes under nitrogen at temperatures of 100, 130 or 160°C was needed to

complete the condensation reaction that introduced bridging and crosslinking, and higher permselectivity resulted. It was postulated that the crosslinking reaction took place in the non-crystalline parts of the PVA membrane, forming denser non-crystalline regions. As shown in Table 2-6, the best result, for a 15% water mix in ethanol at 40°C, was a separation factor of 893 and a flux of 40 g/m^{2}h when the annealing temperature was 130°C. This compared to a separation factor of 329 and a flux of 50 g/m^{2}h when annealing was at 160°C. It was postulated that the crosslinking reaction took place in the non-crystalline parts of the PVA membrane, forming denser non-crystalline regions.

Annealing also improved the selectivity of similar membranes made from poly(vinyl alcohol-co-acrylic acid) (Uragami *et al.* 2005). In one example the separation factor was 250 for a 15% aqueous ethanol at 40°C, with a flux of 18 g/m^{2}h. Blends of PVA and poly(ethylene glycol) (PEG) have been crosslinked with TEOS and annealed at 130°C to produce a membrane with a separation factor of 300 for a 15% water mix in ethanol at 50°C (Ye *et al.* 2007). The presence of PEG increased the flux but sacrificed the separation factor. This was attributed to the decreased crystallinity of PVA with the addition of PEG, which resulted in an increase in the free volume. It favoured the permeation of permeant molecules through the membranes and resulted in an increase in the permeation flux. On the other hand, the -OH moieties decreased with the incorporation of PEG, so the hydrophilicity of the membranes decreased; subsequently, the separation factor decreased.

Similar membranes made from PVA crosslinked with TEOS were reported for the pervaporation separation of water-isopropanol mixtres, with the observation that too much crosslinker made the membrane hydrophobic (Kulkarni *et al.* 2004). Performance was enhanced by modifying the membrane by the incorporation of chitosan (Kulkarni *et al.* 2006). This was because of increased hydrophilicity and intermolecular hydrogen bonding interaction within the membrane.

PVA membranes crosslinked with γ-aminopropyltriethoxysilane (APTEOS) were examined for separation of ethanol/water mixtures (Zhang *et al.* 2007). When APTEOS was used for crosslinking PVA, the hydrophilicity of the membranes increased when the silane content was < 5%, and the permeation increased remarkably while the selectivity increased at the same time, thus breaking the trade-off between the two. With a feed containing 5% water, the separation factor was 537 and the flux was 36 g/m^{2}h at 50°C. This anti-trade-off phenomenon in pervaporation of ethanol/water mixture by the hybrid membranes was

attributed to the increase of the amorphous region of PVA and the free volume of the membrane due to the incorporation of hydrophilic aminopropyl groups in APTEOS.

PVA were crosslinked with γ-glycidoxypropyltrimethoxysilane (GPTMS) to produce PVA-silica hybrid membranes, with the aim of improving both permeability and selectivity in pervaporation separation of benzene-cyclohexane mixtures (Peng *et al.* 2005a). Bridges such as

$$CH_2OH \qquad\qquad OH \quad OH$$
$$| \qquad\qquad\qquad | \qquad |$$
$$-CHCH_2OCH_2CH_2CH_2O-Si-(O-Si-O)_n-Si-$$
$$| \qquad |$$
$$OH \quad OH$$
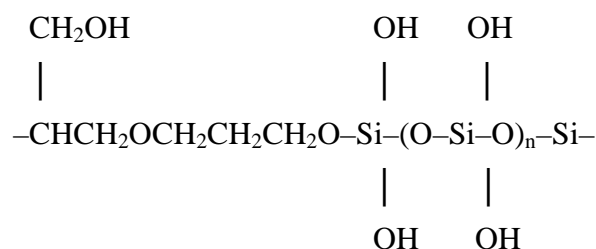
may be formed as links between the oxygen atoms in the PVA. The permeation flux for benzene from a mixture with cyclohexane increased from 20.3 g/m^2h for an unfilled PVA membrane to 137 g/m^2h for the hybrid membrane, while the separation factor increased from 9.6 to 46.9. This was attributed to an increase in the size and number of free volume element size and an elongation of the diffusion path.

A mixture of γ-glycidoxypropyltrimethoxysilane and TEOS has been employed in the crosslinking of PVA for dehydration of ethylene glycol (Guo *et al.* 2006). The γ-glycidoxypropyltrimethoxysilane facilitated the dispersion of silica particles throughout the membrane, enhanced the mechanical properties and gave the best selectivity results. A more compact crosslinked structure was obtained with membranes made from PVA and γ-mercaptopropyltrimethoxysilane (Guo *et al.* 2007). There was no improvement when the mercaptol groups were oxidised to sulphonic acid groups.

PVA has also been crosslinked with the solid acid of sulphated zirconia by an acid-catalysed reaction which affected the degree of swelling and the crosslinking density of the membrane (Kim *et al.* 2001). For the same duty, both flux and selectivity were lower than for the silane products (Table 2-6). The flux increased with feed water content, while the selectivity decreased.

As detailed in this section, PVA based hybrid organic-inorganic membranes, especially PVA/ tetraethoxysilane (TEOS) hybrid membranes have been prepared through sol-gel reaction for pervaporation separation of alcohol-water mixture. In general, hybrid organic-

inorganic membranes effectively controlled the swelling of PVA-based membranes in aqueous solutions with film-forming properties, chemical and physical stabilities. Through chemical crosslinking to control the swelling degree, the permselectivity of the membrane increased, but the permeation flux and hydrophilicity were generally depressed. Therefore how to control the degree of swelling of PVA-based membranes, and to increase or retain the permeation flux is the focus of this work on the modification to the PVA membranes. Zhang *et al.* (2007) and Peng *et al.* (2005a) demonstrated it is possible to enhance both flux and permselectivity at the same time for pervaporation by crosslinking PVA with APTEOS or GPTMS by proper design of the nanostructure of hybrid membranes.

2.8   Factors affecting pervaporation process

The steady-state mass transport regime for the pervaporation process depends on several parameters. It is usually considered with regard to the variations of membrane properties and different operating variables, such as the membrane thickness, the feed composition/concentration, the feed temperature, the permeate pressure, and the feed flow velocity.

2.8.1   Membrane thickness

Membrane thickness plays an important role in pervaporation performance. The influence of membrane thickness on flux and selectivity in separating different mixtures has been studied previously by number of researchers. Binning *et al.* (Binning *et al.* 1961) observed that the flux of a mixture of n-heptane and isooctane (50/50 vol.%) through a plastic membrane was proportional to the reciprocal membrane thickness and the selectivity was independent of the thickness for membrane thicknesses in the range of 20–50 μm. Similar results were reported by Villaluenga *et al.* (2005) in studying the pervaporation separation of methanol/methyl tertiary butyl ether mixtures through cellulose acetate and poly(2,6-dimethyl-1,4-phenylene oxide) membranes. It was found that the permeate flux through both membrane types decreased markedly with increasing the membrane thickness, while the selectivity remained nearly constant. The finding that the flux decreased inversely with membrane thickness was also reported by Qunhui *et al.* and Kanti *et al.* in studying the separation of water/ethanol mixtures by using chitosan (Qunhui *et al.* 1995) and blended chitosan/sodium alginate membranes (Kanti *et al.* 2004). In both cases, they reported the

flux decreased significantly with an increase in the membrane thickness and the flux was proportional to the reciprocal of the membrane thickness.

The constant selectivity with varying membrane thickness reported by Binning *et al.* (1961) and Villaluenga *et al.* (2005) was only observed with thick membranes. However, when thin membranes (<15-17 µm) were used, it was found that the selectivity improved with increasing membrane thickness. Brun *et al.* (1974) studied the influence of the membrane thickness on selectivity using nitrile rubber membranes and a mixture of butadiene and isobutene (60/40 vol%), and concluded that the selectivity was constant above a membrane thickness of 100 μm, and a lower selectivity was found when using membranes of 17 μm. The selectivity lowering for thin membranes was explained by assuming the existence of micropores in the membrane matrix, which allowed the diffusion of molecules through them.

Similar findings were also observed when using grafted polytetrafluoroethylene membranes to separate water/dioxane mixtures (Aptel *et al.* 1974), polysulfone, poly(vinyl chloride) and polyacrylonitrile membranes to separate water/acetic acid mixtures (Koops *et al.* 1994), and chitosan membranes to separate water/ethanol mixtures Qunhui *et al.* (1995). Aptel *et al.* (1974) observed an increased selectivity with a increase of the membrane thickness from 10 to 50 µm. Low selectivity of thin membranes was attributed to the swelling of the membrane. Koops *et al.* (1994) observed that the selectivity was independent of the membrane thickness above 15 μm, but below this limiting thickness, the selectivity decreased with decreasing membrane thickness. This dependence, which could not be explained by differences in the polymer morphology, or by flow coupling, was attributed to the formation of induced defects in the membrane during the pervaporation process. Qunhui *et al.* (1995) found that, the selectivity increased with the membrane thickness for membranes with thicknesses lower than 30 μm, whereas for membranes with thickness higher than 50 μm, the membranes exhibited constant selectivities.

Kanti *et al.* (2004) reported that the selectivity increased with membrane thickness when separating water/ethanol mixtures using blended chitosan/sodium alginate membranes with the membrane thickness varies from 25 to 190 µm. The variation of the selectivity with the membrane thickness was related to the existence of a dry layer in the membrane on the permeate side, which was responsible of the permselective properties of the membrane. It was explained that the thickness of this dry layer increased with the total membrane

41

thickness, causing a rise in the membrane mass transfer resistance. Therefore, the selectivity increased when the membrane thickness was increased.

In summary, all the studies on membrane thickness were consistent. In general, flux decreased inversely with increasing membrane thickness by increasing the membrane resistance, which is in agreement with equation 2-2 and 2-3. On the other hand, the selectivity also improved with increasing membrane thickness until the membranes were very thick. The existence of micropores in the nonporous pervaporation membranes would lead to poor selectivity as defects allow the diffusion of molecules through thin membranes. Therefore, in order to obtain a constant selectivity, an optimal membrane thickness with uniform structure may be required, and the absolute thickness at which this occurs varies between systems.

2.8.2 Operating conditions

For polymeric pervaporation membranes, extensive research was performed to find an optimised membrane material having selective interaction with a specific component of feed mixtures to maximise performance in terms of separation factor, flux and stability (Peivasti *et al.* 2008). However, performance of these membranes was strongly influenced by process conditions such as feed concentration and temperature.

Performance of pervaporation is dependent not only upon the membranes but also upon the operating parameters such as feed concentration, temperature, permeate pressure and feed flow rate. A number of researchers reported the effect of these parameters on various pervaporation systems (Burshe *et al.* 1997, Jiraratananon *et al.* 2002, Ping *et al.* 1990, Marin *et al.* 1992, Kittur *et al.* 2003). Jiraratananon *et al.* (2002) investigated the performance of the blended CS/HEC-CA composite membranes on dehydration of ethanol–water mixtures as affected by the operating conditions. They concluded that pervaporation of low water content feed carried out at high feed flowrate and at low temperature and permeation pressure was an advantage. In a study using ZSM-5 zeolite incorporated PVA membranes for pervaporation separation of water-isopropanol mixtures, Kittur *et al.* found that separation factor and flux were dependent on water composition of the feed mixture, but were comparatively less dependent on temperature. Permeation flux increased with increasing the amount of water up to 30 wt% in the feed and then, decreased with increasing water composition (Kittur *et al.* 2003).

Feed concentration refers to the concentration of the more permeable (usually minor) component in the solution. A change of feed concentration directly affects sorption at the liquid/membrane interface, i.e., the concentration of the components in the membrane tends to increase with the feed concentration, as would be suggested by the term partition coefficient K defined in equation 2-1. Since diffusion in the membrane is concentration dependent, the permeation flux generally increases with feed concentration. Mass transfer in the liquid feed side may be limited by the extent of concentration polarization. In principle, an increase of feed flow rate should reduce concentration polarization and increase flux due to a reduction of transport resistance in liquid boundary layer (Jiraratananon *et al.* 2002). In the water-alcohol system, previous studies show a trade-off relationship between water flux and selectivity (Burshe *et al.* 1997). With an increase in feed water concentration, the flux increased and the selectivity decreased. This phenomenon can be explained in terms of the plasticising effect of water. As the water concentration in the feed increases, the amorphous regions the membrane swell and the polymer chains become more flexible thus lowering the ability of the membrane for selective transport (Huang and Yeom 1990).

Flux and selectivity in pervaporation are also affected by feed temperature. The temperature dependency of flux, generally, follows an Arrhenius law:

$$J_i = A_i \exp\left(-\frac{E_{p,i}}{RT}\right) \qquad (2\text{-}10)$$

where, J_i is the permeation flux of i (g/m^2 s), A_i the pre-exponential parameter (g/m^{2}s), R the gas constant, T the absolute temperature (K) and $E_{p,i}$ is the activation energy for permeation (kJ/mol) which depends on both activation energy for diffusion and heat of solution. If the activation energy is positive, then permeation flux increases with increasing temperature. This was observed in most pervaporation experiments (Burshe *et al.* 1997, Kittur *et al.* 2003). The driving force for mass transport also increases with increasing temperature. As the feed temperature increases, vapour pressure in the feed compartment increases, but vapour pressure at the permeate side is not affected. These result in an increase of driving force due to increase in temperature and subsequently the vapour pressure difference across the membrane, consequently flux increases (Kittur *et al.* 2003). Depending on differences in flux increment of each component with increasing temperature, effect of feed temperature on selectivity in pervaporation is different. In most cases, a small decrease of selectivity

with increasing feed temperature was found (Peivasti *et al.* 2008, Ping *et al.* 1990, Kittur *et al.* 2003). However, an increase of selectivity with feed temperature was also reported for dehydration of ethanol and isopropanol using cellulose acetate membrane, which was explained by the larger flux increment of water compared to ethanol with increasing temperature (Song and Hong 1997).

Permeate pressure is also an important parameter since the operation at high vacuum is costly. The maximum driving force can be obtained at zero permeate pressure. The effect of permeate pressure change on flux was described mathematically and confirmed experimentally by many investigators (Peivasti *et al.* 2008, Jiraratananon *et al.* 2002, Greenlaw *et al.* 1977). For selectivity, its variation with permeate pressure relies on the relative volatility of the permeating components. Peivasti *et al.* (2008) found both permeate flux and selectivity enhances with decreasing permeate pressure (high vacuum) on pervaporation of methanol/methyl tert-butyl ether mixtures.

As can be seen, process operating conditions such as feed temperature and permeate pressure have strong influence on pervaporation performance of membranes. To optimise membrane performance for desalination by pervaporation, it is necessary to study the effect of process parameters such as temperature, permeate pressure and salt concentration on water flux and salt rejection.

2.9   Summary

As a potential low energy membrane technology, pervaporation has been extensively used for separation of mixtures of aqueous-organic or organic liquids. However, there are only limited studies on its application in water desalination. For its application in desalination, it has the advantages of near 100% salt rejection and the energy need is independent of the salt concentration. The main challenge for commercial application of desalination by pervaporation is believed to be the low water flux of current available polymeric membranes.

Among the commonly used hydrophilic polymers, PVA has found increasing applications as a pervaporation membrane material due to its superior properties. However, PVA must be grafted or crosslinked to minimise its swelling in water. Numerous attempts have been made to improve the separation capabilities of the membranes including crossling PVA with maleic acid, glutaraldehyde, and phenylene diamine. These membranes yield better

44

pervaporation performances, but still fail to achieve satisfactory results. In general, there is a trade-off between permeability and selectivity for polymeric membranes. This may account either for greater degree of crosslinking density or for higher degree of swelling due to less crosslinking density. Hybrid organic-inorganic membranes which bridge organic and inorganic components is believed to be a convenient and efficient approach to overcome these problems. Especially, the "class II" hybrid organic-inorganic membranes in which the inorganic and organic components are linked through strong ionic/covalent bonding. Such membranes could provide a solution to overcome the trade-off between flux and selectivity as already been observed for dehydration of ethanol by hybrid PVA membranes crosslinked with APTEOS (Zhang *et al.* 2007).

Based on the solution-diffusion theory and free-volume theory which are used to describe the transport mechanism of pervaporation membranes, it is believed that as long as the hybrid organic-inorganic membranes can be prepared with larger free volume capacity and suitable size of the free volume cavities, the permeability and selectivity will be enhanced simultaneously. Class II organic-inorganic hybrid materials provide the opportunity to do this. Successful preparation of such membranes relies heavily on the appropriate recipe of the hybrid organic-inorganic membranes. Furthermore, to improve the compatibility and mechanical properties of the hybrid membrane, appropriate selection of precursor with sufficient hydrophilicity and ideal structure is also crucial. For PVA/silica hybrid membranes, the hydroxyl groups in PVA molecule could form hydrogen bonds or become involved in the condensation reaction with silanols produced during hydrolysis of the silica precursor during the sol-gel reactions. The primary objective of this work was to develop a PVA based high performance hybrid organic-inorganic pervaporation membrane with transport properties exceeding the performance limits of current commercial polymer membranes for desalination applications. It is expected this work will provide a method to disperse the inorganic particles uniformly in the polymer matrix at a nano-scale to improve the stability. It would also help to gain fundamental understanding of transport mechanism of the pervaporation membranes and establish the structure-performance relationship with respect to water flux and salt rejection.

Pervaporation performance not only depends on the type of membrane materials but is also strongly influenced by operating parameters such as feed concentration, feed temperature, permeate pressure and feed flowrate. A process engineering model to estimate the energy

consumption for desalination by pervaporation will enable potentially applications to be assessed. The results of this research work are expected to offer useful criteria for development of high performance pervaporation membranes and selection of appropriate operating conditions for desalination by pervaporation process. This will identify potential applications where pervaporation desalination might be applicable.

Chapter 3
Experimental and Methods

3.1   Introduction

In this study, highly dispersed non-porous poly(vinyl alcohole) (PVA) based hybrid organic-inorganic membranes were developed via an in-situ sol-gel method. Tetraethoxy-silane (TEOS) was used as the silica precursor with maleic acid (MA) as an additional crosslinking agent. This chapter describes the synthesis and characterisation method of hybrid organic-inorganic membranes based on PVA, maleic acid and TEOS. A range of characterisation techniques were used with the aim to establish the structure-property relationship of fabricated PVA/MA/TEOS membranes. The membrane performance testing procedure for separating aqueous salt solution by pervaporation process is also described.

3.2   Hybrid Membrane Synthesis

3.2.1   Materials

PVA (98-99% hydrolysed, average molecular weight 160,000), tetraethyl orthosilicate (TEOS, 98%), maleic acid (MA), p-toluene sulfonic acid (98.5%, monohydrate), sodium chloride (NaCl) were obtained from Sigma-Aldrich. All the chemicals were of reagent grade and were used without further purification.

Milli-Q de-ionised water (18.1 M$\Omega\cdot$cm@25°C) was used to prepare the PVA and aqueous salt solutions throughout the study.

3.2.2   Hybrid membrane synthesis

Hybrid PVA/MA/silica membranes were synthesised via an aqueous sol-gel route. A schematic drawing of the synthesis process for unsupported hybrid membranes is shown in Figure 3-1:
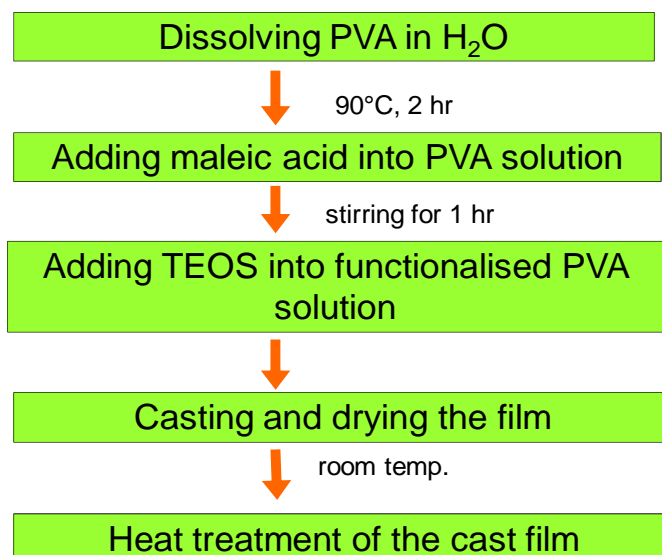
Figure 3- 1: Scheme for hybrid membrane synthesis

For PVA/MA/silica membranes, PVA polymer powder (8 g) was fully dissolved in 100 mL of Milli-Q deionised water at 90°C. The obtained 7.4 wt% PVA solution was allowed to cool to room temperature and the pH adjusted to 1.9±0.1with ~0.5 mL concentrated HCl or 0.08 g of p-toluene sulfonic acid. The given amount of MA (the weight content of MA with respect to PVA = 5-20 wt%) was added to the PVA solution and stirred until fully dissolved. Under steady stirring, a predetermined TEOS and ethanol mixture (mass ratio of TEOS: ethanol = 1:9) was added drop wise to the PVA/MA mixture. The amount of TEOS was added in the SiO_2 weight percentages of 10 and 25 wt% with respect to the amount of PVA in the solution, i.e. the weight content of SiO_2 with respect to PVA = 10-25 wt%. The reaction was held at room temperature by continuously stirring for 2 hr. The resulting homogeneous mixture was cast on Perspex Petri dishes to the desired thickness and dried at 50°C overnight and heated to 140°C for 2 hr in a fan forced oven. Pure PVA membrane samples were also prepared as a reference for comparison.

To study the effect of silica nanoparticles on properties and pervaporation performance of hybrid PVA/MA/silica membranes, a series of PVA/MA and PVA/silica membranes were prepared. In this case, either the step adding TEOS or adding MA was omitted during the synthesis.

To study the effect of heat treatment on pervaporation properties of hybrid PVA/MA/silica membranes, the resulting homogeneous mixture was cast on Perspex Petri dishes to the

desired thickness and dried in air followed by either varying the heat temperature from 100 to 160°C with 2 hours heating time or varying the heating time from 2 to 24 hours at a temperature of 140°C. A membrane sample prepared at room temperature (21°C) without any heat treatment was prepared as a reference for comparison.

Table 3-1 lists a summary of the synthesis conditions for all membranes fabricated in this study:

Table 3- 1: Summary of the membrane synthesis conditions used in the study.

Sample No	Sample	Heating temperature	Heating time
		°C	hour
S1	PVA	21	0
S2	PVA, 20%MA	140	2
S3	PVA, 20%MA, 10%silica	140	2
S4	PVA, 20%MA, 25%silica	140	2
S5	PVA, 5%MA, 10%silica	21	0
S6	PVA, 5%MA, 10%silica	100	2
S7	PVA, 5%MA, 10%silica	120	2
S8	PVA, 5%MA, 10%silica	140	2
S9	PVA, 5%MA, 10%silica	160	2
S10	PVA, 5%MA, 10%silica	140	2
S11	PVA, 5%MA, 10%silica	140	5
S12	PVA, 5%MA, 10%silica	140	16
S13	PVA, 5%MA, 10%silica	140	24

3.3 Membrane Characterisation

3.3.1 *Physical properties of membrane*

Membrane thickness: The thickness of membranes was measured at different positions using a Fowler electronic digital micrometer (accuracy ±1 μm) and the average thickness of 6 measurements is reported.

Fourier transform infrared spectroscopy (FTIR): FTIR was performed on a Perkin-Elmer Spectrum 2000 FTIR instrument to assess the functional structure of hybrid membrane samples. FTIR spectra of thin films were obtained using 128 scans with an 8 cm^{-1} resolution, from 400 to 4000 cm-1 wavelength.

Differential scanning calorimetry (DSC): DSC was conducted using a Perkin-Elmer Pyris-1 differential scanning calorimeter to assess the glass transition temperature (T_g) of PVA and its hybrid membrane samples. The analysis was conducted under nitrogen with samples of approximately 5-10 mg at a scan rate of 10°C min^{-1} from 10 to 250°C. The data were analysed using the Pyris software provided by Perkin-Elmer. The glass transition temperature, T_g, was taken at the midpoint of the heat capacity step change.

Thermogravimetry analysis (TGA): Thermal stabilities of PVA and hybrid membranes were assessed using a Perkin-Elmer Pyris 1 TGA instrument. Experiments were conducted on 3-5 mg thin film samples heated in flowing nitrogen at a heating rate of 20°C min-1 from 30 to 800°C.

Scanning electronic microscope (SEM): The surface morphology of the hybrid membrane samples were imaged using a Philips XL30 SEM. Energy dispersive X-ray spectrometry (EDS) was performed by an EDAX detector on the SEM with a voltage of 15 kV and a working distance of 15 mm. All samples were coated by sputtering with iridium for imaging and with carbon for EDS.

Transmission electron microscope (TEM): The morphology of the hybrid membrane sample was imaged using a TECNAI F30 TEM with an accelerating voltage of 200 kV. TEM samples were prepared by a focused ion beam (FIB) technique with samples sputter coated with gold.

Wide-angle X-ray diffractometry (WAXD): The crystalline diffraction of PVA and hybrid membranes were studied at room temperature using a Bruker D8 advanced WAXD with Cu-Kα radiation (40kV, 40mA) monochromatised with a graphite sample monochromator. Dried membrane samples were mounted on zero background plates and scanned over a 2θ range of 5 to 61° with a step size of 0.02° and a count time of 4 seconds per step.

Swelling properties: The swelling properties or the water uptake of PVA and PVA/MA/silica hybrid membranes was measured by the following procedures: (i) immersing the dried membrane in deionised water at room temperature for 48 h to reach the absorption equilibrium. (ii) blotting the surface of wet membrane with the cleansing tissue to remove surface water and quickly weighing the wet membrane within 10 sec (W_s). (iii) drying the membrane in a vacuum oven at 50°C for overnight and then weighing again to obtain the mass of dried membrane (W_d). The swelling degree (S) or the water uptake of membrane was then calculated according to:

$$S = \frac{W_s - W_d}{W_d} \times 100\% \tag{3-1}$$

Where W_s and W_d are the weight of wet and dry membrane, respectively.

Contact angle: The hydrophilic properties of membrane samples were assessed by a KSV contact angle meter (CAM200) equipped with an image capturing system. Static contact angles were measured by the sessile drop method. A minimum of three drops were measured and a 6 µL water drop was formed on the levelled surface of the membrane for contact angle measurements.

3.3.2 Salt transport properties

Salt transport properties of membranes were characterised using the kinetic desorption method (Lonsdale *et al.* 1965, Yasuda *et al.* 1968, Ju *et al.* 2010, Sagle *et al.* 2009). A film membrane sample with thickness of 60 µm was immersed in 50 mL of 5 wt% NaCl solution for 48 hours at room temperature. Following that, the film was taken out of the NaCl solution and blotted dry with tissue paper. The film was then quickly transferred to a beaker containing 80 mL of deionised water which was stirred vigorously using a stirring bar to achieve a uniform distribution of NaCl in the solution during desorption. To minimise solution conductivity change due to CO_2 absorption by the water, the water in the beaker

was air-saturated before adding the film sample. Solution conductivity was measured as a function of time using an Oakton® Con 110 conductivity meter and the data were recorded at 5 s intervals.

Analysis of the desorption results plotted (M_t/M_∞) versus $t^{1/2}$. The desorption process was considered to follow a Fickian diffusion model and the NaCl diffusivity D_s in the membrane was calculated using (Yasuda *et al.* 1968, Ju *et al.* 2010, Sagle *et al.* 2009):

$$D_s = \frac{\pi \cdot l^2}{16} \left[\frac{d(M_t / M_\infty)}{d(t^{1/2})} \right]^2$$

(3-2)

Where M_t is the amount of NaCl in the solution at time t and M_∞ is the total amount of NaCl desorbed from the membrane into the solution, and l is the thickness of the membrane. The NaCl solubility, K_s, is the ratio of NaCl in the membrane (M) per unit membrane volume to the concentration of NaCl in the original solution (i.e. 5 wt%). According to the solution-diffusion model, NaCl permeability, P_s, is the product of D_s and K_s (Lonsdale *et al.* 1965, Yasuda *et al.* 1968, Ju *et al.* 2010, Sagle *et al.* 2009).

$$P_s = D_s K_s$$

(3-3)

3.3.3 *Diffusion coefficients of water and global mass transfer coefficients*

Diffusion coefficient is an important factor to estimate the diffusion of the penetrants through membranes and permeation flux. Based on Fick's law, the permeation flux of component i can be expressed as (Zhang *et al.* 2007, Peng *et al.* 2006b, Villaluenga *et al.* 2004)

$$J_i = -D_i \frac{dC_i}{dx}$$

(3-4)

Where J_i, D_i and C_i are the permeation flux (kg/m^2·hr), the diffusion coefficient (m^2/s) and the concentration (kg/m^3) of component i in the membranes, respectively; x is the diffusion length (m). For simplicity, the apparent diffusion coefficient can be calculated by the equation (Villaluenga *et al.* 2004):

$$D_i = \frac{J_i \delta}{C_{i,f}}$$
(3-5)

Where J is the permeate flux, δ is the membrane thickness, and $C_{i,f}$ is the concentration of component i in the feed.

The global mass transfer coefficient (K_{ov}) was determined using the following equation as explained in (Khayet *et al.* 2008, Gronda *et al.* 2000).

$$K_{ov} = \frac{V}{At} \ln\left(\frac{C_0}{C}\right)$$
(3-6)

where *V* is the initial liquid volume of the feed solution, *A* is the membrane area, C_0 is the initial feed concentration and *C* is the feed concentration at time *t*.

3.3.4 *Positron annihilation lifetime spectroscopy (PALS)*

PALS analysis of hybrid membrane samples was conducted using an automated EG&G Ortec fast-fast coincidence system at ambient temperature with a time resolution of 240 ps. Radioactive isotope [22]Na, which was sealed between thin Mylar films, was used as the positron source. Prior to the wet film measurement, the samples were immersed in a 0.2 wt% NaCl solution for 2 days, which represented the feed solutions used in pervaporation testing prior to measurement. The Mylar source was then sandwiched between stacks of wet films with 2 mm thickness. A minimum of 5 spectra were collected with each containing 1 x 10^6 integrated counts. The spectra were analysed using the LT v9 software. The longest lifetime, τ_3, and its intensity, I_3, were interpreted as the ortho-positronium (o-Ps) annihilation signature. The o-Ps components were used to characterise the sample's free volume (Ju *et al.* 2010). Assuming that the o-Ps is localised in a spherical potential well surrounded by an electron layer of thickness ΔR of 0.166 nm, the free volume element size, R, can be calculated using the following equation (Peng *et al.* 2006, Ju *et al.* 2010, Yampolskii and Shantarovich 2006, Tao 1972):

$$\tau_3 = \frac{1}{2}\left[1 - \frac{R}{R + \Delta R} + \frac{1}{2\pi}\sin\left(\frac{2\pi R}{R + \Delta R}\right)\right]^{-1}$$
(3-7)

The average volume of the free volume elements, VFVE can be calculated as (Peng *et al.* 2006, Ju *et al.* 2010, Yampolskii and Shantarovich 2006, Tao 1972):

$$V_F = \frac{4\pi}{3} R^3 \qquad\qquad\qquad (3\text{-}8)$$

The fractional free volume (FFV) was estimated from the following equation:

$$FFV = V_F I_3 \qquad\qquad\qquad (3\text{-}9)$$

3.4   Membrane testing

The pervaporation experiments were carried out on a laboratory scale pervaporation unit as shown in Figure 3-2 and Figure 3- 3. The membrane was placed in the middle of a pervaporation cell with an effective surface area of the membrane of 12.6 cm^2. An aqueous solution containing 2000 ppm NaCl was used as the feed solution. During the experiment, the feed solution was preheated in a water bath to the required temperature and pumped to the pervaporation cell using a Masterflex® peristaltic pump. The feed flowrate was varied from 30 to 150 mL/min. The pressure on the permeate side of the membrane cell was maintained at 6 Torr with a vacuum pump. The permeate was collected in a dry-ice cold trap. A K-type thermocouple installed in the feed chamber was used to measure the operating temperature of feed solution and the feed temperature was varied from 21 to 65°C in the study.
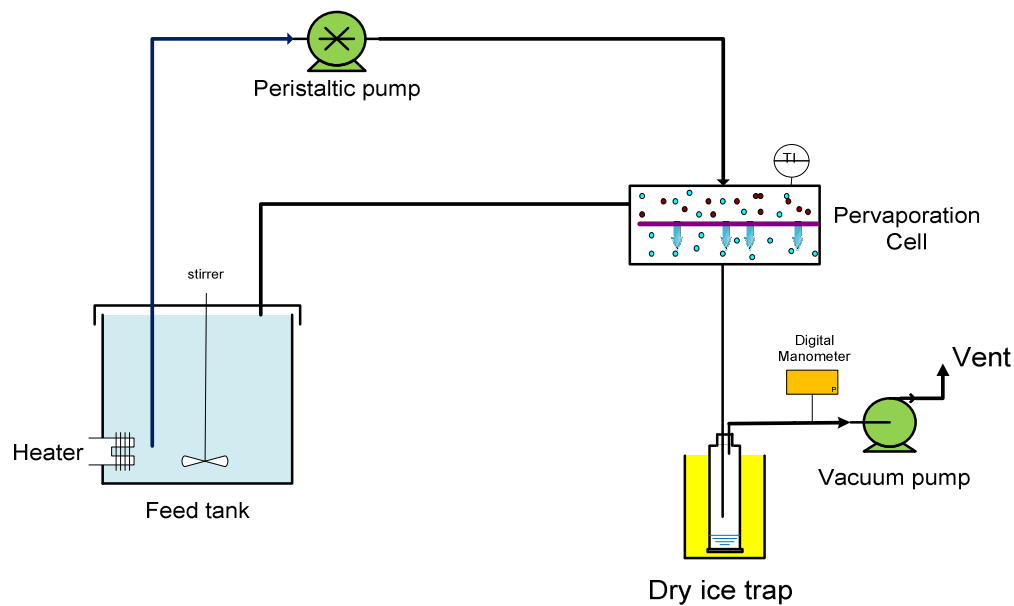
Figure 3- 2: Schematic drawing of the pervaporation unit.
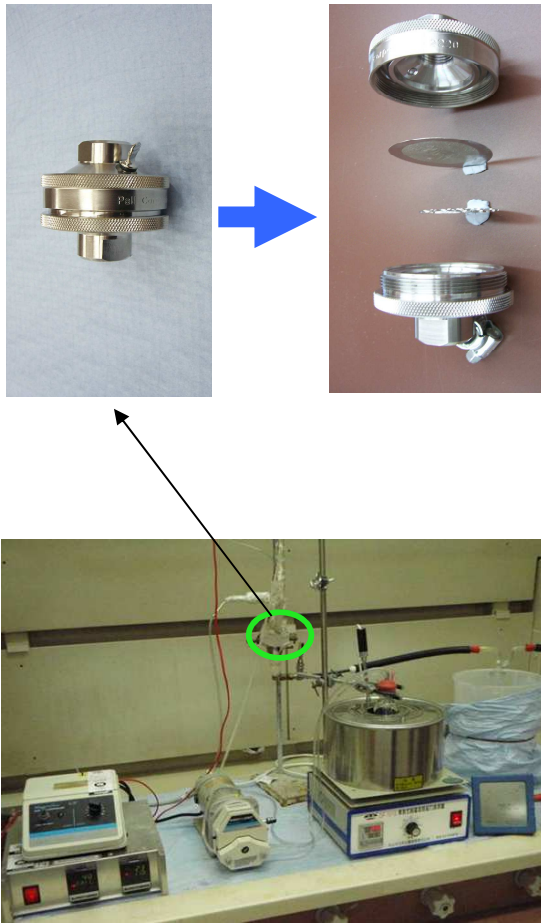
Figure 3- 3: Experimental setting up of the pervaporation unit

The desalination by pervaporation performance of hybrid membranes were characterised by water flux and salt rejection. The water flux (J) was determined from the mass (M) of permeate collected in the cold trap, the effective membrane area (A) and the experimental time (t).

$$J = \frac{M}{A*t} \qquad (3\text{-}10)$$

The salt concentration of the feed (C_f) and permeate (C_p) were derived from measured conductivity with an Oakton® Con 110 conductivity meter. Salt rejection (R) was determined by the following equation:

$$R = \frac{C_{f,i}W_{f,i} - C_{f,f}W_{f,f}}{C_{f,i}W_{f,i}} \times 100\% \qquad (3\text{-}11)$$

where $C_{f,i}$ and $C_{f,f}$ are NaCl concentrations in the feed at the beginning and end of the experiment, respectively; $W_{f,i}$ and $W_{f,f}$ are masses of feed at the beginning and end of the experiment, respectively.

Each experiment was run for 3 hours. At the end of each experiment, the membrane and membrane housing were inspected to check for signs of salt precipitation or fouling. In this study, membranes remained clean and there was no evidence of salt precipitation or crystallisation occurring in the membrane. The results during pervaporation testing were reproducible, with the variation generally within ± 0.2 kg/m^2·hr for water flux and $\pm 0.5\%$ for salt rejection.

3.5   Salt analysis

The salt concentration of the feed and permeate during membrane testing were calculated based on the relationship between NaCl concentration and conductivity measured with an Oakton$^{\circledR}$ Con 110 conductivity meter. The conductivity meter was calibrated using a series of prepared standard NaCl solutions with known concentration in the range of 0-7700 ppm. A calibration curve and equation between NaCl concentration and conductivity was then constructed and used to calculate the NaCl concentration (Figure 3- 4).
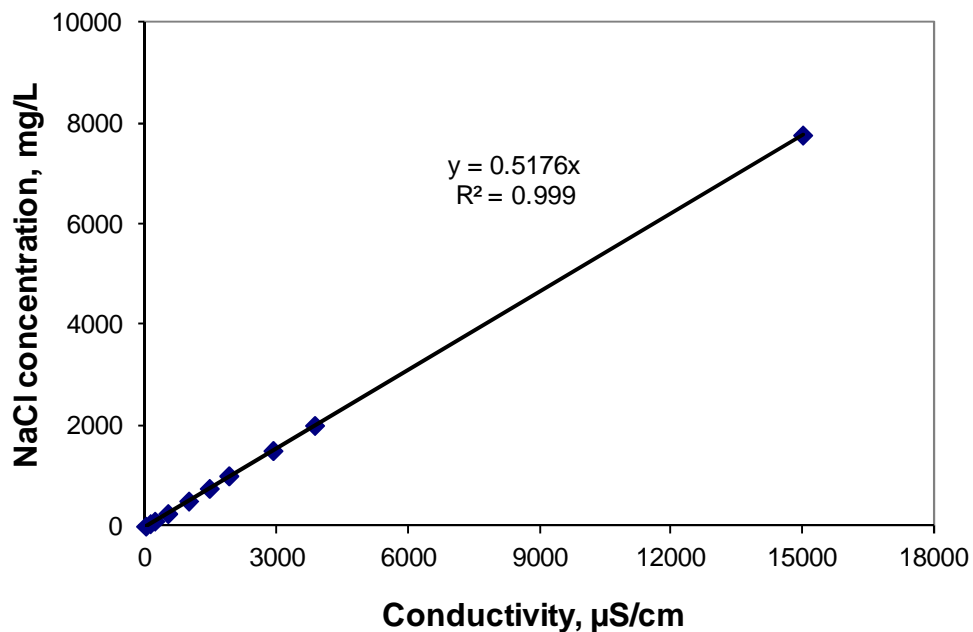
Figure 3- 4: NaCl calibration curve of the conductivity meter.

Chapter 4

Synthesis and Characterisation of Sol-gel Derived Hybrid PVA/MA/Silica Membrane for Desalination by Pervaporation

4.1 Introduction

Pervaporation has been extensively used for separation or concentration of mixtures of aqueous-organic or organic liquids. However, there is little published information on application of this technology for water desalination. In desalination applications, pervaporation has the advantage of near 100% of salt rejection. The pervaporation of an aqueous salt solution can be regarded as separation of a pseudo-liquid mixture containing free water molecules and bulkier hydrated ions formed in solution upon dissociation of the salt in water (Kuznetsov *et al.* 2007). Previous studies have demonstrated the possibility of applying pervaporation to produce distilled water from aqueous salt solutions. However, the water flux reported so far is generally quite low, at <6 kg/m^2·hr (Kuznetsov *et al.* 2007, Zwijnenberg *et al.* 2005). One of the main limitations for desalination using pervaporation is the lack of the high performance membranes with high permeate flux.

Hybrid organic-inorganic nanocomposite materials, in which polymers serve as hosts for inorganic nano-particles, are promising materials for many applications due to their extraordinary properties. The combination of these two different building blocks at a molecular level could provide novel properties that are not obtained from conventional organic or inorganic materials (Guo *et al.* 2006, Peng *et al.* 2006b, Tamaki and Chujo 1998, Ulbricht 2006). The sol-gel method is a common process to synthesise polymer-inorganic nanocomposites. It consists of an initial hydrolysis reaction, a subsequent condensation reaction followed by removal of the solvents, resulting in formation of metal oxides.

Poly(vinyl alcohol) (PVA), a water soluble hydrophilic polymer, has been studied intensively for membrane applications because of its good chemical stability, film-forming ability and high hydrophilicity. High hydrophilicity is critical for desalination membranes to minimise membrane fouling by natural organic matter (Bolto *et al.* 2009). However, PVA

has poor stability in water. Therefore, it must be insolubilised by modification reactions such as grafting (Nguyen *et al.* 1993) or crosslinking (Yeom and Lee 1996, Isklan and Sanl 2005) to form a stable membrane with good mechanical properties and selective permeability to water. Among various insolubilisation techniques, hybridisation between PVA and inorganic particles has received significant interest as it not only restricts the swelling of PVA but also provides the inherent advantages of the organic and inorganic compounds (Ye *et al.* 2007). Previous studies have shown that introducing an inorganic component derived from Si-containing precursors into PVA can form a homogeneous nanocomposite membrane with enhanced physicochemical stability and separation performance in pervaporation separation of benzene/cyclohexane mixtures (Uragami *et al.* 2002, Peng *et al.* 2006b) and aqueous ethanol solution (Uragami *et al.* 2002). However, there are few published results on application of this type of membrane for desalination by pervaporation.

This chapter reports the development of a new type of hybrid polymer-inorganic membrane based on PVA/MA/silica for desalination by pervaporation. The hybrid membrane was synthesised via a sol-gel route by using tetraethoxy-silane (TEOS) as the silica precursor with maleic acid (MA) as an additional crosslinking agent. The resulting hybrid membranes with varying silica and MA contents were characterised with a range of techniques including FTIR, SEM, WAXD, TGA, DSC and contact angle described in previous chapter. The pervaporation separation of aqueous salt solution of hybrid PVA/MA/silica membranes was examined in relation to the diffusion coefficient of water.

4.2   Membranes

Table 4-1 lists a summary of membranes used in this study. The synthesis method and conditions have been detailed in chapter 3.

Table 4- 1: Summary of the membrane synthesis conditions used in the study.

Sample	Heating temperature, °C	Heating time, hr
PVA	21	0
PVA, 20%MA	140	2
PVA, 25% silica	140	2
PVA, 20%MA, 10%silica	140	2
PVA, 20%MA, 25%silica	140	2

4.3   Results and discussion

4.3.1   FTIR analysis

Figure 4-1 shows the ATR-FTIR spectra of PVA/silica and PVA/MA/silica membrane with a pure PVA sample as a reference. FTIR spectra confirmed the formation of PVA/MA/silica hybrid with network crosslinking. The pure PVA sample (Figure 4-1-a) shows the typical C-H broad alkyl stretching band (2800-3000 cm^{-1}) and the hydrogen bonded hydroxyl band (3200-3570 cm^{-1}) (Reis *et al.* 2006). The peak at 1000-1100 cm^{-1} was assigned to the C-O stretching vibration of the secondary alcohol (-CH-OH) of PVA. For the hybrid PVA/silica membrane (Figure 4-1-b) and PVA/MA/silica membrane (Figure 4-1-c), it was noticed there was an increase in the peak intensity compared to the PVA membrane at these wavelengths. For the hybrid PVA/MA/silica membrane (Figure 4-1-c), there was also a new peak observed at 1726 cm^{-1} assigned to the ester group (-CO-O-) (Gohil *et al.* 2006).

In preparing the hybrid PVA/silica and PVA/MA/silica membranes, TEOS was initially hydrolysed in the presence of acid catalyst to form silanol groups which were subsequently condensed to form a silicon oxide network. Under acid conditions, the hydrolysis reaction is more rapid than condensation reactions and linear or random branches of silica network tend to form (Orgaz-Orgaz 1988). The resulting silanol groups formed siloxane bonds from subsequent condensation reactions during membrane drying. These reactions led to cohesive bonds between siloxane in the membrane which were dispersed in the polymer matrix (Uragami *et al.* 2002, Ye *et al.* 2007). In fabricating the hybrid PVA/MA/silica membranes,

the hydroxyl groups in the repeating units of PVA and the carboxylic groups in MA were expected to produce strong secondary interactions with these silanol groups to form hydrogen and covalent bonds. Therefore, the increase in peak intensity at 1000-1100 cm^{-1} could be explained by the formation of Si-O-Si bonds (1080 cm^{-1}) resulting from the condensation reaction between hydrolysed silanol Si-OH groups, and also covalent Si-O-C bonds resulting from the crosslinking reaction between PVA and TEOS (Ye *et al.* 2007). A new peak at 950 cm^{-1} may be attributed to Si-OH bonds resulting from the hydrolysis reaction of TEOS and the hydrogen bonds between the organic groups and the silica. Obviously, introduction of Si-OH and Si-O-Si through hydrolysis and condensation reactions of TEOS has modified the PVA structure.

In addition, PVA and MA go through esterification reactions via grafting or crosslinking under heat treatment to form the ester group. This would explain the new peak at 1726 cm^{-1} for the hybrid PVA/MA/silica membrane (Figure 4-1-c). In the hybrid PVA/MA/silica membrane, MA is also believed to act as an organic-inorganic coupling agent. This idea is supported by comparing the optical properties of hybrid PVA/MA/silica and PVA/silica membranes. The sample with MA (PVA/MA/silica) was clear and transparent. On the other hand, the film sample in the absence of MA (PVA/silica) was dark brown in colour and not transparent, as shown in Figure 4-2.
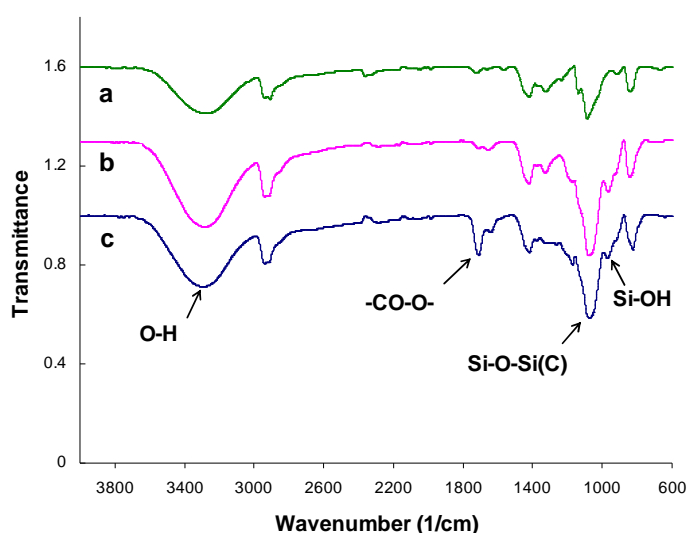
Figure 4- 1: FTIR spectra of pure PVA and hybrid membranes (a: PVA, b: PVA/silica, 25% SiO$_2$, c: PVA/MA/silica, 20%MA and 10% SiO$_2$).
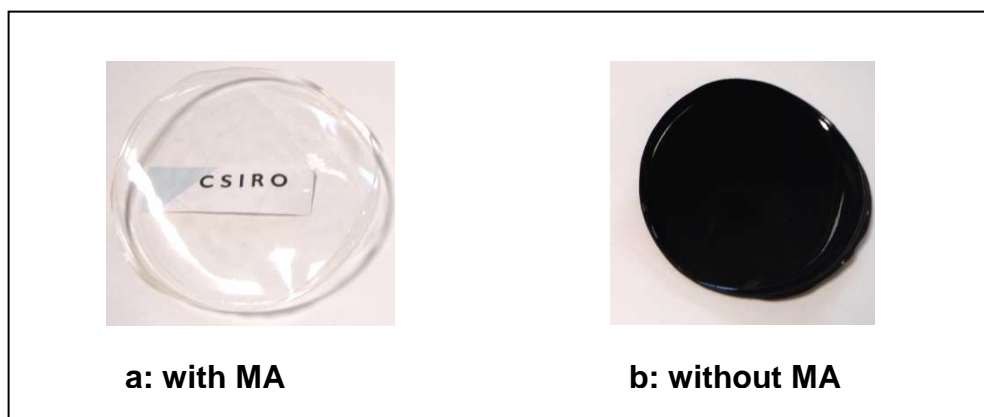
Figure 4- 2: Optical images of hybrid membranes with and without MA (a: PVA/silica, 25% SiO_2; b: PVA/MA/silica, 20%MA and 25% SiO_2).

4.3.2 Morphology

In the hybrid polymer-inorganic membrane, the inorganic phase is dispersed in the polymer phase. It is believed that the inorganic phase, resulting from the hydrolysis and condensation of TEOS in the casting solution, changes the microstructure or nanostructure of the hybrid membranes and consequently leads to the improved physical properties and performance. The uniform dispersion of silica nanoparticles and avoidance of aggregation in the polymer matrix is, therefore, critical for the performance of hybrid membranes. The phase morphology of the hybrid PVA/MA/silica membrane was studied by TEM. The typical TEM image and EDS spectra of the hybrid membrane are shown in Figure 4-3. The EDS spectra confirmed the formation of silica particles through sol-gel reaction of TEOS. No particles or agglomeration greater than 10 nm was observed in TEM image, indicating that the silica nanoparticles were well dispersed in the polymer matrix.
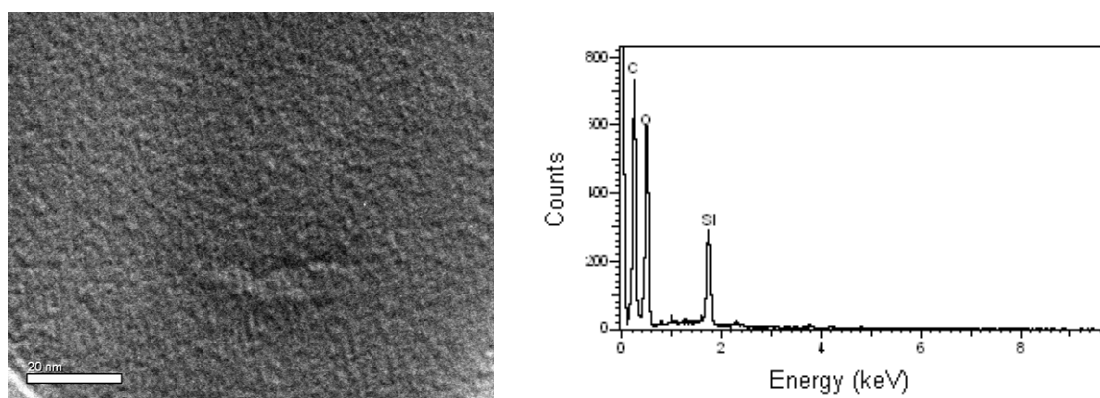
Figure 4- 3: TEM image and EDS spectra of the hybrid PVA/MA/silica membrane (membrane containing 20wt% MA and 10wt% SiO_2 with respect to PVA).

61

The crystallinity of PVA and its hybrid membranes was studied by WAXD analysis and the results are shown in Figure 4-4. For the PVA film sample, it showed a typical spectra of semi-crystalline materials and a characteristic peak of PVA appeared at approximately $2\theta = 20°$. This is in agreement with the results obtained by Kulkarni *et al.* (2004) and Uragami (2002) working with pure PVA films. With the addition of MA and silica, diffraction patterns of the hybrid membrane samples showed that the intensity of the typical peak of PVA (at 20°) became smaller (PVA/MA, PVA/silica) and the peak shape became broader (PVA/silica and PVA/MA/silica). This indicates a decrease of crystallinity for hybrid materials and an increase of amorphous character due to the crosslinking among PVA, MA and silica. It was also noted there was a slight shift in the peak position of hybrid PVA/silica and PVA/MA/silica sample. As explained by Kulkarni *et al.* (Kulkarni *et al.* 2004) and Burshe *et al.*(Burshe *et al.* 1997), this implies silanol groups of TEOS crosslink with the reactive –OH groups of PVA in a crystalline domain, leading to a more compact structure in the amorphous region due to the expansion of the crystal lattice. This is supported by the higher d-spacing value of the crystalline peak of the hybrid membrane which increased from 4.462 (PVA membrane) to 4.560 (PVA/MA/silica membrane).
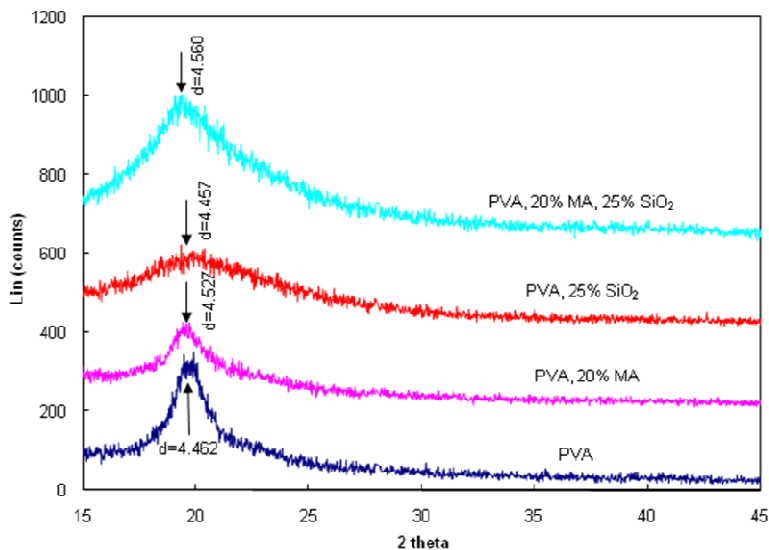
Figure 4- 4: WAXD spectra of PVA and its hybrid membranes.

4.3.3 *Thermal properties of hybrid membranes*

Thermal gravimetric analysis (TGA) was carried out for PVA, PVA/MA, PVA/MA/silica membrane samples in the temperature range of 30-800°C under nitrogen at a heating rate of

10°C min^{-1}, and the results are shown in Figure 4-5. In general, thermal stability increased for hybrid membranes. For PVA/MA membranes (Figure 4-5b), both the decomposition temperature and the residual weight increased when compared with pure PVA membrane (Figure 4-5a). With the addition of silica (Figure 4-5c and d), the residual weight of the PVA/MA/silica membrane increased further as expected. However, the degradation temperature became unclear, especially at the high silica content. When the silica content was increased from 10 wt% to 25wt%, the residual weight at 800°C increased by about the same percentage, from 21.6 wt% to 36.7 wt%.
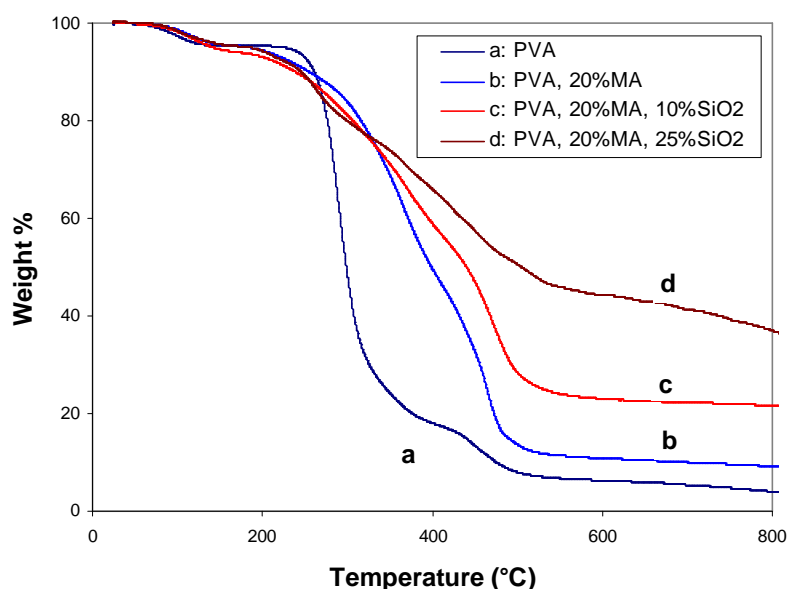
Figure 4- 5: TGA curves of PVA and its hybrid membranes.

Thermal properties of these membranes were also studied by differential scanning calorimetry (DSC) performed at a heating rate of 10°C min^{-1}. Figure 4-6 shows the DSC thermograms of PVA and its hybrid membranes. PVA is a semi-crystalline polymer exhibiting both a glass transition temperature (T_g) and a melting isotherm (T_m), as evidenced in the DSC thermogram (Figure 4-6a). The pure PVA membrane exhibited a T_g of 84°C and a T_m of 220°C. The pure PVA had the lowest T_g. For the PVA/MA membrane (Figure 4-6b), the T_g increased to 94°C. The increase in T_g is consistent with an esterification reaction between MA and PVA. With the introduction of silica into the membrane (Figure 4-6c), the T_g of hybrid PVA/MA/silica increased to 103°C. As the silica content increased, the T_g

increased further, indicating the polymer chains were becoming more rigid with the introduction of inorganic silica.
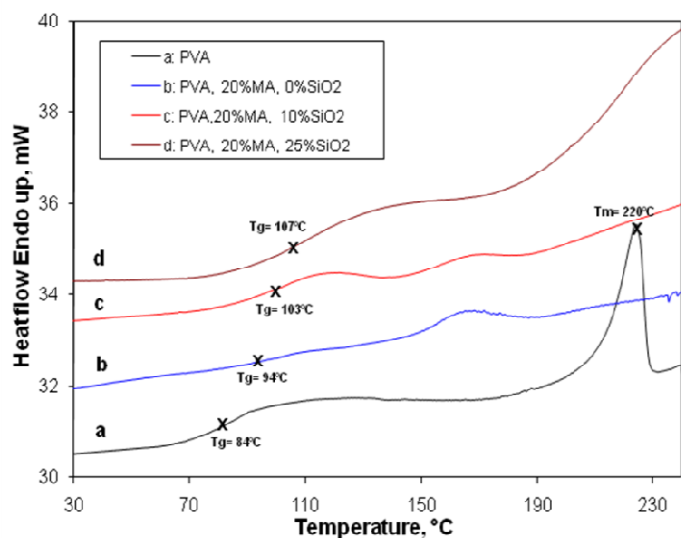
Figure 4- 6: DSC curves of PVA and its hybrid membranes.

4.3.4   *Swelling studies and contact angle*

The swelling of any polymer film in a solvent depends upon the diffusion coefficient of the solvent, the relaxation rate of the amorphous regions of the polymer chain and its degree of crystallinity (Gohil *et al.* 2006). Table 4-2 shows the swelling properties of pure PVA and hybrid membranes.

Table 4- 2: Swelling properties of PVA and its hybrid membranes.

Sample details	Swelling degree, %
PVA	301±25%
PVA, 20% MA	61±5%
PVA, 20% MA, 10% SiO$_2$	22±2%
PVA, 20% MA, 25% SiO$_2$	11±1%

The PVA used in the study has a degree of hydrolysis >98% and possesses a large number of hydroxyl group with extensive hydrogen bonding. Pure PVA membrane showed a very high degree of swelling in cold water. This is due to the relaxation of the amorphous region. For the PVA/MA membrane, the swelling was greatly suppressed. This could be explained by the grafting or crosslinking of the PVA polymer chains via an ester linkage between PVA and MA. Esterification of PVA with MA involves the reaction between carboxylic groups of MA and the hydroxyl group of PVA chains, resulting in intermolecular and intramolecular type ester linkages (see Figure 4- 7).
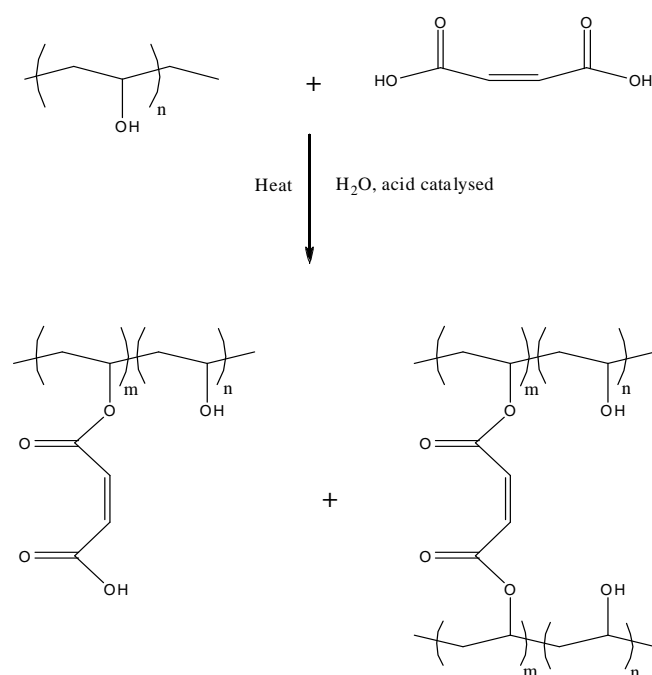
Figure 4- 7: Reaction scheme of PVA with MA.

For PVA/MA/silica membranes, the swelling was further suppressed with the addition of silica. This could be explained by the formation of chemical bonds between polymer and silica. Figure 4-8 shows reaction schemes of PVA and MA with TEOS. The silica, generated from the hydrolysis and condensation of TEOS, linked with the organic polymer chains through the polar hydroxyl group of PVA and carboxylic group of MA in the polymer. This results in a dense inorganic network and rigid hybrid structure. Therefore, the extent of the water absorption for hybrid membranes was greatly suppressed. Similar findings were also

reported by Kotoky and Dolui (Kotoky and Dolui 2004), who demonstrated that there was a considerable decrease in the water absorption in the PVA/silica hybrid films and the swelling in water was greater for those samples with less incorporated silica.
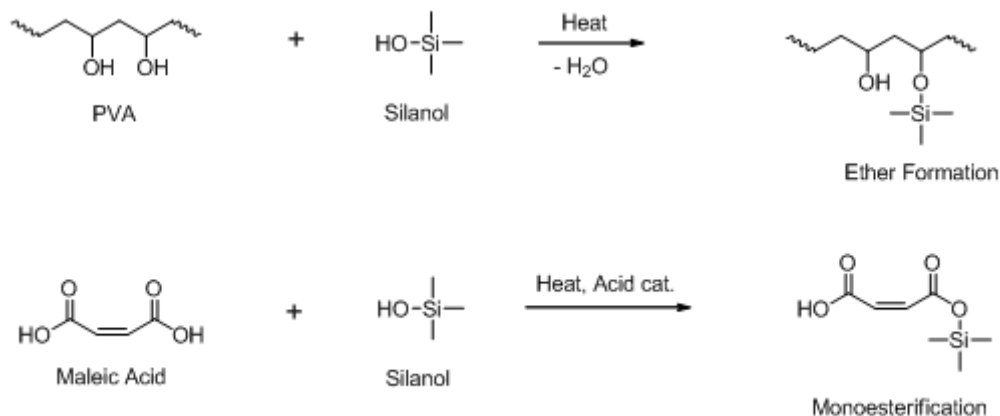
Figure 4- 8: Reaction scheme of PVA and MA with TEOS.

Table 4-3 shows the water contact angles of PVA and its hybrid membranes. Overall, all membrane samples were hydrophilic. Pure PVA film was very hydrophilic, with a water contact angle of 45.3°. With the incorporation of MA and silica, the contact angle increased, indicating that the surface of the hybrid membrane became more hydrophobic. When MA and silica were incorporated with PVA, the crosslinking among PVA, MA and TEOS led to the consumption of –OH group and the hydrophobicity increased.

Table 4- 3: Water contact angle of PVA and its hybrid membranes.

Sample details	Contact angle, ±2 degree
PVA	45.3
PVA, 20%MA, 0% SiO_2	59.4
PVA, 20%MA, 10%SiO_2	63.5
PVA, 20%MA, 25%SiO_2	79.4

4.3.5 *Pervaporation testing*

Figure 4-9 shows the desalination performance by pervaporation with PVA/MA/silica hybrid membranes with same thickness (5 µm) at a feed temperature of 22°C and a vacuum of 6 Torr. All prepared membranes had the same amount of MA (20 wt% with respect to PVA) but various silica contents (0-25 wt% with respect to PVA). Overall, the PVA based hybrid membranes demonstrated good desalination performance with high flux while maintaining a high salt rejection (>95.5%). The salt rejection increased with the silica content and achieved >99.5%. The water flux initially increased as the silica content was raised (0-10%) but then decreased with further increasing silica content (10-25%). A high flux of 5.5 kg/m^2·hr. was obtained for PVA/MA/silica membrane containing 20 wt% MA and 10 wt% silica.
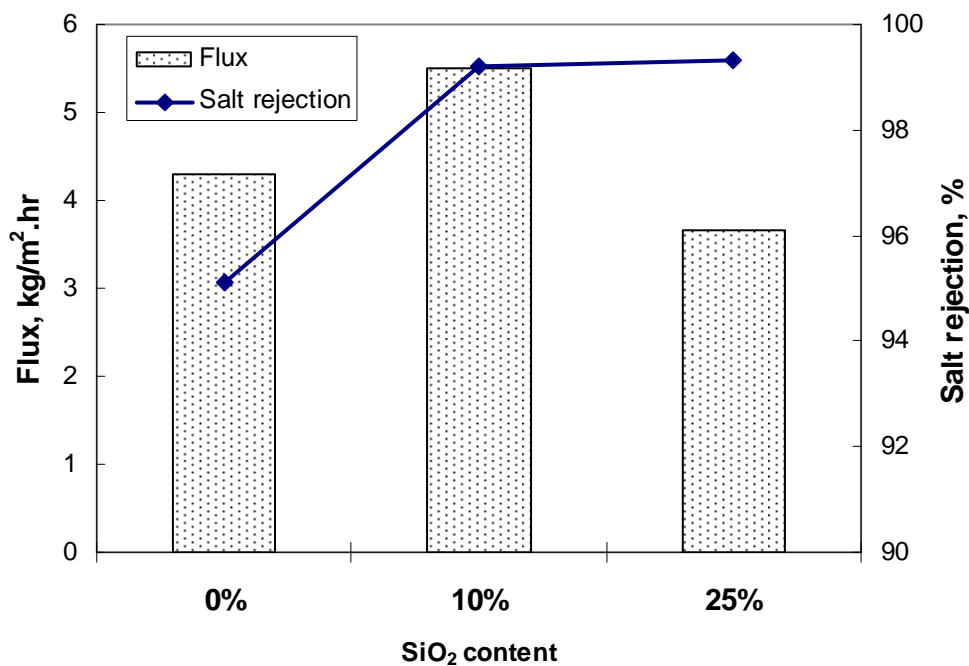
Figure 4- 9: Pervaporation testing results of hybrid membranes (all containing 20 wt% MA with respect to PVA, feed flowrate 30 mL/min, feed temperature 21°C, vacuum 6 Torr).

The solution-diffusion model is usually used to describe the transport mechanism of the pervaporation process which involves three steps: sorption at the membrane surface, diffusion through the dense membrane and desorption into the vacuum (Heintz and Stephan 1994). Under the high vacuum used in the study, the desorption step on the permeate side of the membrane is believed to be a fast step and diffusion is generally considered to be the controlling step (Kulkarni *et al.* 2004). In the solution step, the sorption selectivity is more

dependent on the affinity between the PVA and the permeants (Uragami *et al.* 2002). As mentioned earlier, all the hybrid membranes prepared in the study were hydrophilic (Table 4-3). This hydrophilic property provides a strong driving force for water affinity and its sorption. As a result, water is both preferentially dissolved and transported in the hydrophilic membranes due to its small molecular size and affiniity to hydrogen bond (Uragami *et al.* 2002).

Another set of experiments was carried out to study the effect of the membrane thickness on the desalination by pervaporation performance of aqueous salt solution. A series of hybrid PVA/MA/silica membranes with varying thickness (6-110 µm) were prepared and results are shown in Figure 4-10. As the membrane thickness increased from 6 to 110 µm, the salt rejection remained constantly high (>99%) and the water flux gradually decreased from 6.93 to 0.82 kg/m^2·hr. With increasing membrane thickness, the resistance across membrane increases, therefore the water flux decreases.
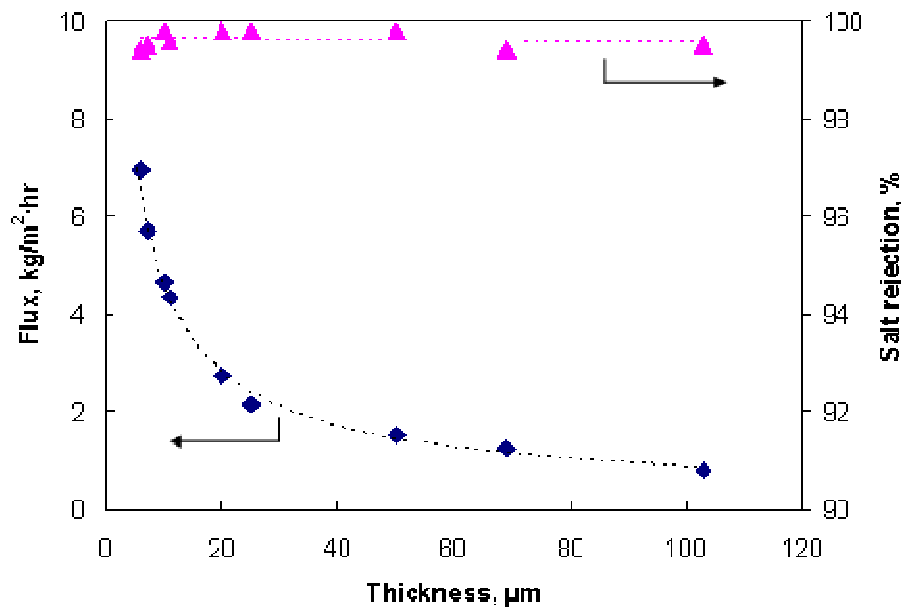
Figure 4- 10: Effect of membrane thickness on water flux (membrane containing 5 wt% MA and 10% SiO$_2$ with respect to PVA, feed temperature 21°C, feed flowrate 30 mL/min, vacuum 6 Torr).

According to the solution-diffusion model, at steady state, diffusion flow is constant and there is an inverse relationship between the flux and membrane thickness (Isklan and Sanl 2005, Heintz and Stephan 1994, George and Thomas 2001). Figure 4-11 shows a linear relationship between the water flux and the reciprocal of the membrane thickness, as

predicted by the Fick's law from the solution-diffusion model (Equation 2-2). Işıklan and Şanlı also reported that the permeation rate was proportional to the reciprocal of membrane thickness on the pervaporation performance of acetic acid-water mixtures through malic acid modified PVA membranes (Işıklan and Şanlı 2005). Therefore, for this system, diffusion through the membrane is the rate limiting step.
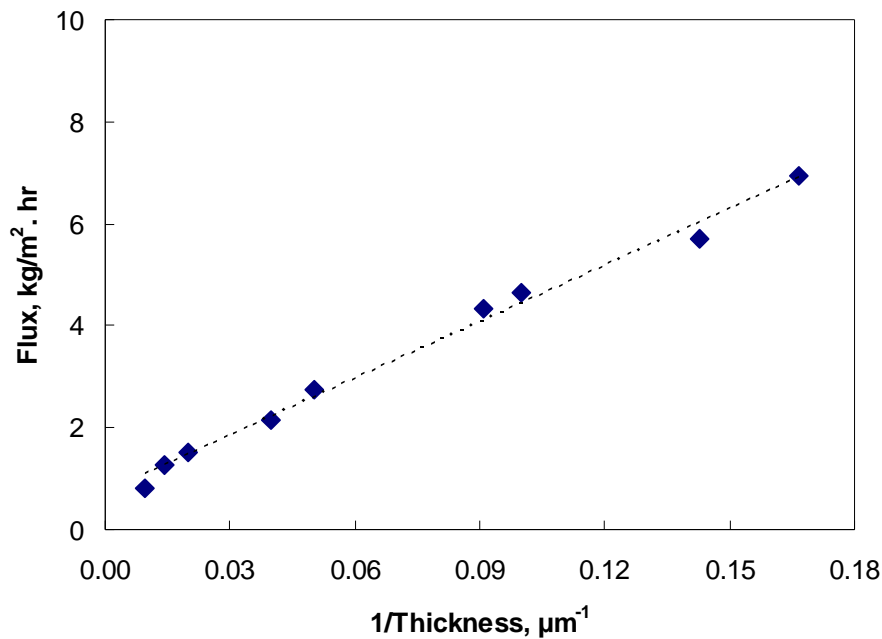
Figure 4- 11: Water flux versus the reciprocal of the membrane thickness.

The salt rejection remained high for all the membranes considered (Figure 4-9). This could be due to either of two reasons. Firstly, NaCl is a non-volatile compound. Secondly, water is preferentially diffused and permeated through the membrane due to the hydrophilic nature of the membranes. The PVA/MA membrane with 0% silica showed a higher degree of swelling compared to the PVA/MA/Silica membranes (Table 4-2). Therefore, a small fraction of hydrated salt molecules could possibly diffuse through the membrane under swelling conditions, which led to the lower salt rejection of only 95.5%. With increasing silica content, the degree of crosslinking increased and the membrane structure became more compact. Consequently, the salt rejection increased to nearly 100%.

As the silica content increased, salt rejection increased due to an increase of the degree of crosslinking. It was expected the water flux would consequently decrease due to lower sorption selectivity for water resulting from the increased hydrophobicity (Table 4-3) upon depletion of hydrophilic hydroxyl groups. However, it was noted that water flux increased

for PVA/MA/silica membrane containing 10% SiO_2 (Figure 4-9). This may be attributed to size effect of silica nanoparticles dispersed in the polymer matrix. The incorporation of silica particles in the polymer chain at the nano-scale may disrupt the polymer chain packing and increase free volume, therefore leading to an increase in water flux. A defining feature of polymer nanocomposites is that the small size of the inorganic fillers leads to a dramatic increase in interfacial area as compared with traditional composites. This interfacial area creates a significant volume fraction of interfacial polymer with properties different from the bulk polymer even at low loadings (Balazs *et al.* 2006). This is especially important for enhancing the permeation property of membranes in water separation applications.

Positron annihilation lifetime spectroscopy (PALS) has emerged as an advanced and relatively new approach to investigate the size and size distribution of free volume elements in polymers (Tung *et al.* 2009, Dong *et al.* 2008). It can provide an atomic scale probe of the free volume in polymers. This method is based on the measurement of positron lifetime and lifetime intensity in a material. The free volume model applied to PALS data interpret the lifetime and orthoPositronium (oPs) located in inter- and intra-molecular spaces as a measure of the size of those spaces. Typical oPs lifetimes in polymers range from 1 to 3 ns corresponding to free volume cavity diameters ranging from 0.3 to 0.7 nm. The annihilation of positrons in a polymer occurs via several pathways. One of the pathways, based on o-Ps in the triplet spin state, is typically sensitive to free volume elements in a polymer, including their size (characterised by o-Ps lifetime τ_3) and concentration (characterised by intensity I_3), respectively (Dong *et al.* 2008).

Table 4-4 lists the PALS and Fractional Free Volume (FFV) results of various membrane samples used in the study. As can be seen, when maleic acid was introduced into the network, FFV decreased significantly from 1.8 nm^3 for PVA sample to 0.7 nm^3 for PVA/MA sample. This could be due to the crosslinking reaction between PVA and MA disrupting the PVA polymer chain packing and adjusting the size and number of free volume cavities. However, it was noted there was no further reduction in FFV when silica was introduced into the network. In fact, compared with PVA/MA sample, the FFV for PVA/MA/silica membrane containing 10 wt% silica actually increased from 0.7 to 0.9 nm^3. This confirmed the incorporation of inorganic silica nanoparticles did have positive impact on free volume. Previous study by Peng *et al.* (2006a) also demonstrated that introducing inorganic silica derived from γ-(glycidyloxypropyl)trimethoxysilane (GPTMS) into PVA

70

increased free volume and simultaneously enhanced both permeation flux and separation factor in pervaporation of benzene/cyclohexane mixtures. In their study, they also reported that the remarkable increase in free volume cavity was only observed at the lower GPTMS content. Further increase of GPTMS content had no enhancing effect on free volume and the small free volume cavity radius even decreased when the weight ratio of GPTMS/PVA was increased from 0.2 to 1.2. As a consequence, the permeate flux increased at first and then decreased with increasing GPTMS content (Peng *et al.* 2006a). This is consistent with our current finding. The water flux increased first when silica content was increased from 0 to 10 wt% but then decreased when the silica content was increased further to 25 wt%. This could be due to further increases of the silica content from 10 to 25 wt% reducing the free volume (Table 4-4). In addition, the increased hydrophobicity (Table 4-3) of membrane would result in reduced sorption of water, thereby reducing the diffusion rate. Therefore, the water flux decreased.

Table 4- 4: PALS results and fractional free volume of membranes.

Sample	τ_3(ns) ± 0.01	I_3(%) ± 0.2	R_{FVE}(nm) ± 0.002	V_F(nm³) ± 0.001	FFV(nm³) ± 0.02
PVA	1.916	20.0	0.278	0.090	1.8
PVA, 20%MA	1.759	9.77	0.262	0.075	0.7
PVA, 20%MA, 10%SiO$_2$	1.772	11.7	0.264	0.077	0.9
PVA, 20%MA, 25%SiO$_2$	1.799	9.2	0.266	0.079	0.7

The apparent diffusion coefficients of water through various PVA based hybrid membranes are shown in Table 4-5. It was noted that the diffusion coefficients of water increased first with the addition of silica and then decreased with further increase of silica content. The PVA/MA/silica membrane containing 20 wt% MA and 10 wt% silica had a highest diffusion coefficient of 7.67 x10^{-12} m^2/s. It is known the diffusivity is generally dependent on both the size of the penetrant and the polymer structure (Villaluenga *et al.* 2004). As water has a very small molecular size (0.278 nm), diffusion of water through membrane is determined by the nanostructure of the membrane. PVA is a semicrystalline polymer. The

crystalline region is impermeable to the water. This reduces the chain mobility and increases the path length of diffusion. When MA and silica are introduced into the polymer matrix, the amorphous character of the membrane increases due to crosslinking among PVA, MA and TEOS. This leads to an increase in both number and size of free volume elements (Table 4-4) and consequently, results in the increase in diffusion of water molecules when silica content was increased from 0 to 10%. Further increasing silica content from 10 to 25% leads the polymer chains becoming less mobile due to the increased crosslinking density and reduced swelling (Table 4-2). As a result, number of free volume elements (I_3) and fractional free volume (FFV) decreases (Table 4-4), thereby leading to a reduced diffusion rate.

Table 4- 5: Apparent diffusion coefficient of water for PVA based hybrid membranes.

Sample details	Diffusion coefficient ($10^{-12} m^2/s$)
PVA, 20%MA, 0% SiO$_2$	5.97
PVA, 20%MA, 10%SiO$_2$	7.67
PVA, 20%MA, 25%SiO$_2$	5.08

4.4   Summary

A new type of PVA/MA/silica hybrid membranes has been synthesised via a sol-gel route and a solution casting method. Tetraethoxy-silane (TEOS) was used as the silica precursor for sol-gel reaction and MA was added as an additional crosslinking agent. The prepared membrane samples were annealed at 140°C for 2 hr to complete the polycondensation reaction of TEOS and the esterification between PVA and MA. FTIR results confirmed the crosslinking among PVA, MA and TEOS. The crystallinity of hybrid membranes decreased as evidenced by WAXD, leading to a more compact membrane nanostructure with increasing amorphous character. TEM images indicated that silica nanoparticles were uniformly dispersed at less than 10 nm scales in the polymer matrix. The thermal properties of the hybrid membranes were significantly enhanced with increased T_g and decomposition temperature when compared with pure PVA membrane. Water uptake measurement of

membranes confirmed that the swelling of hybrid membranes in water was greatly suppressed.

Pervaporation testing results on separating aqueous NaCl solution demonstrated a potential application of this type of hybrid membrane for desalination. A high flux of 6.9 kg/m^2·hr and salt rejection above 99.5% were achieved at a 6 Torr vacuum and 21°C for the hybrid PVA/MA/silica membrane containing 5 wt% MA and 10% silica. The hydrophilic nature of hybrid membranes provides a strong driving force for water affinity and its sorption, consequently water is preferentially dissolved and transported through the membranes. Incorporation of silica nanoparticles into the polymer matrix enhanced the free volume of the membrane and diffusion of water molecule through the membrane, thus enhanced both water flux and salt rejection. However, there is an optimum silica content for achieving the best pervaporation performance. The PVA/MA/silica membrane containing 20 wt% MA and 10 wt% silica had the highest water diffusion coefficient of 7.67 x10^{-12} m^2/s and the highest salt rejection. The effect of membrane thickness on water flux followed the solution-diffusion model, as the flux was proportional to the inverse of the membrane thickness. The salt rejection remained high with varying membrane thickness due to its non-volatile nature. Diffusion through the membrane was found to be the rate-limiting step in desalination by pervaporation process for the hybrid membranes considered.

Chapter 5

Effect of Heat Treatment on Pervaporation Performance of Hybrid PVA/MA/Silica Membrane

5.1 Introduction

It is well known that heat treatment is an important step in controlling the structural morphology and swelling of the membranes which is central to the separation performance of the hybrid organic-inorganic membranes (Peng *et al.* 2006). For example, Ye *et al.* (2007) studied the annealing condition of PVA/PEG/TEOS membranes for pervaporation separation of an ethanol-water mixture. Increasing the heating temperature or time made the water permselectivity increase and the permeation flux decrease. Uragami *et al.* (2002) prepared PVA/TEOS membranes for the pervaporation of aqueous ethanol, with the aim of minimising the swelling of the PVA. Heat treatment was needed to complete the condensation reaction that introduced bridging. The water permselectivity in the hybrid membrane increased significantly with annealing temperature and time. It was postulated that the crosslinking reaction took place in the non-crystalline parts of the PVA membrane, forming denser non-crystalline regions. The importance of heat treatment was also reported by Peng *et al.* (2006) on pervaporation properties of hybrid PVA/γ-GPTMS membranes for separation of benzene/cycloheane mixtures. With increasing annealing temperature and time, the permeation flux of benzene decreased and the separation factor towards benzene increased, which was ascribed to the changed free volume under different heat treatment conditions.

In chapter 4, we have demonstrated that a new type of hybrid organic-inorganic membrane could be fabricated via a sol-gel route based on PVA, MA and TEOS. The hybrid membrane showed significantly improved thermal properties and swelling supression. Incorporation of silica nanoparticles into the polymer matrix disrupted the polymer chains and enhanced the diffusion of water molecules through the membrane and consequently enhanced both the

water flux and the salt rejection. Its performance for desalination of aqueous salt solution was demonstrated and a high flux of 6.9 kg/m^2·hr and salt rejection up to 99.9% at room temperature and a 6 Torr vacuum were achieved.

This chapter presents the effect of heat treatment of hybrid PVA/MA/silica membranes on their pervaporation performance. In this study, the synthesised hybrid PVA/MA/TEOS membranes were subjected to various heat treatment conditions including different heating temperatures and heating times. Effects of heating temperature and heating time on pervaporation separation performance of aqueous salt solution was studied in relation to swelling and hydrophilic properties, the free volume characteristics, salt transport properties, and membrane water diffusivity. The free volume of the hybrid membrane under different heat treatment conditions was characterised by Positron Annihilation Lifetime Spectroscopy (PALS) and were correlated with the pervaporation test results. In addition, the overall mass transfer of the hybrid membrane was also investigated based on the solution-diffusion model.

5.2   Membranes

The hybrid PVA/MA/silica membrane containing 5 wt% MA and 10 wt% silica was used in this study. Table 5-1 lists a summary of various heat treatment conditions. An un-heated sample was also prepared for comparison.

Table 5- 1: Summary of the membrane heat treatment conditions used in the study.

Sample	Heating temperature, °C	Heating time, hr
PVA, 5%MA, 10%silica	21	0
PVA, 5%MA, 10%silica	100	2
PVA, 5%MA, 10%silica	120	2
PVA, 5%MA, 10%silica	140	2
PVA, 5%MA, 10%silica	160	2
PVA, 5%MA, 10%silica	140	2
PVA, 5%MA, 10%silica	140	5
PVA, 5%MA, 10%silica	140	16
PVA, 5%MA, 10%silica	140	24

5.3   Results and discussion

5.3.1   Swelling behaviour and contact angle analysis

The swelling behaviour of membranes is generally described by the water uptake results. Figure 5-1 shows the effect of heating temperature on water uptake and hydrophilic properties of PVA/MA/TEOS hybrid membranes. The heating time was kept constant at 2 h and the heating temperature was increased from room temperature (21°C) to 160°C. When compared with the un-heated membrane, heat treatment had a significant effect on water uptake. The water uptake decreased significantly from 154 to 43wt% when the temperature was increased from 21 to 100°C and then gradually decreased to 22 wt% when the temperature was further increased to 160°C. As mentioned in chapter 4, in fabricating the hybrid PVA/MA/silica membranes, the hydroxyl groups in the repeating units of PVA and the carboxylic groups in MA were shown to produce strong secondary interactions with the residual silanol groups generated from acid catalysed hydrolysis and polycondensation of TEOS to form hydrogen and covalent bonds. In addition, PVA and MA went through an esterification reaction via grafting or crosslinking under heat treatment to form ester groups.

As a result, the hybrid PVA/MA/silica membranes formed a compact structure with network crosslinking due to above mentioned reactions among PVA, MA and TEOS. As the heating temperature increased, it was expected that the crosslinking degree in the hybrid membrane would increase. In addition, polycondensation of silanol groups resulting from hydrolysis of TEOS was also favoured upon heating. Therefore, the swelling was suppressed.

The effect of heating temperature on the hydrophilic properties of hybrid membrane is less straight forward although the hybrid membrane remained hydrophilic upon the change of heating temperature. At heating temperatures less than 140°C, the water contact angle remained almost unchanged at about 45°. This could be explained by the contribution of hydrophilic –OH groups from silanol that resulted from hydrolysis reactions of TEOS and -COOH group from MA. At lower heating temperatures, the crosslinking reaction among PVA, MA and TEOS, and the polycondensation of TEOS may be incomplete. This will result in many free –OH and –COOH functional groups which contribute to the hydrophilic properties of membranes. As the heating temperature was further increased to 160°C, there was a significant increase in water contact angle, indicating that the hybrid membrane became less hydrophilic at the higher heating temperature. This could be due to the fact that crosslinking reactions among PVA, MA and TEOS, and the polycondensation of TEOS, were more complete at higher temperatures. This will lead to consumption of hydrophilic groups, consequently increasing the hydrophobicity of the membrane.
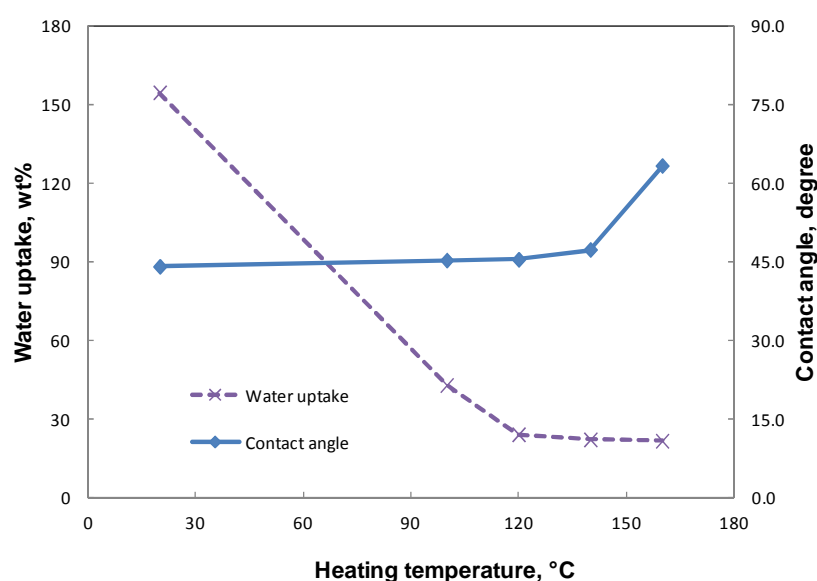
Figure 5- 1: Effect of heating temperature on water uptake and contact angle (heating time: 2 hours).

Figure 5-2 shows the effect of heating time on water uptake and hydrophilic properties of PVA/MA/TEOS hybrid membranes at a heating temperature 140°C. Compared with un-heated membranes, the water uptake decreased sharply from 154 to 24 wt% when the membrane was heat treated for 2 h. Further increase of heating time from 2 to 16 h only had a marginal effect on the swelling properties of the membrane.

Unlike heating temperature, the heating time has more effect on the hydrophilic properties of the membrane. Although the membrane remained hydrophilic following the various heating period, the water contact angle increased gradually with increasing treatment time due to the increased extent of crosslinking and polycondensation of TEOS. This indicates that long heating time favours completion of the crosslinking reaction among PVA, MA and TEOS, and polycondensation of TEOS.
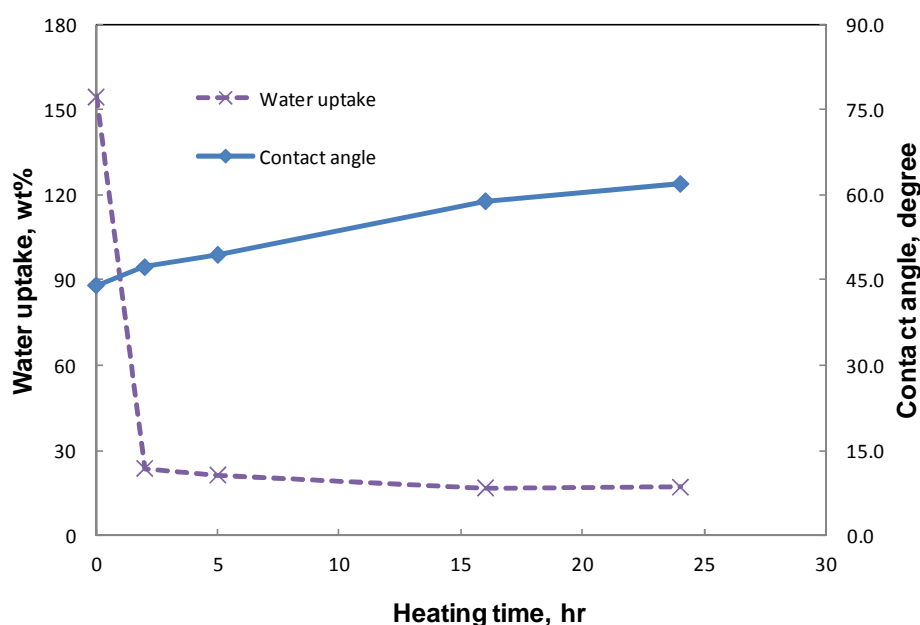
Figure 5- 2: Effect of heating time on water uptake and contact angle (heating temperature: 140°C).

5.3.2   *Free volume analysis*

As mentioned in chapter 4, incorporation of silica nanoparticles leads an increase in interfacial area and consequently creates a significant volume faction of interfacial polymer with properties different from the bulk polymer. This resulting FFV change enhanced the permeation properties of hybrid PVA/MA/silica membrane for water separation. In this

study, the free volume of this hybrid membrane which has been heat treated under various conditions was analysed in wet condition as it closely represents the operating condition of membranes used in pervaporation testing for desalination applications. It is of most interest to understand how the PALS parameters change upon wetting and how the free volume correlates with the transport properties of hybrid membranes upon heating.

Table 5-2 shows PALS results of wet hybrid PVA/MA/TEOS membranes including o-Ps lifetime (τ_3) and intensity (I_3), average radius (R_{FVE}), volume of the free volume elements (V_F) and fractional free volume (FFV) as a function of heat treatment conditions. The average radius (R_{FVE}), volume of the free volume elements (V_F) and fractional free volume (FFV) were estimated from equation 3-6, 3-7 and 3-8 respectively. As can be seen, the average radius R_{FVE} (~0.27-0.28 nm) are typical network pores which are in the range of 0.1-0.3 nm and represents the small cavities between polymer chains constituting the polymer aggregates. There was a slight decrease in the size of network pores (R_{FVE}) and the average volume of the free volume elements (V_F) upon more severe heat treatment conditions. In addition, concentration of the free volume elements as characterised by intensity I_3 decreased significantly upon heating. Consequently, the fractional free volume FFV which is characterised by the product of V_f and I_3 changed significantly upon heat treatment. Generally, the fractional free volume decreased with either increasing heating temperature or heating time, indicating changes in the microstrcuture of the hybrid membrane upon heating. At low heating temperatures or short heating times, the crosslinking reaction among PVA, MA and TEOS including the polycondensation of TEOS may be incomplete. Upon increasing heating temperature or extending heating time, the crosslinking reaction and the polycondensation reaction of TEOS proceed towards complete reaction. This could disrupt the PVA polymer chain packing and accordingly reduce the size and concentration of free volume cavities, in particular the concentration of free volume cavities. As a result, the fractional free volume decreases.

Table 5- 2: PALS results of wet hybrid membrane at different heat treatment conditions.

Heating temperature, °C	τ_3(ns) ± 0.03	I_3(%) ± 0.3	R_{FVE}(nm) ± 0.002	V_F(nm³) ± 0.008	FFV ± 0.03
Un-heated	1.925	19.5	0.278	0.090	1.77
100	1.947	18.9	0.280	0.092	1.75
120	1.925	17.8	0.278	0.090	1.61
140	1.910	17.0	0.277	0.089	1.52
160	1.875	14.9	0.274	0.086	1.26
Heating time, H	τ_3(ns) ± 0.03	I_3(%) ± 0.3	R_{FVE}(nm) ± 0.002	V_F(nm³) ± 0.008	FFV ± 0.3
Un-heated	1.925	19.5	0.278	0.090	1.77
2	1.910	17.0	0.277	0.089	1.52
5	1.876	15.4	0.274	0.086	1.32
16	1.878	14.3	0.274	0.086	1.23
24	1.872	13.2	0.273	0.086	1.13

It is also noted that the average radius (R_{FVE}) of the free volume elements (~0.27-0.28 nm) is bigger than the radius of water molecules (0.14 nm) (Franks 2000) but smaller than the radius of the first hydration shell of sodium ions (0.34 nm) and chloride ions (0.38 nm) (Jardón-Valadez and Costas 2004). This assists in understanding how high salt rejection is achieved by the hybrid PVA/MA/silica membrane, as the pores are large enough to pass water molecules but too small to allow salt to pass.

5.3.3   Salt transport properties

The kinetic desorption method is well established for characterising the salt transport properties of polymer membranes (Ju *et al.* 2010, Lonsdale *et al.* 1965, Yasuda *et al.* 1968b, Sagle *et al.* 2009). A typical NaCl desorption curve from the kinetic desorption experiments is shown in Figure 5-3 by plotting (M_t/M_∞) versus $t^{1/2}$. Similar to the study of

PEG-based hydrogel membrane coating by Ju *et al.*, the NaCl diffusion coefficient, D_s, for each membrane was calculated from the slope of the linear portion of the desorption curve using Equation 3-2 (Ju *et al.* 2010).
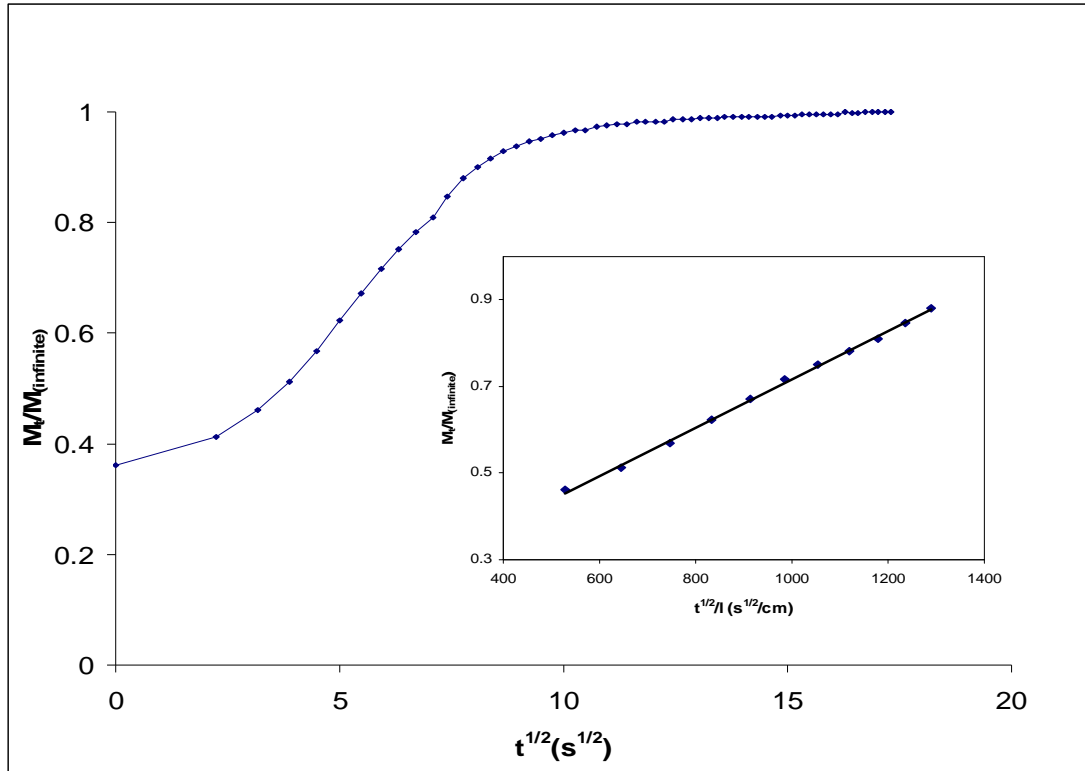
Figure 5- 3: Typical NaCl desorption curve for PVA/MA/silica membranes (membrane containing 5 wt% MA and 10 wt% silica).

Table 5-3 presents the salt transport properties of hybrid membranes as a function of heat treatment conditions. NaCl solubility decreased with increasing heating temperature or time. The results agree well with the water uptake data (Figure 5-1& 5-2). In theory, no salt (NaCl) is expected to dissolve in a pure polymer matrix, so any NaCl in the membrane phase is assumed to be solvated by the water within the membrane (Yasuda *et al.* 1968b). Therefore, the amount of NaCl in the membrane will be closely connected to the amount of water in the membrane. With increasing heating temperature or time, the swelling degree in the membrane decreases, and as a result, there is a tendency to accommodate less NaCl along with water in the membrane.

Table 5- 3: Transport properties of NaCl as a function of heat treatment conditions.

Heat treatment temperature, °C (2 hours)	NaCl diffusivity ($x10^6$ cm^2/s)	NaCl solubility (dimensionless)	NaCl permeability ($x10^6$ cm^2/s)
Unheated	4.96	1.93	9.54
100	2.88	1.82	5.23
120	2.32	1.74	4.03
140	1.91	0.99	1.90
160	1.04	0.67	0.70
Heat treatment time, hour (140˚C)	NaCl diffusivity ($x10^6$ cm^2/s)	NaCl solubility (dimensionless)	NaCl permeability ($x10^6$ cm^2/s)
Unheated	4.96	1.93	9.54
2	1.91	0.99	1.90
5	1.21	0.97	1.17
16	0.70	0.74	0.52
24	0.45	0.43	0.19

It is worth mentioning that the diffusion coefficients of NaCl in the study were in the range of 0.45-4.96x10^{-6} cm^2/s. These are significantly lower than the diffusion coefficient of NaCl in pure water, 1.47x10^{-5} cm^2/s (Yasuda *et al.* 1968b). As explained by Yasuda *et al.*, this could be due to the effect of concentration polarisation at the interface of the membrane sample and the extraction water during the desorption measurement (Yasuda *et al.* 1968). A similar finding was also reported by Ju *et al.* (2010) in a study of crosslinked poly(ethylene oxide) hydrogels, and they reported NaCl diffusivities in a similar range of 0.3 to 4.4x10^{-6} cm^2/s.

Compared with the un-heated membrane, both NaCl diffusivity and permeability decreased significantly upon heating. With increasing heating temperature or time, NaCl diffusivity and permeability decreased due to the changes in free volume resulting from the increased crosslinking degree upon heating. Figure 5-4 shows NaCl permeability as a function of free volume under different heat treatment conditions. NaCl permeability data correlated well with the free volume. In general, NaCl permeability increased exponentially with increasing fractional free volume, suggesting the salt transport properties of the membrane is strongly influenced by the microstructure of the hybrid membrane.
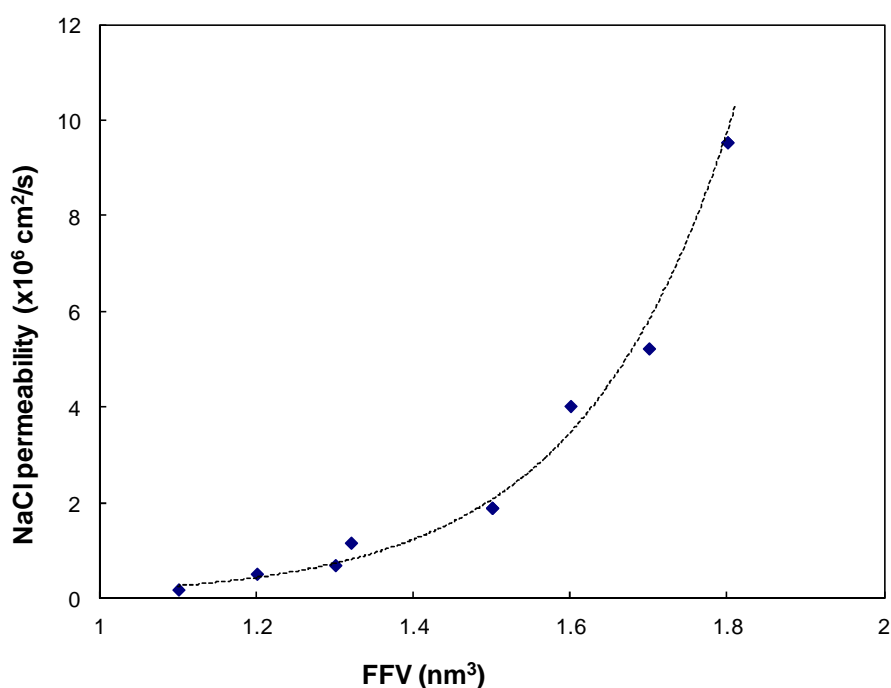
Figure 5- 4: NaCl permeability versus fractional free volume (FFV) of hybrid PVA/MA/silica membrane (membrane containing 5 wt% MA and 10 wt% silica).

5.3.4 *Pervaporation testing*

Figure 5-5 and 5-6 show the effect of heating temperature and time on pervaporation separation performance of aqueous salt solution through hybrid PVA/MA/TEOS membranes at a feed temperature of 21°C and a vacuum of 6 Torr, respectively.
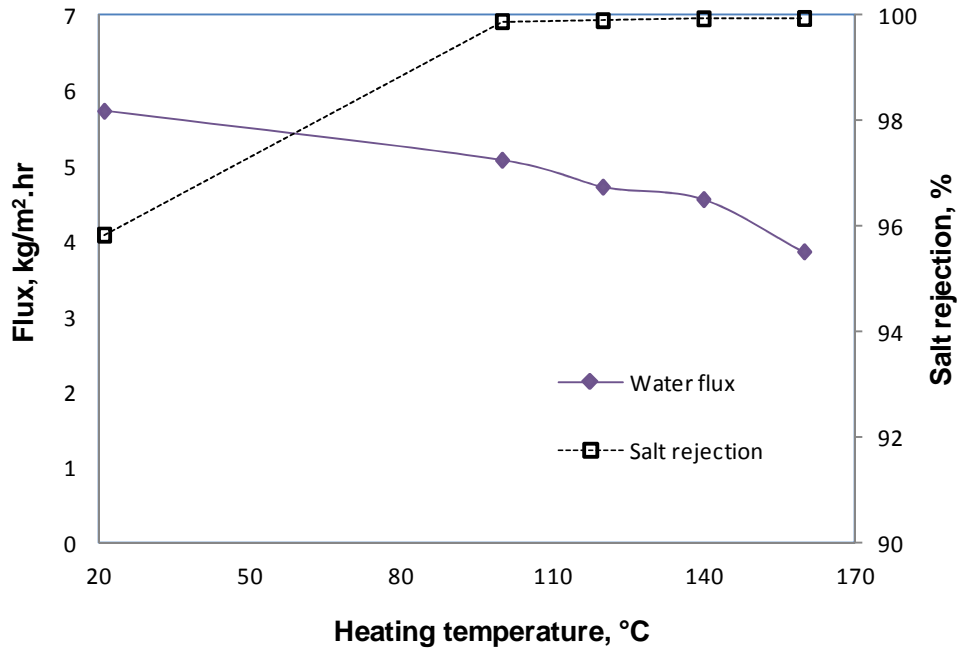
Figure 5- 5: Effect of heating temperature on water flux and salt rejection (heating time 2 hours, membrane thickness 10 µm, feed temperature 21°C, feed flowrate 30 mL/min, vacuum 6 Torr).
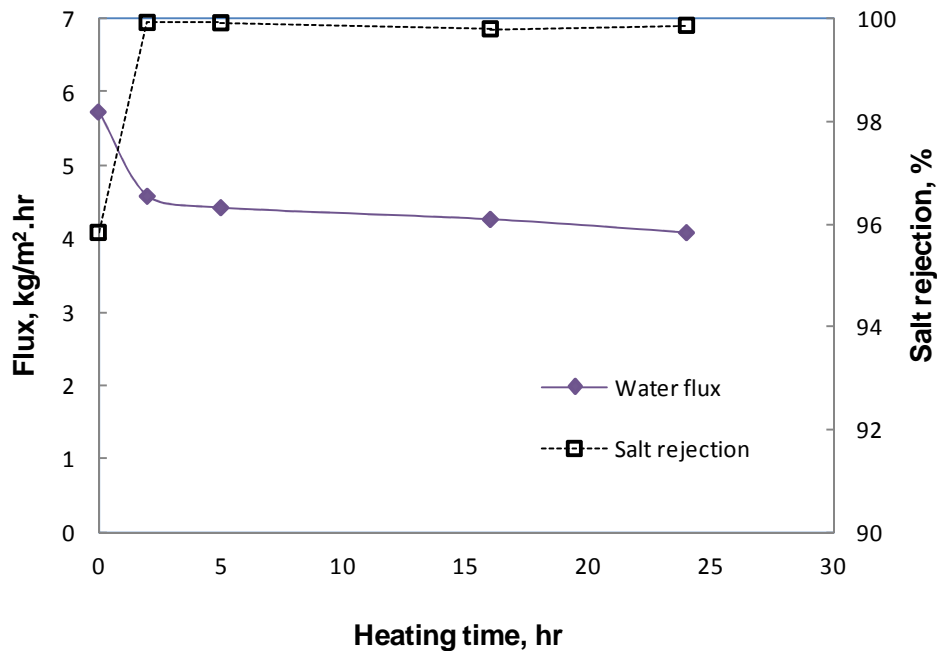
Figure 5- 6: Effect of heating time on water flux and salt rejection at 140˚C. (Membrane thickness 10 µm, feed temperature 21°C, feed flowrate 30 mL/min, vacuum 6 Torr).

The water flux generally decreased with increasing heating temperature and time. This could be explained by the solution-diffusion model and free volume theory. Based on the solution-diffusion model, there are three steps in the pervaporation transport mechanism: sorption at the membrane surface, diffusion through the dense membrane and desorption into the vacuum (Heintz and Stephan 1994). As mentioned in chapter 4, under the high vacuum used in the study, the desorption step on the permeate side of the membrane is believed to be a fast step. Either sorption at the membrane surface or diffusion through membrane is the more likely controlling step. In the solution step, the sorption selectivity is more dependent on the affinity between the membrane and the permeants (Uragami *et al.* 2002). Increasing heating temperature or time will increase the degree of crosslinking among PVA, MA and TEOS, and consequently increased the hydrophobicity of hybrid membranes upon depletion of hydrophilic –OH and -COOH groups (Fig. 5-1 and 5-2). The increased hydrophobicity will result in less sorption of water at the membrane surface with significantly decreased water solubility (Table 5-4). Therefore, the sorption of water at the membrane surface will be significantly decreased. This would reduce numbe of water molecules available for diffusion through the membrane. In the diffusion step, the transport of molecules through the dense membrane is limited by the fractional free volume available in the membrane. At higher fractional free volumes, more water could be accommodated and consequenly diffused through the membrane. As explained earlier, increasing heating temperature or time will change the microstructure of PVA/MA/TEOS membrane and consequently affect the free volume of the membrane. In general, increasing heating temperature or time leads to a more compact structure with decreased fractional free volume (Table 5-2) and reduced swelling (Fig. 5-1 and 5-2). This would result in less accommodation for water in the membrane during the diffusion step. Combining the effect of less water sorption on the membrane surface during the sorption step and less fraction free volume in the membrane for diffusion upon heating, the water flux decreased.

Figure 5-7 shows the relationship of water flux versus fractional free volume. There was a linear dependency of water flux on the fractional free volume. As the fractional free volume increased, the water flux increased. Similar results were reported by Peng *et al.* (2006b) for pervaporation properties of PVA-GPTMS hybrid membrane through PALS. With increasing heating temperature and time, the permeation flux of benzene decreased and separation factor towards benzene increased. This was ascribed to the suitable adjustment of size and

number of network pores and aggregate pores, and fractional free volume under different heating temperatures and times.
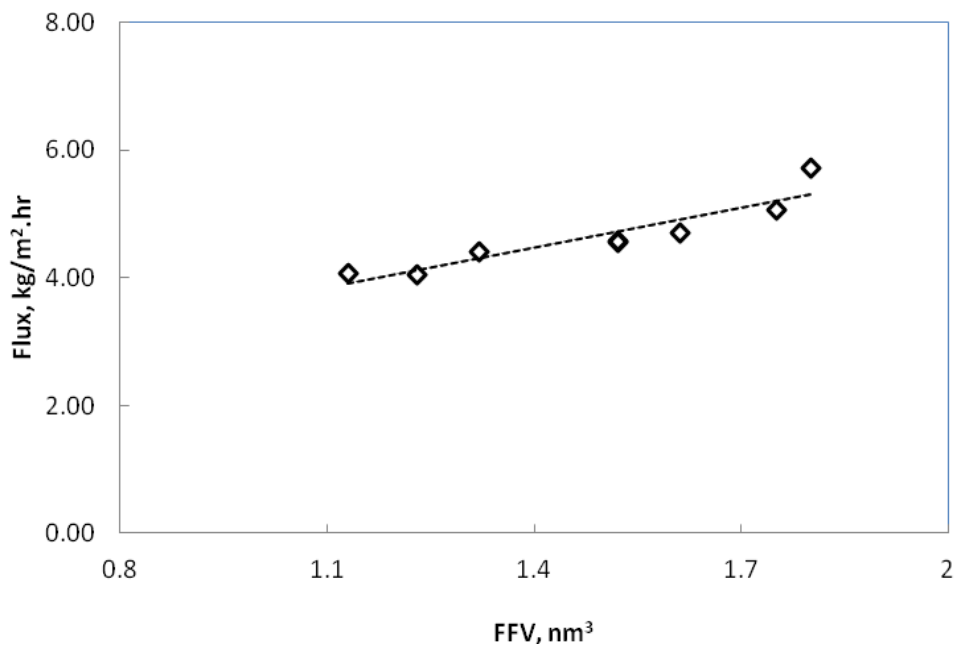

Figure 5- 7: The water flux versus the fractional free volume (FFV) of hybrid PVA/MA/silica membranes (membrane containing 5 wt% MA and 10 wt% silica).

Based on the solution-diffusion model, there are three mass transfer resistances which exist on the feed side, the membrane and the permeate side. Under the high vacuum used in this study, the resistance to mass transport at the permeate side of the membrane was eliminated. Thus, the overall mass transfer resistance could be controlled by either the feed side boundary layer or by the membrane itself (Khayet *et al.* 2008, Gronda *et al.* 2000). Table 5-4 lists the global mass transfer coefficients and water transport properties of hybrid PVA/MA/TEOS membrane at different heat treatment conditions. The diffusion coefficient of water and the global mass transfer coefficient were estimated using Equations 3-5 and 3-6 while the water solubility was estimated using Equation 2-1. As expected, both global mass transfer coefficients and water diffusivity generally decreased with increasing heating temperature or heating time.

Table 5- 4: Global mass transfer coefficients and water transport properties of hybrid membranes as a function of heat treatment conditions (membrane containing 5 wt% MA and 10 wt% silica).

Heat treatment temp, °C (2 hours)	Kov (x10⁻⁹ m/s)	Water solubility (dimensionless)	Water diffusivity (x10⁻⁷ cm²/s)
Un-heated	3.35	382	1.59
100	3.24	105	1.41
120	2.95	58	1.30
140	2.93	54	1.27
160	2.38	49	1.11
Heat treatment time, hour (140°C)	Average Kov (x10⁻⁹ m/s)	Water solubility (dimensionless)	Water diffusivity (x10⁻⁷ cm²/s)
Un-heated	3.35	382	1.59
2	2.93	58	1.27
5	2.75	52	1.21
16	2.65	41	1.19
24	2.54	40	1.14

Yasuda *et al.* (1968b) have proposed that the free volume theory of diffusion to interpret the water and salt diffusion through hydrogel. Based on Yasuda's version of free volume theory, water or salt diffusion coefficients vary exponentially as the reciprocal free volume varies. Figure 5-8 shows the NaCl and water diffusivity as a function of fractional free volume. As can be seen, both water and NaCl difusivity increased exponentially with decreasing 1/FFV. When 1/FFV increased from 0.54 to 0.91, water diffusivity decreased about 30% while NaCl diffusivity decreased about 10 times. This indicates that changing free volume has more pronounced effect on changing NaCl diffusivity than water diffusivity. Similar finding was also reported by Ju et al (2010). These results agrees well with the free volume theory: the transport properties of the larger penetrant is more sensitive to changes in free volume

than those of smaller penetrant. In our study, hydrated NaCl is the larger penetrant and water is the smaller penetrant. Therefore, it is expecting that increasing free volume will increase the water flux but decrease water/NaCl selectivity (i.e., salt rejection).
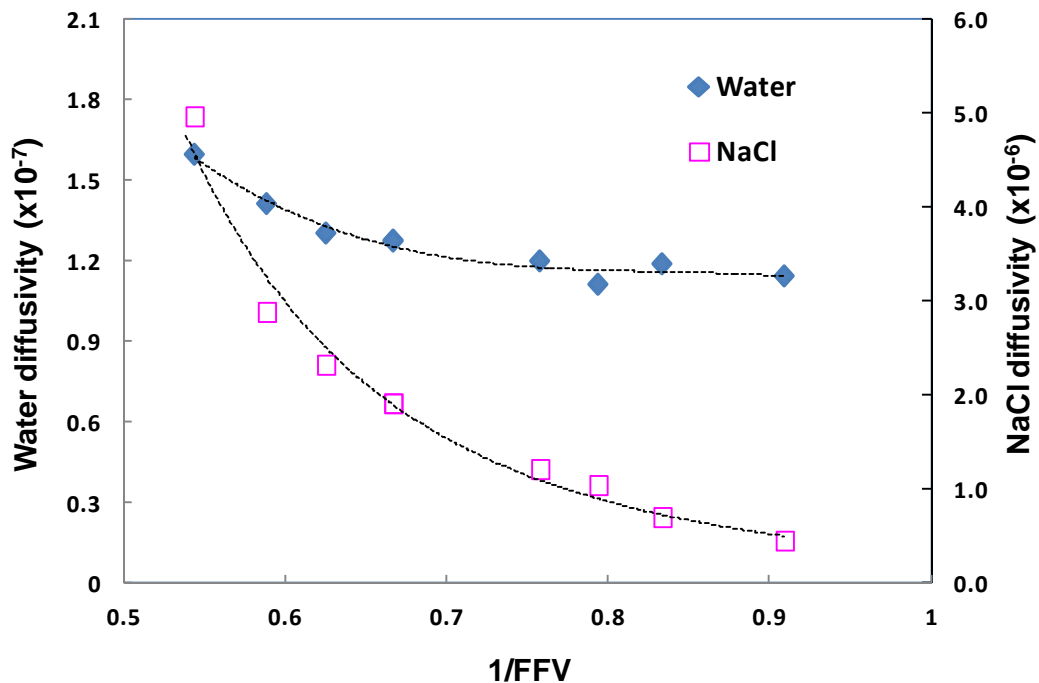
Figure 5- 8: NaCl and water diffusivity of hybrid PVA/MA/silica membranes as a function of 1/FFV (membrane containing 5 wt% MA and 10 wt% silica).

Figure 5-9 shows the relationship of global mass transfer coefficients versus the fractional free volume. Similar to the water flux, the global mass transfer coefficients were also closely related to the fractional free volumes. The trend in change of the global mass transfer coefficient is consistent with the trend in the water flux. With fractional free volume increasing, the mass transfer increases. As the free volume is directly related to the diffusion of molecules through the membrane, this close correlation of pervaporation properties of membrane and fractional free volumes confirms that the diffusion through membrane is the most likely controlling step of the pervaporation separation of aqueous salt solution.
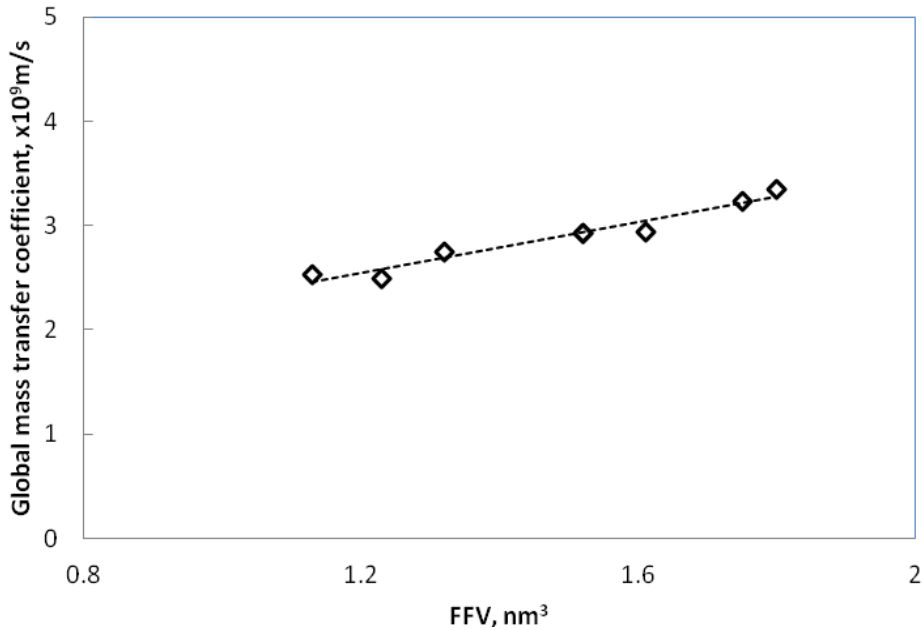
Figure 5- 9: Global mass transfer coefficient versus fractional free volume (FFV) of hybrid PVA/MA/silica membranes (membrane containing 5 wt% MA and 10 wt% silica).

Except for the un-heated membrane, the salt rejection remained at >99.5% with either increased heating temperature or heating time (Fig. 5-5 and 5-6). This was mainly due to the non-volatile nature of NaCl and the rigid structure of hybrid membranes resulting from crosslinking among PVA, MA and TEOS (Xie *et al.* 2010). According to the solution-diffusion model, the sorption selectivity is more dependent on the affinity between the membrane and the permeants in the solution step. Due to the hydrophilic nature of hybrid membranes used in this study (Fig. 5-1 and 5-2) and very dilute solution (0.2 wt% NaCl concentration), the water molecules were preferentially diffused and permeated into the membranes. This is supported by the low NaCl solubility (Table 5-3) and high water solutibility (Table 5-5) results obtained from the transport study of hybrid membranes. Water solubility was generally 2 magnitudes higher than NaCl solubility, e.g, for un-heated membrane, water solubility was 382 while NaCl solubity was only 1.9. The relatively low salt rejection (95.9%) of un-heated membrane could be explained by the high swelling of the membrane. Without heat treatment, the crosslinking reactions among PVA, MA and TEOS, and also the polycondensation of TEOS are most likely incomplete. Especially, the esterification reactions between PVA and MA in the aqueous phase is generally favoured under heating. As a result, membrane tended to swell due to the less rigid structure. This

resulted in bigger FFV due to higher concentration of free volume size elements (Table 5-2). Consequently, some hydrated NaCl was solvated by the water in the membrane. Therefore, the salt rejection was lower. Introducing heat treatment to the hybrid membrane tended to form a more rigid structure. This resulted in a decrease in free volume size, consequently reduced FFV and swelling and increased the salt rejection.

5.4   Summary

In this study, the synthesised hybrid PVA/MA/silica membranes underwent different heat treatment conditions and were tested for pervaporation separation of aqueous salt solution. Heating temperature and heating time were found to strongly affect the microstructure and pervaporation performance of membranes. Increasing heating temperature or time favoured the completion of the crosslinking reaction among PVA, MA and TEOS, and also favoured the polycondensation reaction of TEOS. This resulted in a less hydrophilic membrane with reduced swelling due to the consumption of hydrophilic –OH groups of PVA and –COOH groups of MA during the crosslinking reactions. Increasing heating temperature or time changed the microstructure of PVA/MA/silica membrane. Free volume analysis by PALS indicated that both the size and concentration of free volume elements decreased, leading to an overall decrease in FFV upon heating.

Upon increasing heating temperature or time, the water flux reduced but the salt rejection increased. This was explained by the solution-diffusion mechanism and free volume theory. The increased hydrophobicity upon heating led to less sorption of water at the membrane surface due to significantly decreased water solubility in the sorption step. Moreover, the reduced free volume upon heating led to less accommodation of water in the diffusion step. Combined together, the water flux decreased with either increased heating temperature or time.

The transport properties of hybrid membranes upon heating were attributed to the free volume change characterised by PALS. Both NaCl and water diffusivity increased exponential with decreasing 1/FFV and changing free volume had a more pronounced effect on NaCl diffusivity than water diffusivity. This result agrees well with the free volume theory and indicates that a trade-off between water permeability and salt rejection was present for hybrid PVA/MA/silica membrane. It is believed that NaCl was solvated by the water in the membrane in the hydrate form. The average radius of the free volume elements (RFVE)

(~0.27-0.28 nm) was bigger than the radius of water molecules but smaller than that of the first hydration shell of sodium ions and chloride ions provides a strong evidence for the mechanism of high salt rejection achieved by the hybrid PVA/MA/silica membrane in this study. The increased salt rejection upon heating was attributed to a more rigid membrane structure with reduced free volume.

The close correlation among pervaporation properties (e.g., global mass transfer coefficients, water flux and salt rejection), transport properties (e.g., NaCl/water diffusivity and permability) and fractional free volume of the membrane confirmed that the diffusion through membrane is the controlling step of pervaporation separation of aqueous salt solution.

Chapter 6

Effect of Operating Conditions on Pervaporation Performance of Hybrid PVA/MA/Silica Membrane

6.1 Introduction

Pervaporation processes are able to separate mixtures in contact with a membrane via preferentially removing one component from the mixture due to its higher affinity with, and/or faster diffusion through the membrane. In order to ensure continuous mass transport, very low absolute pressures are usually maintained on the downstream side of the membrane, removing all molecules migrating to the surface, and thus rendering a concentration difference across the membrane (Shao and Huang 2007). The mechanism of mass transfer of liquids across non-porous polymeric membranes includes successive stages of sorption of a liquid and its diffusion through the free volume of the polymeric material (Kuznetsov *et al.* 2007).

It is well known that the pervaporation performance is not only dependent on the properties of membranes, but also the operation conditions such as feed concentration, temperature, permeate pressure and feed flowrate (Jiraratananon *et al.* 2002). For scale up, it is important to design and operate the system under optimum operating conditions to make the process more efficient and also economically viable.

This chapter presents a study of the effect of operating conditions on pervaporation separation performance of aqueous salt solutions. A synthesised hybrid PVA/MA/silica membrane containing 5 wt% MA and 10 wt% silica was tested for separation of aqueous salt solution by the pervaporation process at various salt concentrations and operating conditions. The activation energy of permeation was calculated from the Arrhenius relationship. The performance was discussed in relation to the diffusion coefficient of water to understand the fundamental transport mechanism within the membrane.

6.2 Materials

The hybrid PVA/MA/silica membrane used in this study contained 5 wt% MA and 10 wt% silica relative to PVA. The synthesis method and conditions has been detailed in Chapter 3. The synthesised membrane was heat treated 2 hours at 140°C prior to use.

6.3 Results and discussion

6.3.1 Salt rejection

The salt (NaCl) rejection remained high (about 99.9%) irrespective of variation in operating conditions. This is not surprising as NaCl is a non-volatile compound and it is unlikely to enter the vapour stream on the permeate side. This low volatility of NaCl will lead to high salt rejection in the pervaporation process. Varying operating conditions could have significant effect on the transmembrane concentration (driving force for mass transport of the pervaporation membrane) of water but not on salt. Therefore, the operating condition has little effect on the salt rejection. Secondly, according to the solution-diffusion model, the sorption selectivity is dependent on the affinity between the PVA and the permeants in the sorption step. As the hybrid PVA/MA/silica membrane used in the study is hydrophilic in nature (Figure 5-1) and the major component in the feed solution is water, the water molecules will be preferentially diffused and permeated into the membrane (Uragami *et al.* 2002). As a result, the salt rejection remained high. Thirdly, in our previous chapter, we have mentioned, for hybrid PVA/MA/silica membranes, the crosslinking among PVA, MA and silica resulted in a more rigid, compact structure. In particular, the incorporation of silica nanoparticles in the polymer chain may disrupt the polymer chain packing and therefore lead to reduced free volume radius and consequently a high salt rejection. In the following section, only effects of operating conditions on water flux are discussed.

6.3.2 Effect of feed concentration

Figure 6-1 shows the effect of salt concentration in the feed solution on separation performance of aqueous salt solution at various feed temperatures. At room temperature, salt concentration has negligible effect on water flux. At a higher temperatures (50°C), the water flux decreases with increasing salt concentration. This increase became more significant as the feed temperature was increased further to 65°C.
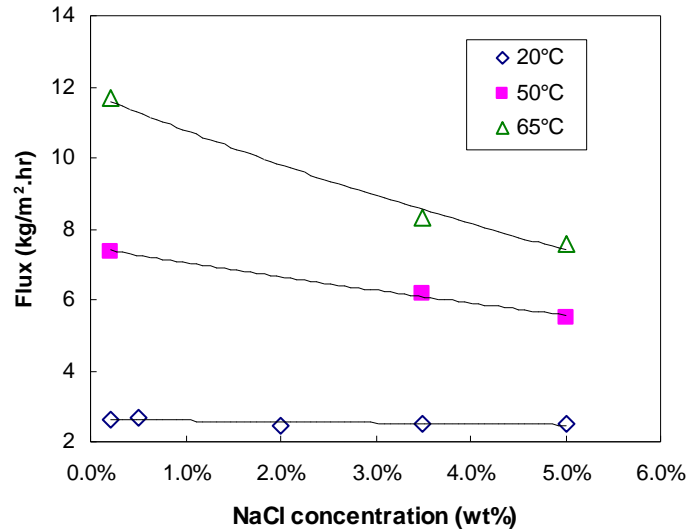
Figure 6- 1: Effect of feed concentration on water flux (membrane thickness 20 µm, feed flowrate 30 mL/min, vacuum 6 Torr)

Feed concentration is believed to directly affect the sorption of its components at the liquid/membrane interface (Jiraratananon *et al.* 2002). That is, the concentration of the components in the membrane tends to increase with its increase in the feed concentration. Since diffusion in the membrane is concentration dependant, the permeate flux generally increases with the bulk feed concentration. As the salt concentration increased from 0.2 wt% to 5.0 wt%, the water concentration decreased from 99.8 wt% to 95.0 wt%. At room temperature, this decrease in water concentration may not have any effect on diffusion within the membrane as the majority of the feed is water and there is no major difference of water vapour pressure in the water concentration range of 95.0-99.8%. It is expected that the diffusivity of the membrane towards water remained constant at room temperature. Therefore, there was no or negligible change on the flux. On the other hand, at higher temperatures, as the vapour pressure is exponentially related to the temperature, differences in bulk feed water concentration would have a pronounced effect on the water concentration in the membrane surface, and consequently affect the diffusivity and flux. Therefore, it is expected that, at the higher temperature, increasing salt concentration would lead to a decrease in diffusivity in the membrane due to the decreased water concentration. The trend in diffusion coefficients of water has been confirmed by the calculated apparent diffusivity results as shown in Table 6-1.

Table 6- 1: Apparent diffusion coefficients of water at various salt concentrations and feed temperatures.

Salt concentration	Diffusion coefficient of water (10^{-11} m^2/s)		
	20°C	50°C	65°C
0.2 wt%	1.45	4.09	6.51
3.0 wt%	1.45	3.56	4.78
5.0 wt%	1.47	3.22	4.42

6.3.3   Effect of feed velocity

Figure 6-2 shows the effect of the feed velocity on the pervaporation performance of the hybrid PVA/MA/silica membrane when the feed velocity varied from 0.01-0.05 m/s at a feed temperature of 21°C. It seems the feed velocity has little or negligible effect on the water flux. The water flux remained constant at around 2.5 kg/m^2·hr over the feed velocity range of 0.01-0.05 m/s.

Mass transfer in the liquid feed side may be limited by the extent of concentration polarisation. Generally an increase of feed flowrate reduces concentration polarisation and increases flux due to a reduction of transport resistance in liquid boundary layer (Jiraratananon *et al.* 2002). However, this positive effect is not observed in the study. In the studied feed velocity range (0.01 to 0.05 m/s), the corresponding Reynolds numbers in the membrane cell are 21-105, indicating that the flow is in the laminar flow regime. This implies that increasing feed velocity had little effect on the turbulence and fluid dynamics of the feed stream in the laminar flow region, and the mass transfer from the feed to the membrane was not a rate limiting step. Therefore, concentration polarisation was not a significant issue for these experiments.
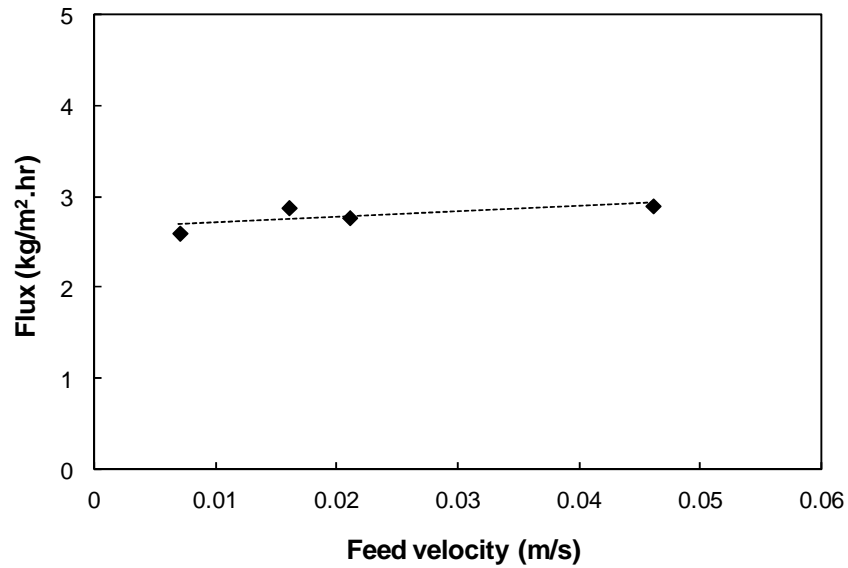
Figure 6- 2: Effect of feed velocity on water flux (membrane thickness 20 µm, feed temperature 21°C, vacuum 6 Torr)

Table 6-2 presents the diffusion coefficient of water at various feed velocity. The diffusion coefficient remained almost constant over the studied feed velocity range, again confirming that the rate of pervaporation was not affected by the feed velocity and therefore the transport of water to the membrane surface.

Table 6- 2: Apparent diffusion coefficients of water at various feed velocity (feed temperature 21°C, vacuum 6 Torr).

Feed flowrate (mL/min)	30	70	85	150
Feed velocity (m/s)	0.007	0.016	0.021	0.046
Diffusion coefficient of water (10^{-11} m^2/s)	1.46	1.60	1.54	1.61

6.3.4   *Effect of permeate pressure*

Permeate pressure is another important operating parameter as a high vacuum is directly related to a high energy cost. Theoretically, the maximum flux is achieved at zero absolute permeate pressure. Figure 6-3 shows the effect of permeate pressure on water flux. The water flux decreased as the permeate pressure increased. For pervaporation processes, the driving force of transmembrane concentration (ΔC) is provided by the vapour pressure

difference between the feed and permeate side of the membrane. With increasing permeate pressure (i.e. decreasing vacuum), as the feed side pressure remains unchanged, the transmembrane vapour pressure difference is reduced. This leads to a decreased transmembrane concentration (i.e. driving force) and consequently a decreased water flux (see equation 2-3).
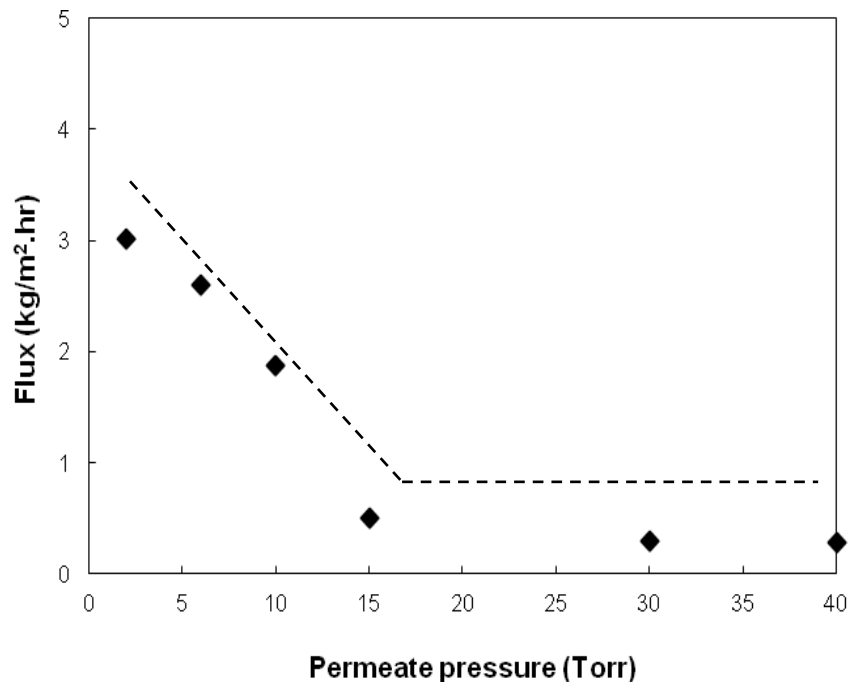
Figure 6- 3: Effect of vacuum on water flux (membrane thickness 20 µm, feed temperature 21°C, feed flowrate 30 mL/min)

It was observed that the water flux dropped down to less than 0.5 kg/m^2·hr when the permeate pressure increased to >15 Torr. At room temperature, the saturation vapour pressure of water is about 17 Torr (Shakhashiri 1992). When the permeate pressure is increased above 15 Torr, the driving force for water vaporisation approaches zero, leading to near zero net evaporation and consequently the low mass transport of water. Table 6-3 presents the diffusion coefficient of water at various permeate pressures. Decreasing diffusion coefficient with permeate pressure indicates that the permeation process is mainly controlled by diffusion through the hybrid membrane. As permeate pressure increased above 15 Torr, the diffusion coefficient dropped significantly, by nearly 90%, indicating the diffusion of water has been greatly reduced.

Table 6- 3: Apparent diffusion coefficients of water at various permeate pressure (feed temperature 21°C, feed flowrate 30 mL/min).

Permeate pressure (Torr)	2	6	10	15	30	40
ΔP between permeate pressure and saturation pressure (Torr)	-15	-11	-7	-2	13	23
Diffusion coefficient (10^{-11} m^2/s)	1.68	1.45	1.05	0.28	0.16	0.16

6.3.5   Effect of feed temperature

Figure 6-4 shows the effect of feed temperature on the desalination by pervaporation performance of hybrid PVA/MA/silica membrane at a feed flowrate of 30 mL/min and a vacuum 6 Torr. For all feed concentrations, there was an exponential increase of water flux when the feed temperature increased from 21°C to 65°C. A high water flux of 11.7 kg/m^2·hr was achieved at the feed temperature of 65°C. This is not surprising, as firstly, the driving force for the pervaporation process is the partial vapour pressure difference of permeant between the feed and permeate conditions. As the feed temperature increased, the water vapour pressure on the feed side increased exponentially. As the vapour pressure on the permeate side was held constant, the increasing vapour pressure in feed led to an increase in the driving force and consequently the water flux. Secondly, an increase in temperature also raises the diffusion coefficient for transport through the membrane, making it easier for the transport of the water molecules. This is confirmed by the diffusion coefficient results as shown in Table 6-1. As can be seen, there is an increasing trend in the diffusivity coefficient of water in the hybrid membrane as the feed temperature is increased. In addition, the mobility of the polymer chains also increased with the feed temperature, which could lead to an increase of the free volume of the membranes. According to the free volume theory, the thermal motion of polymer chains in the amorphous region creates momentary free volumes (Burshe *et al.* 1997). As the temperature increases, the frequency and amplitude of the chain motion increase and the resulting free volumes become larger. Consequently, water

molecules which have smaller size can diffuse through these free volumes more easily. Therefore, the water flux increases.
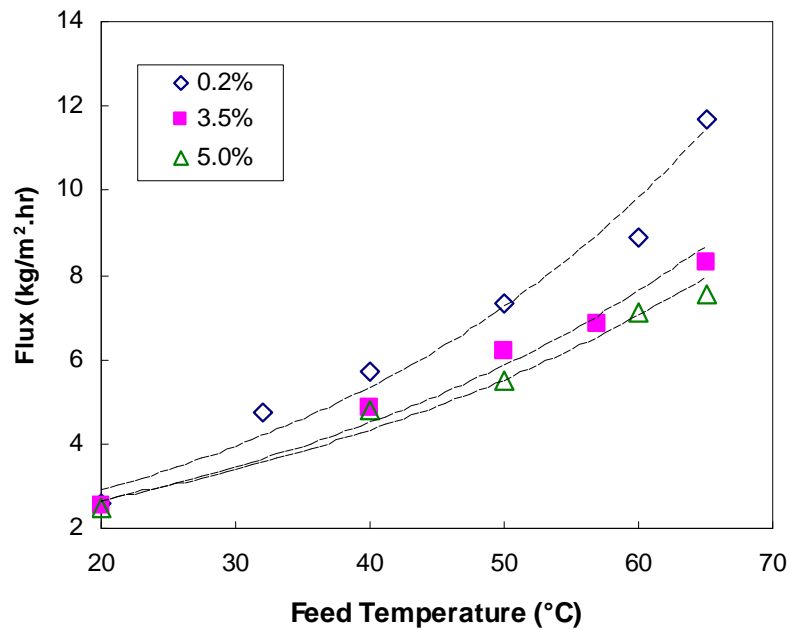
Figure 6- 4: Effect of feed temperature on water flux (membrane thickness 20 µm, feed flowrate 30 mL/min, vacuum 6 Torr, feed concentration: 0.2-5.0 wt% NaCl)

As mentioned in Chapter 2, the temperature dependence of permeate flux for pervaporation generally follows an Arrhenius type relationship (Yeom and Lee 1996, Jiraratananon *et al.* 2002, Peng *et al.* 2006b).

$$J_i = A_i \exp\left(-\frac{E_{p,i}}{RT}\right)$$ (6-1)

Where J_i is the permeate flux of i, A_i is the pre-exponential factor, R is the gas constant, T is the absolute temperature and $E_{p,i}$ is the apparent activation energy for permeation which depends on both the activation energy for diffusion and heat of sorption.

Figure 6-5 shows the Arrhenius plot of the water flux and feed temperature at different feed concentrations. The linear relationship was observed between fluxes and the reciprocal of the absolute temperature. The activation energy of permeation of water ($E_{p,w}$) in the membrane was taken from the slope of the Arrhenius plot (equation 6-1) and the results are shown in Table 6-4. There was no significant variation in activation energy of permeation of

water as the salt concentration in the feed solution increased from 0.2 to 5.0wt%, with the activation energy only varying from 23.8 to 20.1 kJ/kmol. The positive activation energy implies that permeation flux increases with increasing temperature (Kittur *et al.* 2003), as confirmed from the results shown in Table 6-4. This indicates that sorption is mainly dominated by the Henry's model of sorption, giving an endothermic contribution. Henry's law states that the heat of sorption will be positive for liquid transport, leading to the dissolution of chemical species into that site within the membrane, giving an endothermic contribution to the sorption process (Kulkarni *et al.* 2006). The relatively low activation energy could be attributed to the high water content over the studied feed concentration range. At the higher water content in the feed, the significance of the plasticising effect of water on the membrane can significantly enhance free volume and diffusion of water. Therefore, the activation energy is low. As explained by Jiraratananon *et al.*, an increase of temperature can reduce the amount of water-water clusters*(Jiraratananon et al. 2002)*. As a result, the permeation of water is significantly enhanced.
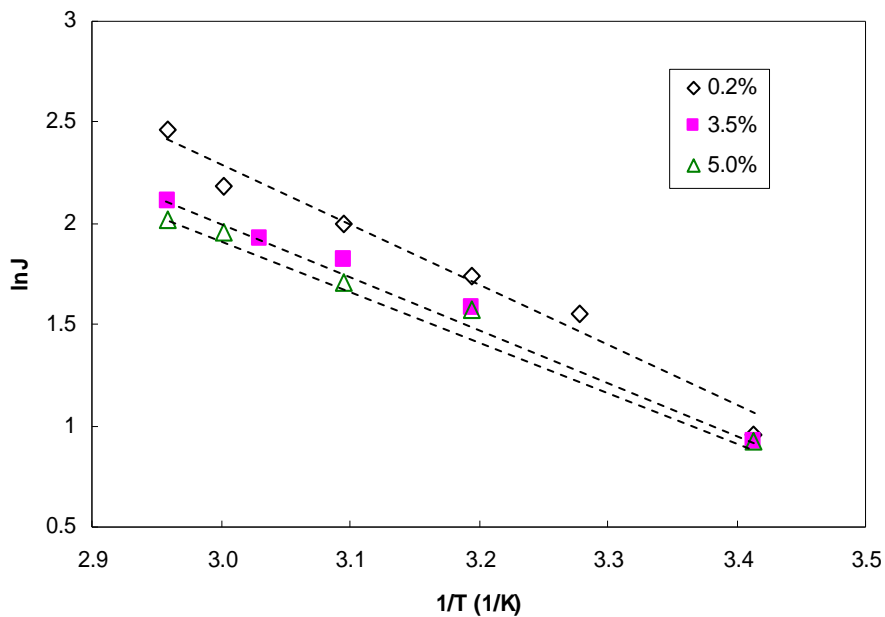
Figure 6- 5: Arrhenius plot of the water flux at various feed concentrations (feed concentration: 0.2-5.0 wt% NaCl).

Table 6- 4: Activation energy of permeation of water at different feed concentration (feed flowrate 30 mL/min, vacuum 6 Torr).

NaCl concentration	0.2 wt%	3.0 wt%	5.0 wt%
Activation energy (kJ/kmol)	23.8	21.6	20.1

6.4   Summary

In this study, pervaporation under various operating conditions was carried out to evaluate the separation performance of aqueous salt solution through the hybrid PVA/MA/silica membrane. A high water flux of 11.7 $kg/m^2 \cdot hr$ could be achieved at a feed temperature of 65°C and a vacuum of 6 Torr. Under all operating conditions, salt rejection remain high (up to 99.9%), indicating salt rejection performance of hybrid PVA/MA/silica membrane is independent of the operating conditions mainly due to the non-volatile nature of NaCl. In the studied laminar flow region, feed velocity had little or negligible effect on the water flux and diffusion coefficients of water, and this confirmed that the sorption of water onto the membrane surface was not the rate controlling step of pervaporation separation of aqueous salt solution. Rather the diffusion through the membrane was the rate controlling process.

High feed temperature and high vacuum had a significant enhancing effect on the water flux and diffusivity coefficients of water due to the increased driving force and increased free volume of the membrane. The activation energy of permeation of water was found to be around 21.8±1.8 kJ/kmol when the salt concentration in the feed was increased from 0.2 to 5.0 wt%. The positive activation energy implied that permeation flux would increase with increasing temperature and the relatively low activation energy was attributed to the high water content over the studied feed concentration range. The effect of feed concentration had differing impacts depending on the operating temperature. At low feed temperatures, the salt concentration in the feed solution had little or negligible effect on water flux and diffusion coefficients. However, at high feed temperature (50-60°C), feed flux and diffusivity of water decreased with increasing salt concentration due to the decreased water vapour pressure and consequently water concentration in the membrane surface.

Chapter 7

Process Engineering Modelling for Desalination by Pervaporation

7.1　Introduction

Increasing population growth and global warming have created greater disparities between the supplies and demands of reliable fresh water sources. Seawater and brackish water desalination technologies have been a promising technology to overcome the water scarcity issue (McGinnis and Elimelech 2007). Among various desalination technologies used in the world, RO accounts for >65% of total world desalination capacity and distillation accounts about 30%. As mentioned earlier, the energy requirement of RO operation is very high, with as much as 23% of total water cost for seawaer desalination attributed to energy cost (Figure 1-1). The energy requirement vary between 6 and 10 kWh/m^3 and investment costs vary between 600 and 2000 US$/m^3/d, according to the size of the unit and the type of process used (Korngold *et al.* 1996). The osmotic pressure for seawater of salinity 35,000 mg/L is 2800 kPa, versus 140 kPa for brackish water of salinity 1600 mg/L. This means that for seawater RO, a significantly higher pressure must be applied to prevent osmotic transfer of water through the semi-permeable membrane. Consequently energy requirements are high at 12 kWh/kL if there is no energy recovery and 4 kWh/kL if there is energy recovery (Cabassud and Wirth, 2003). The survey data show that the average energy consumption in Australia is 3-3.7 kWh/kL for sea water RO, 0.7-1 kWh/kL for brackish water and 1.2 kWh/kL for industrial effluent (Hoang *et al.* 2009).

Despite much progress being made in lowering the energy requirements and cost of RO, challenges remain to be overcome. The energy costs of RO seawater desalination are still too high for economic widespread application; and large brine discharge streams continue to cause concern over the environmental impacts they may cause (McGinnis and Elimelech 2007). In Australia, the future production cost of desalinated water will be heavily influenced by the cost of plant construction and the anticipated increasing cost of energy due to the carbon tax (Hoang *et al.* 2009). In an effort to address some of these challenges, the desalination by pervaporation process has been investigated.

The pervaporation process has been used extensively for separation of mixtures of aqueous-organic or organic liquids. However, there are only limited studies on application of pervaporation for desalination although it has advantages of high salt rejection and energy needs practically independent of the feed concentration. It is believed this is mainly due to the low water flux associated with current commercial membranes, as low water flux increases the amount of membrane area required and consequently increases the capital cost required for the membranes. For good performance of pervaporation, high water flux must be obtained with moderate energy consumption. The performance of pervaporation, like other membrane processes, mainly depends on: 1) the membrane properties; 2) the operating conditions; and 3) the module design (Criscuoli *et al.* 2008). There are extensive literatures available on the effect of membrane properties and operating conditions (Burshe *et al.* 1997, Jiraratananon *et al.* 2002, Ping *et al.* 1990, Kittur *et al.* 2003). However, only few studies refer to the energy requirement and economics of the pervaporation process (Suggala and Bhattacharya 2003, Ji *et al.* 1994).

The economy of the pervaporation process can be assessed with following parameters: the specific energy required for heating, the specific power required for circulating feed and vacuum pump operation, and the specific membrane area (Alklaibi 2008a). The energy used in the desalination by pervaporation process is primarily heat and electricity.

In this chapter, a process engineering model is developed to evaluate the energy consumption of desalination by pervaporation process. The energy consumption considered in this work refers to the external heating/cooling required for feed/permeate stream, as well as the energy consumptions associated with pumps for re-circulating feed and maintaining vacuum. The energy requirement for pervaporation process was compared to other desalination process such as reverse osmosis (RO), multi stage flash (MSF) and multi evaporation distillation (MED) with the aim to identify the potential applications/conditions which would be suitable for pervaporation.

7.2   Energy Balance and Estimation

Figure 7-1 shows a schematic flow chart of the desalination by pervaporation process in recirculation mode. The system consists of a feed pump, a heater, membrane modules, a cooler/condenser and a vacuum pump. The reject stream from the membrane modules are

recirculated back to the feed tank. It should be noted that this process engineering model is focused on the major energy consuming components that contribute to the desalination performance. The pre-treatment of the feed stream and post-treatment of permeate stream are outside the scope of this study.
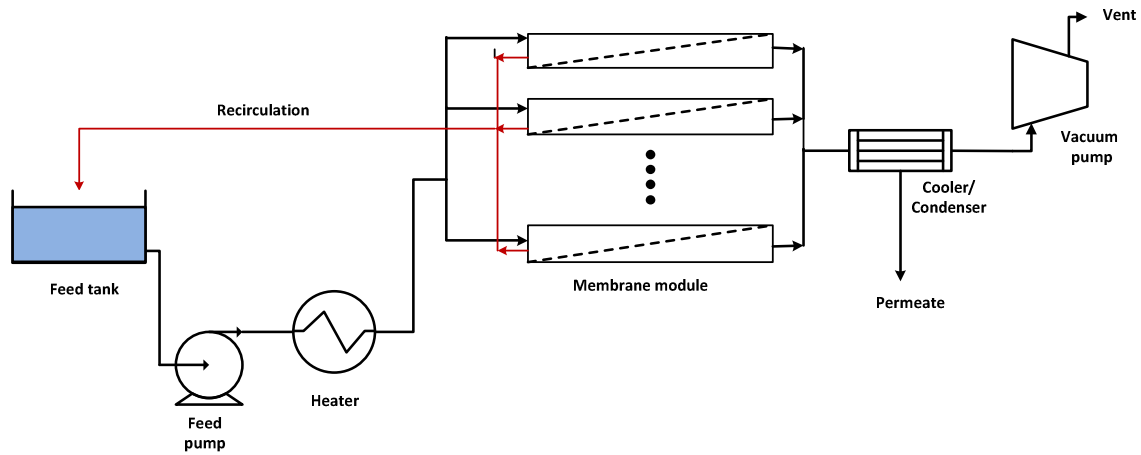
Figure 7- 1: Schematic flow chart of pervaporation process in recirculation mode.

As shown in Figure 7-1, major energy-consuming components for the pervaporation process include the feed stream heating, the permeate stream cooling/condensation, the feed pump and vacuum pump. Figure 7-2 shows a breakdown of energy requirement for pervaporation. Feed heating (Q_h) and permeate cooling energy (Q_c) are classified as the thermal energy requirement whereas the electrical power associated with feed pump (E_f) and vacuum pump (E_v) are classified as the electrical energy requirement. The latent heat of condensation E_r from cooling the water vapour of the outlet permeate stream could be potentially recovered in the process and used for heating the feed.
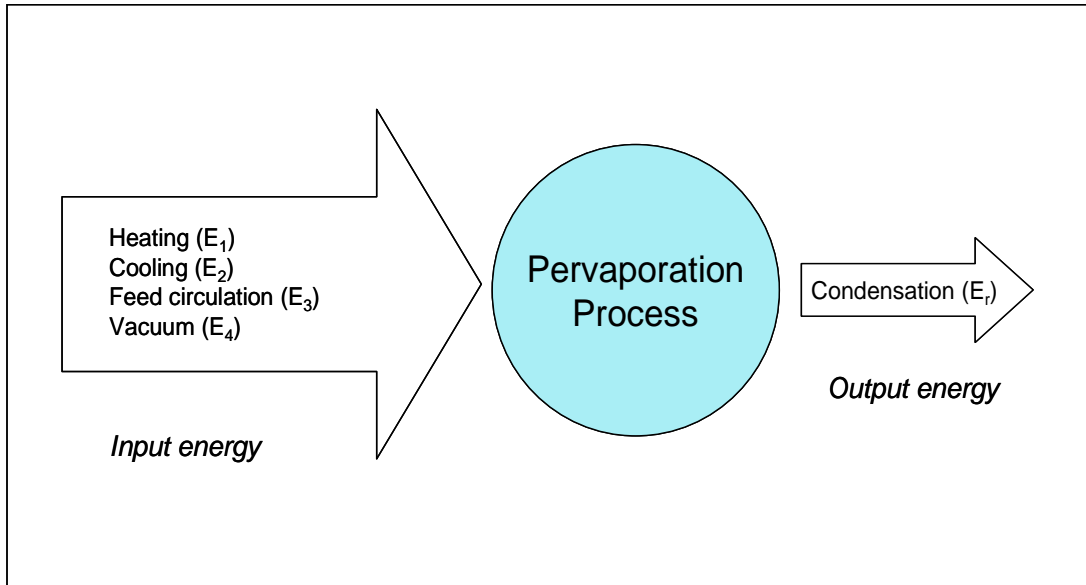
Figure 7- 2: Breakdown of energy requirement for pervaporation.

The overall energy requirement is therefore:

$$E_{Total}=Q_h+Q_c+E_f+E_v \qquad (7\text{-}1)$$

If the heat recovery option is considered, depending on the heat recovery efficiency (x%), E_{Total} could be calculated from:

$$E_{Total}=Q_h+Q_c+E_f+E_v\text{-} x\% E_v \qquad (7\text{-}2)$$

7.2.1 Heating energy required for heating the feed stream

In pervaporation, permeate is in the vapour phase on the downstream side of the membrane. The energy for this phase change is supplied by the sensible heat of the feed (Howell 1990). In addition, pervaporation normally operates at a temperature higher than ambient temperature which is normally the temperature of the feed reservoir. In this case, energy is required to raise the temperature of the feed stream to the pervaporation operating temperature (T_{fi}). The energy required to heat the feed stream (Q_h) in the pervaporation process can be calculated based on the operating conditions of the pervaporation (feed flow rate and feed inlet/outlet temperatures). When the feed stream is recirculated (Fig. 7-1), a one-off heating (Q_{init}) is required to increase the temperature of the feed reservoir (T_{res}) to the desired operating feed temperature. At steady state, a lesser amount of energy is required

to compensate for the heat loss and boost the recirculating stream to the desired feed temperature:

$$Q_{init} = m_f C_{pf}(T_{fi} - T_{Res})$$ (7-3)

$$Q_h = m_f C_{pf}\left(T_{fi} - T_{fo}\right)$$ (7-4)

Where m_f is the mass flow rate of the feed (kg s^{-1}), C_{pf} is its heat capacity (J kg^{-1} K^{-1}), T_{Res} and T_{fi} are the temperatures of the feed reservoir and feed inlet (K), respectively. Lower feed reservoir temperatures will increase the energy requirement for heating and vice versa.

7.2.2 Cooling energy required for permeate condensation/cooling

In pervaporation, the water vapour on the permeate side needs to be condensed. Theoretically this portion of energy consumption equals the total energy used to evaporate permeants from the feed stream (Shao and Kumar 2011). Condensation is normally carried out at temperature between 0 and 10°C to achieve the desired operating permeate pressure. This condensing temperature is lower than that of tower cooling water. Therefore, further energy is required. However, this can often be minimised by using low temperature cooling devices which are often available on fine chemical sites (Howell 1990).   The thermal energy required to condense the water vapour (Q_c) is calculated as:

$$Q_c = m_p \lambda$$ (7-5)

Where m_p is the mass flow rate of the permeate (kg s^{-1}), and λ is latent heat of condensation of water vapour at the permeate temperature (J kg^{-1}). When the temperature of condensed permeate stream is to be lowered, additional heat needs to be removed, thus Q_c becomes:

$$Q_c = m_p \lambda + m_p \int_{T_{pi}}^{T_{po}} C_{p(l)} dT$$ (7-6)

Where T_{pi} and T_{po} are the permeate inlet and out temperatures.

7.2.3 Electrical energy required for circulating the feed stream

The feed side pump is used to circulate the feed stream to the membrane module and also overcome the pressure head loss across the membrane module. The electrical power consumption required for circulating the feed stream through the pervaporation system is a

function of the pressure drop and the volumetric flow rate of the feed. It was calculated as (Alklaibi 2008b):

$$E_3 = \frac{\Delta P_f V_f}{\eta_{p1}}$$ (7-7)

where V_f is the volumetric flow rate of feed, η_{p1} is the pump efficiency which is assumed to be 80%, and ΔP is the pressure drop on due to friction determined by (Munson *et al.* 2002):

$$\Delta P = f \frac{L}{D_H} \rho \frac{u^2}{2}$$ (7-8)

In the above equation, f is the Darcy friction factor, L is the channel length, D_H is the hydraulic diameter, ρ is the density, and u is the linear velocity of the feed. For stream velocity in the laminar region ($Re<2100$), the following correlation is applied:

$$f = \frac{64}{Re}$$ (7-9)

with the Re defined as:

$$Re = \frac{u \rho D_H}{\mu}$$ (7-10)

μ is the fluid viscosity and u is the linear velocity. The hydraulic diameter D_H is calculated from the geometry of the flow channel.

For turbulent flows (Re>2100), the pressure drop is also affected by the changes in the feed channel such as the expansion, constriction, joint and valves.

$$\sum f = f(\mathrm{Re}, \frac{\varepsilon}{D}) + \sum (e_v)$$ (7-11)

where the first term on the right hand side refers to the friction loss due to the material of the piping or tubing and can be estimated from the Moody chart based on the knowledge of the Reynolds number. For common polymeric materials, a smooth surface can be assumed. The second term on the right hand side of the equation (e_v) represents the friction loss due to the disturbances in the flow channel. Some common values are listed in Table 7-1.

Table 7-1: Common values for friction loss factors (Bird *et al.* 2002)

Disturbances	e_v
Changes in cross-section area:	
Sudden contraction	0.45 (1-β)*
Sudden expansion	$\left(\dfrac{1}{\beta}-1\right)^2$
Fittings and valves:	
90° round elbows	0.4-0.9
45° elbows	0.3-0.4
Open globe valve	6-10

* $\beta = \dfrac{smaller\ cross\ section}{larger\ cross\ section}$

7.2.4 Electrical energy required for vacuum pump

In pervaporation, the vacuum pump is generally used after a condenser/cooler for start-up and removal of non-condensable vapours. For desalination applications, as the permeate contains water vapour which is condensable, the proportion of non-condensable vapour will be very small. This mainly includes dissolved non-condensable gases from the feed stream and air leakage from the vacuum system as few vacuum systems are completely airtight. Consequently the power requirement for the vacuum pump will be very low at steady state as the condenser does most of the job for maintaining the vacuum by efficient condensation of the permeate (Ji *et al.* 1994). The electrical power consumption of a vacuum pump in the pervaporation unit can be estimated based on the principle of adiabatic vapour expansion and contraction from the following equations (Choedkiatsakul *et al.* 2011):

$$E_v = -m_{nc} \int_{T_{in}}^{T_{out}} C_p dT \qquad (7\text{-}12)$$

$$T_{out} = T_{in}\left[1 + \frac{1}{\eta_{p2}}\left(\left(\frac{p_{out}}{p_{in}}\right)^{(\gamma-1)/\gamma} - 1\right)\right] \qquad (7\text{-}13)$$

where m_{nc} is non-condensable flow rate (mol s^{-1}), C_p is the heat capacity of non-condensables at constant pressure (kJ kmol^{-1} K^{-1}), T_{in} and T_{out} are the vacuum pump inlet and outlet temperatures, η_{p2} is the vacuum pump efficiency which is assumed to be 80%, p_{out} is the vacuum pump outlet pressure (normally atmospheric pressure), p_{in} is the vacuum pump inlet pressure, and γ is the adiabatic expansion coefficient defined as (Choedkiatsakul *et al.* 2011):

$$\gamma = \frac{C_p}{C_p - R} \tag{7-14}$$

where R is the gas constant (8.3145 J mol^{-1}K^{-1})

Assuming that dissolved non-condensable gases from the feed and air leaking into the vacuum system are at a rate of 1% of the permeate vapour, the above equations for calculating the electrical power consumption of the vacuum pump can be simplified to the following equation (Ji *et al.* 1994, Vallieres and Favre 2004)

$$E_v = \frac{1\% J \; R \; T_{in}}{\eta_{p2}} \frac{A_m}{MW} \frac{\gamma}{\gamma - 1} \left[\left(\frac{p_{out}}{p_{in}} \right)^{(\gamma-1)/\gamma} - 1 \right] \tag{7-15}$$

where J is the permeate flux *(kg/m^{2}h)*, T_{in} is the absolute temperature of the noncondensable vapour at the vacuum pump inlet condition (K) and *MW* is the molecular weight of the non-condensable gases (assumed to be air).

7.3 Results and discussion

7.3.1 Specific energy requirement

The pervaporation testing results obtained in Chapter 6 have been used as the basis to estimate the energy consumption required for the desalination by pervaporation process. As mentioned earlier, the energy requirement for pervaporation is divided into thermal energy and electrical energy. The thermal energy includes initial heating of the feed stream from the feed reservoir temperature to the desired feed inlet temperature, intermediate re-heating of the feed stream to compensate the heat loss and to maintain the desired feed inlet temperature during circulation, and the cooling energy required to condense and cool the permeate stream. The electrical energy includes the power associated with feed pump and vacuum pump.

Figure 7.3 shows a breakdown of the thermal energy requirement and electrical power consumption for desalination by pervaporation in recirculation mode using the experimental water flux of 11.7 kg/m²h and an evaporation efficiency of 90% at a feed inlet temperature of 65°C, feed velocity 0.05 m/s and vacuum level 6 Torr (800 Pa). The thermal energy required is significant. 5643 MJ/m³ is required to heat the feed reservoir from 21°C to 65°C and 2609 MJ/m³ of thermal energy is required to maintain the feed stream at 65°C. The heat of condensation removed in the condenser is almost equal to the intermediate heat required for permeate evaporation, with 2350 MJ/m³ required for permeate condensation and 201 MJ/m³ for cooling the permeate stream. In terms of electrical energy requirement, the vacuum pump requires most of the power and its value is about 1.43 kWh/m³. The circulation power required for the feed pump is negligible (<1% of total electrical energy requirement) compared with the vacuum pump energy. This is because the feed flow is in laminar region with a Reynolds number of 220.
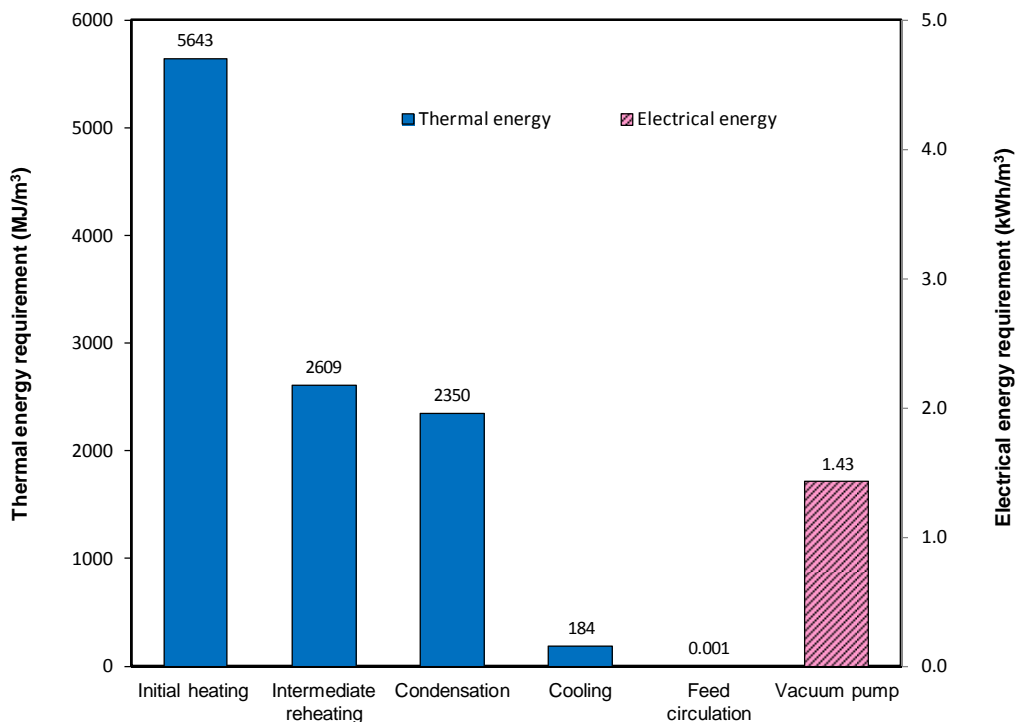
Figure 7- 3: Breakdown of thermal and electrical energy requirement for pervaporation process in recirculation mode (feed temperature 65°C, feed velocity 0.05 m/s, vacuum 6 Torr).

Figure 7-4 shows the effect of feed temperature on the feed heating (including initial heating and intermediate reheating for the feed stream), permeate cooling/condensation thermal energy, and the electrical power required for operating the pervaporation process at a feed velocity of 0.05 m/s and a 6 Torr permeate pressure. As the feed temperature increases from 21 to 65°C at constant feed velocity and permeate pressure, the feed heating required increases from none to 5643 MJ/m^3 to bring the feed from ambient temperature (21°C) to 65°C. In addition, more heat is transferred from the feed stream, across the membrane and to the permeate stream resulting in an increase in permeate temperature. Therefore more cooling energy is required to remove the heat from the permeate stream at higher feed temperature. When the feed temperature increases from 21 to 65°C, cooling energy increases from 17 to 184 MJ/m^3. Combined together, more thermal energy is required with increasing feed temperature, from 2714 MJ/m3 at 21°C to 8252 MJ/m^3 at 65°C.

The feed temperature has less influence on the electrical energy requirement. The electrical energy required includes the power consumption associated with the vacuum pump and the feed circulation pump. When the feed inlet temperature increases from 21 to 65°C, it is found that the power consumption remains constant for the vacuum pump and reduces for the feed circulation pump. This is because the power consumption for the vacuum pump mainly depends on the pump inlet pressure and permeate flowrate (equation 7-15). The vacuum pump directly affects the permeate pressure and the pressure affects permeate flowrate. At a fixed production capacity (i.e. permeate flowrate) and permeate pressure (i.e. pump inlet pressure), the electrical power required by the vacuum pump per unit of product water remains unchanged (i.e. it is not a function of temperature). On the other hand, the electrical power requirement for the feed recirculation pump decreases with the increasing feed inlet temperature due to the reduced viscosity and consequently increased Re at higher temperatures. In this study, the flow remained in the laminar region, with only a marginal increase of Re from 98 at 21°C to 220 at 65°C. As a result, the electrical energy required for the feed circulation pump was negligible compared with the vacuum pump. Consequently, the total electrical energy required remains at ~1.43 kWh/m^3 regardless of feed temperature change.
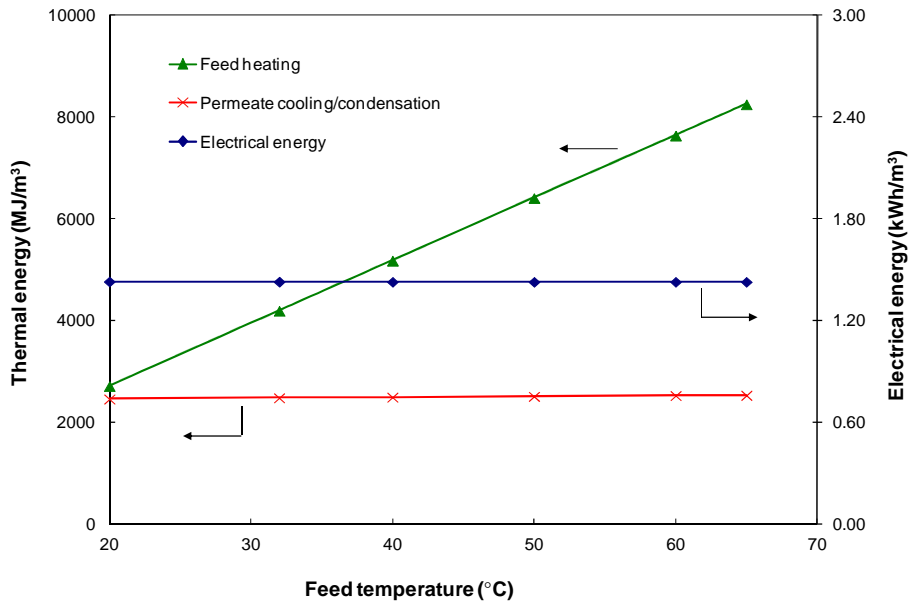
Figure 7- 4: Effect of the feed temperature on thermal and electrical energy requirement (feed velocity 0.05 m/s, vacuum 6 Torr).

Figure 7-5 shows the effect of permeate pressure on feed heating, permeate cooling/condensation thermal energy, and the electrical power required for operating the pervaporation process at an ambient feed temperature (21°C) and 0.05 m/s feed velocity. The thermal energy (both feed heating and permeate cooling) remains constant while the electrical energy required decreases continuously with increasing the downstream permeate pressure. This is because, at a fixed production capacity, thermal energy is only related to the feed inlet temperature and permeate temperature which are normally constant.

The permeate pressure has negligible influence on the electrical power required for the feed recirculation pump due to the constant feed flowrate and pressure drop. On the other hand, as permeate pressure increased from 1 to 40 Torr, the electrical power required for the vacuum pump decreased from 1.97 to 0.87 kWh/m^3. As mentioned earlier, the power consumption for the vacuum pump is only related to the pump inlet pressure at a given production capacity. Higher permeate pressure indicates that less power is required to operate the vacuum pump. However, it should be noted that the water flux also decreases at higher permeate pressure due to the lower driving force, especially when the permeate pressure is above the saturation pressure. E.g, the water flux at room temperature dropped to ~0.29 kg/m^2·h when the permeate pressure was more than the water saturation pressure of 17 Torr (Figure 6-3).
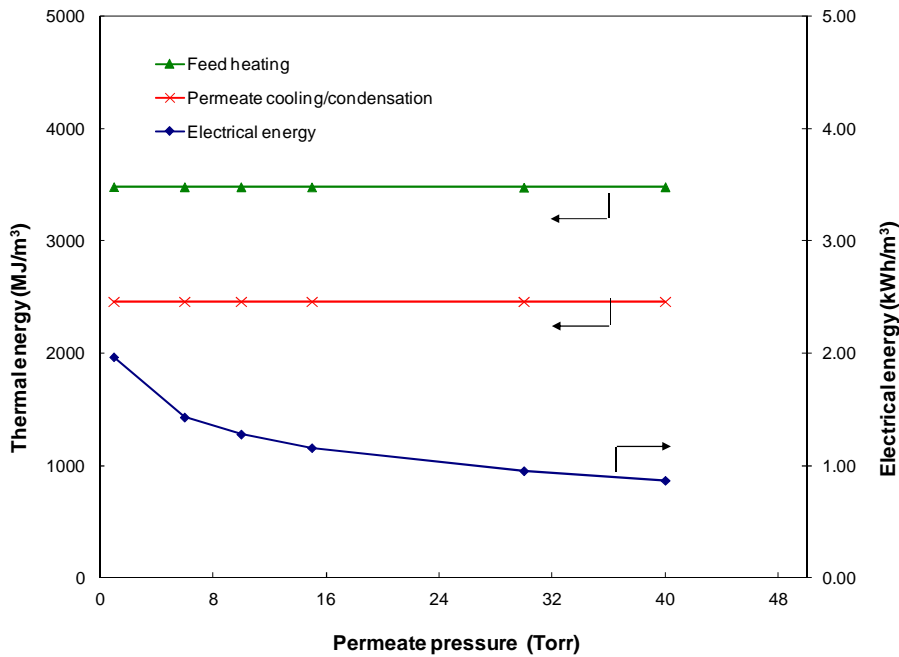
Figure 7- 5: Effect of the permeate pressure on thermal and electrical energy requirement (feed velocity 0.05 m/s, feed temperature 21°C).

As mentioned earlier, the thermal energy requirement is significant in pervaporation processes. To reduce the process energy required, alternative low-grade or waste heat can be used to provide the thermal energy for heating the feed. In addition, if the heat recovery option is adopted to recover the latent heat of condensation gained in the condenser, the total energy required for the system could be potentially reduced down to a much improved level. Figure 7-6 compares the total thermal energy and electrical energy with or without the heat recovery option and the use of a waste heat source. Assuming low grade waste heat is readily available and 100% heat recovery of latent heat from the permeate stream can be obtained, the thermal energy is significantly reduced. That is, only the electrical power consumption for the vacuum pump and small amount of thermal energy for cooling the permeate is required if ignoring any limitation of heat recovery from the permeate stream, e.g. 1.43 kWh/m^3 of electrical energy and 140 MJ/m^3 of thermal energy are required at 65°C feed temperature and 6 Torr permeate pressure in laminar flow regime. At 21°C, the required thermal energy reduces to 140 MJ/m^3 while the electrical energy remains constant at 1.43 kWh/m^3. It should be noted that the value of the low-grade thermal energy becomes higher when the feed temperature is high. It is, therefore, desirable to improve the membrane permeability as it lowers the required feed temperature and the specific membrane area. Consequently, this

113

reduces the required low-grade thermal energy and the membrane related capital and operating cost.
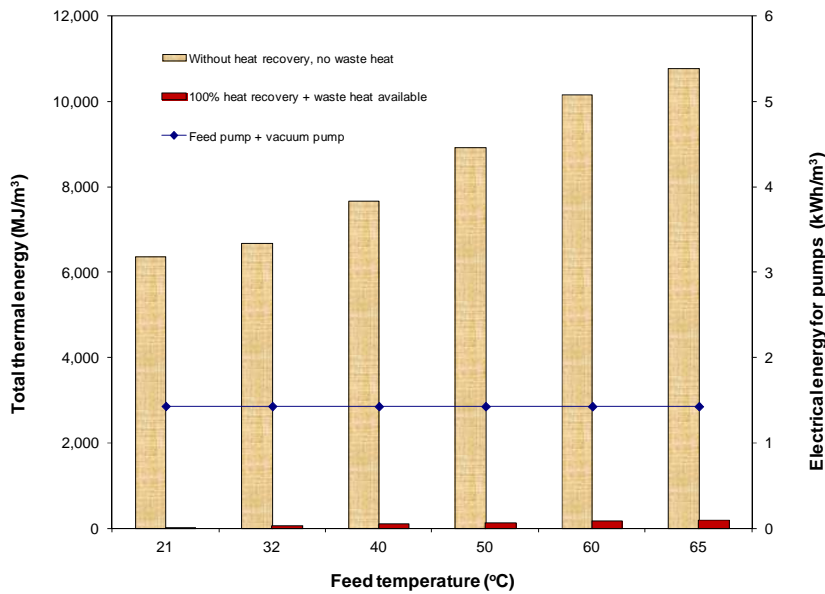
Figure 7- 6: Total thermal and electrical energy requirement with/without heat recovery and alternative heat source (feed velocity 0.05 m/s, vacuum 6 Torr).

Table 7-2 compares the energy consumption of pervaporation against other desalination technologies such as RO, multi stage flash (MSF), multi effect distillation (MED) and vapour compression (VC). Except for RO using electrical power only, the energy used in other desalination process such as MSF, MED and VC consists of thermal and electrical energy. As can be seen, the energy needed for RO is considerably lower than the distillation options. With the option of a free low grade waste heat source and heat recovery, the thermal energy needed for pervaporation is significantly lower than distillation technologies and the electrical energy is generally lower than RO-seawater. Assuming the fuel cost of 1.5 US$/GJ and electricity price of 0.03 US$/kWh (Wade 2001), the energy related water production cost for pervaporation is 0.07-0.25 US$/m^3, which is comparable to RO production cost (Table 7-2). It should be noted use of waste heat can have big impact as it is sometimes not practical to transport heat energy over long distances. However, if a free waste heat source and the heat recovery option are available, the results in Table 7-2 indicates pervaporation has advantage against RO at high salt concentration as its energy needs for pervaporation is essentially independent of the salt concentration in the feed solution. This suggests that pervaporation could be applied in niche markets where RO has limitations, such as RO brine concentration.

Table 7- 2: Energy consumption for various desalination technologies.

Process	Thermal[1] (MJ/m³)	Electrical[1] (kWh/m³)	Energy related product cost[2] (US$/m³)
Multi stage flash (MSF)	250-300	3.5-5	0.48-0.60
Multi effect distillation (MED)	150-220	1.5-2.5	0.27-0.41
Vapour compression (VC) –thermal	220-240	1.5-2	0.36-0.39
Vapour compression (VC) - mechanical	None	11-12	
RO – seawater	None	5-9	0.05-0.27
RO – brackish water	None	0.5-2.5	
Pervaporation	4-140	0.9-2	0.07-0.25

[1] Thermal and electrical energy of MSF, MED, VC and RO are extracted from ref. (Khalifa 2010).

2 Hypothesis: fuel cost 1.5 US$/GJ, electricity price 0.03 US$/kWh (Wade 2001).

7.3.2   *Specific membrane area requirement*

In addition to the energy requirement, specific membrane area is the other main factor influencing the economics of the process, as it not only affects the capital cost but also the operating cost via membrane cleaning and replacement. For a typical RO desalination plant, the capital cost of the system will be approximately $500 US/m^2 membrane area (I. Koyuncu *et al.* 2001). Membrane cost usually represents about 20–30% of the total capital cost and about13.5% of water production cost (Wade 2001). It is, therefore, desirable to keep the membrane area as low as possible to maximise productivity and lower the membrane related capital cost. Figure 7-7 shows the effect of feed temperature on relative specific membrane area requirement. With increasing the feed temperature, the specific membrane area required decreases, as the water flux increases with the increasing feed temperature due to the increased driving force (Figure 6-4). When feed temperature increases from 21 to 65°C, the required membrane area decreased by 80%.
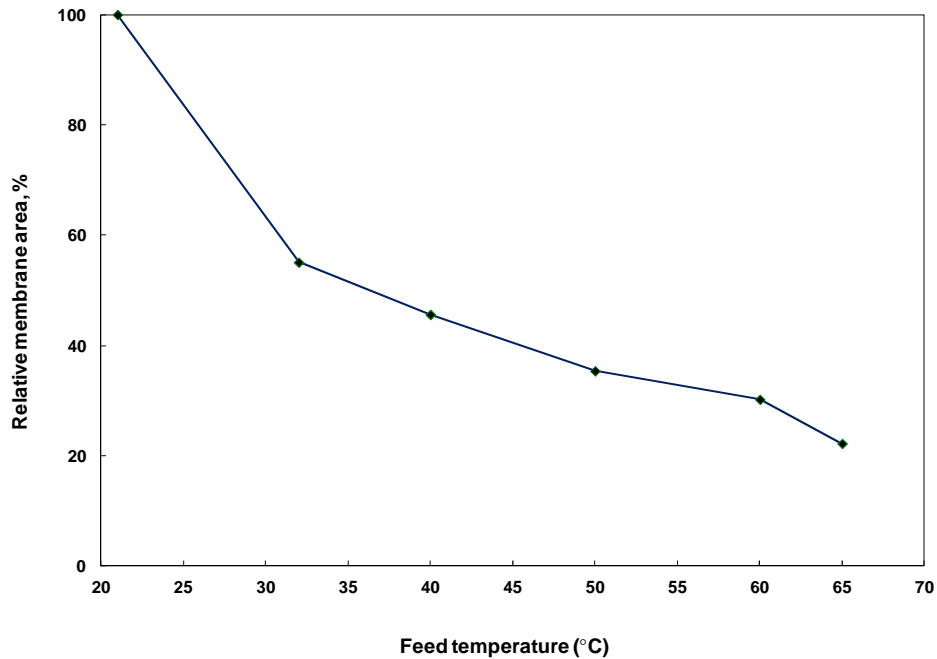
Figure 7- 7: Relative specific membrane area versus feed temperature (feed velocity 0.05 m/s, vacuum 6 Torr).

Figure 7-8 shows the effect of permeate pressure on relative specific membrane area requirement. At the low permeate pressure range (from 1 to 10 Torr), the required membrane area increases slightly with increasing permeate pressure due to a decrease of water flux (Figure 6-3). However, when the permeate pressure is increased to 15 Torr, which is approaching the water saturation pressure of 17 Torr at 20°C, the required membrane area increases by more than 4-folds due to the significantly reduced driving force. Once the permeate pressure is increased above the water saturation pressure (>15 Torr), the required membrane area is more than 8 times than required at 6 Torr and remains high when the permeate pressure is further increased from 30 to 40 Torr. When the permeate pressure is approaching or greater than the water saturation pressure, the driving force for water transport across the membrane becomes very low and consequently very low water flux and high membrane area requirement.
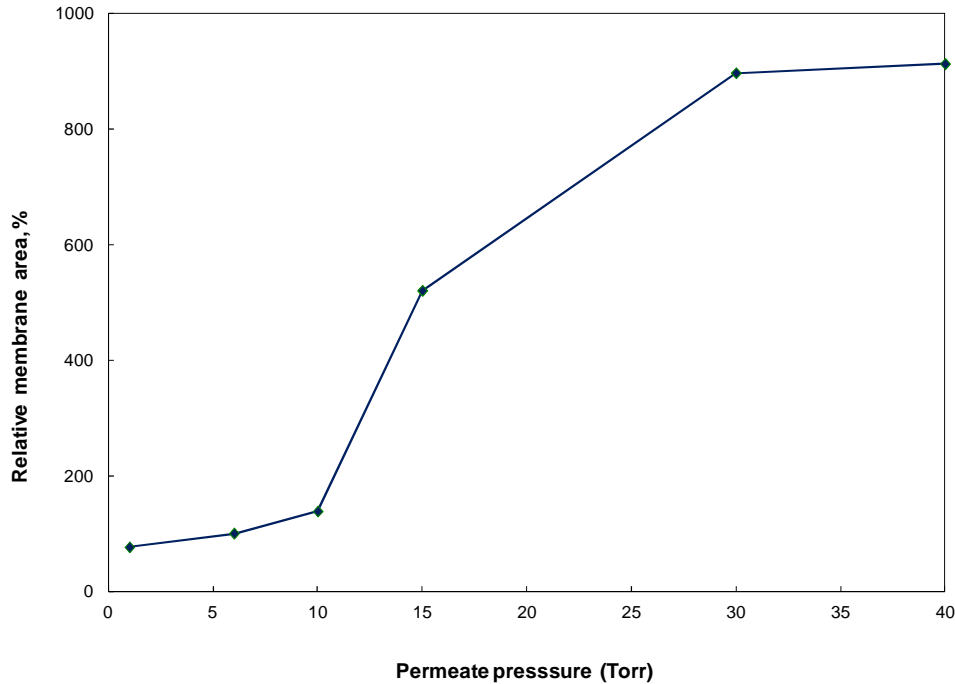
Figure 7- 8: Relative specific membrane area versus permeate pressure (feed velocity 0.05 m/s, feed temperature 21°C).

To lower the membrane related capital and operating cost, it is therefore advantageous for the pervaporation process to operate at high feed temperature and low permeate pressure to maximise the productivity and reduce the membrane area requirement. This is because the water flux increases with high feed temperature and low permeate pressure. Howell (Howell 1990) reported that the flux increased by approximately 50% with every 10°C rise in temperature. On the other hand, to lower the energy consumption required for the pervaporation process, it is advantage to operate the system at low feed temperature and high permeate pressure (Figure 7-4 and 7-5). Especially, if there is no free low grade heat resource available and no heat recovery option, operating at higher temperatures will be too expensive due to high thermal energy consumption. In addition, there is also a limitation to lower the permeate pressure due to the increased electrical power consumption associated with the vacuum pump (Figure 7-5).

In seawater desalination, current commercial RO membranes (e.g. crosslinked full aromatic polyamide membrane) can achieve up to 41 kg/m^2·h of water flux with 99.2% salt rejection operating at 55 bar (Lee *et al.* 2011). Although the energy consumption of pervaporation is comparable to the RO process, the required specific membrane area is still higher than RO due to the low water flux in pervaporation. This indicates that the pervaporation may not be

117

able to directly compete with RO technology unless there is significant improvement in water flux. This could be possibly done by developing thin film composite membranes to improve the water flux by reducing the membrane thickness. In addition, since pervaporation has the advantage of the energy requirement being nearly independent of the feed concentration, it may be possible to use pervaporation for RO brine concentration.

7.3.3   Single pass Vs. recirculation

Whether to operate the system in single pass or recirculation mode needs also to be considered in scale up operation. The electrical energy required will remain relatively constant regardless of the mode of operation as the flows associated with the electrical power consumption remains stable. However, the mode of operation will have an impact on the thermal energy required which varies with the feed temperature. In single pass mode, the reject stream from the membrane module is discharged. On the other hand, this stream is recirculated back to the feed reservoir in recirculation mode at a higher temperature than the fresh feed. Therefore, while only initial heat is required to bring the feed stream to the required feed temperature in single pass, extra thermal energy is required to compensate the heat loss of the feed stream in recirculation mode. Figure 7-9 compares the thermal energy requirement for single pass and recirculation mode at two different feed inlet temperatures (21°C and 65°C) in the absence of waste heat and any heat recovery. At low feed temperature (<30°C), negligible or minimum amount of heating is required for the feed stream in single pass. However, greater heating is required in recirculation mode as the recirculated feed is returned at a lower temperature than the fresh feed and therefore requires additional heating to compensate the heat loss. E.g, at 21°C, 2462 MJ/m^3 of thermal heating is required in single pass compared to 5176 MJ/m^3 in recirculation mode. On the other hand, the opposite is true at a higher feed temperature (65°C), more thermal energy is required in single pass mode than recirculation mode (8194 MJ/m^3 in single pass versus 5160 MJ/m^3 in recirculation mode). This is because, at higher temperatures, the recirculated feed is returned at a temperature higher than the fresh feed and therefore requires less heat. On the other hand, the feed stream always needs to be heated from ambient temperature to the desired feed inlet temperature in single pass. Therefore, more thermal energy is expected. In addition, large quantities of fluid also need to be discharged after the membrane module in single pass. Thus, recirculation mode is the preferred configuration at higher feed temperatures. Moreover,

recirculation mode is generally preferred regardless of feed temperature as discharging large quantities of reject stream in single pass could be avoided in recirculation mode.
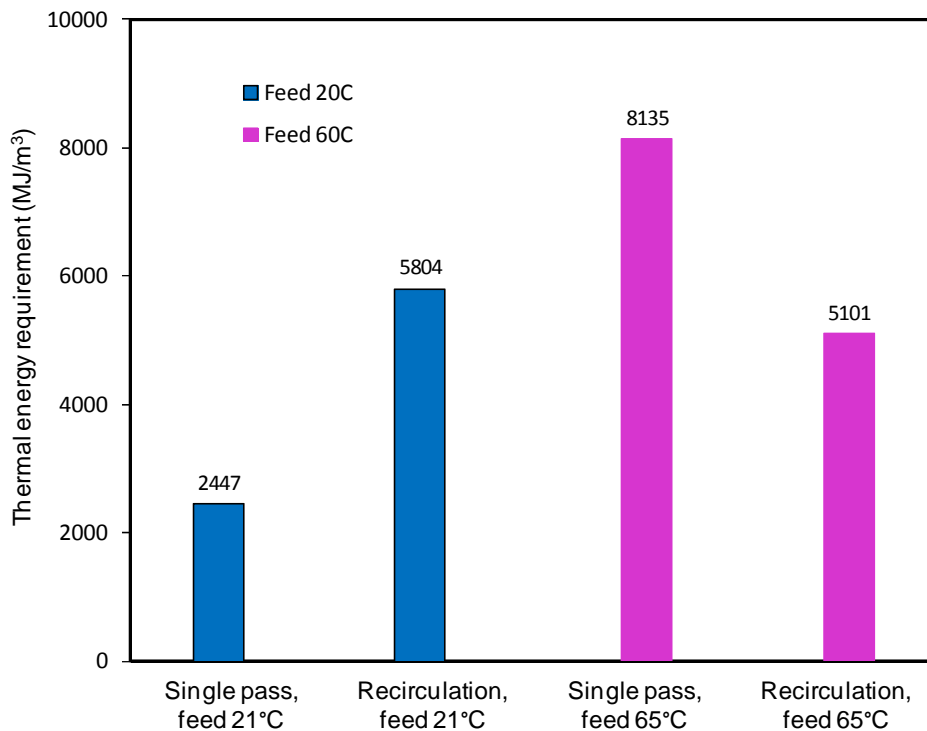
Figure 7- 9: Thermal energy requirement for single pass and recirculation mode (feed velocity 0.05 m/s, vacuum 6 Torr).

7.4   Summary

A process engineering model was developed to assess the specific energy required for desalination by pervaporation. The energy requirement for pervaporation was divided into thermal energy and electrical energy. The thermal energy includes feed heating and permeate cooling/condensation, and the electrical energy includes the power required for feed circulation and maintaining vacuum. In pervaporation process, the thermal energy requirement is significant. E.g, 5643 MJ/m^3 of thermal energy is required to heat the feed reservoir from 21°C to 65°C and 2609 MJ/m^3 is required to maintain the feed stream at 65°C in recirculation mode. Assuming laminar flow, the power required for feed circulation is negligible. The vacuum pump contributes to the majority of the electrical energy, with 1.43 kWh/m^3 of electrical power required at 65°C feed temperature.

The specific energy and membrane area requirement of the pervaporation process were assessed as a function of feed inlet temperature and permeate pressure. Thermal energy increases with the feed temperature but remains constant with permeate pressure. On the other hand, electrical energy decreases with increasing permeate pressure but remains constant with feed temperature. To reduce the process energy requirement, the waste heat sources and heat recovery could be used to provide the thermal heating and recover the heat of condensation in the condenser. The specific membrane area required decreases with increasing feed temperature and decreasing permeate pressure. When the permeate pressure is above the water saturation pressure, the specific membrane area required increases significantly due to low water flux. To lower the membrane related capital and operating cost, it is advantages for the pervaporation process to operate at high feed temperature and low permeate pressure to maximise the productivity as the flux increases with high feed temperature and low permeate pressure. However, the thermal energy requirement becomes significant at high feed temperature and the electrical energy increases with decreasing permeate pressure.

With the option of free low grade waste heat source and heat recovery, the thermal energy needed for pervaporation is significantly lower than other distillation technologies and the electrical energy is generally lower than RO-seawater. Assuming the fuel cost of 1.5 US$/GJ and electricity price of 0.03 US$/kWh, the energy related water production cost for pervaporation is 0.07-0.25 US$/m^3, which is comparable to RO. However, the required specific membrane area for pervaporation is higher than RO due to low water flux in pervaporation. This indicates that the pervaporation may not be able to directly compete with RO technology unless targeting niche markets where RO has limitations, such as RO brine concentration or further improving the water flux of pervaporation membranes.

Moreover, whether to operate the pervaporation system in single pass or recirculation mode will have significant impact on the thermal energy requirement. Recirculation is generally preferred as it has the advantage of reducing discharge large quantities of the brine stream and, reducing the thermal energy requirement when high temperature waste heat is available. In the absence of a waste heat source and heat recovery, operating the system in single pass will provide an advantage at low feed temperatures when the initial heating is not required.

Chapter 8

Conclusions and Recommendations

8.1   Introduction

As mentioned in Chapter 1, the objective of this study was to develop a scalable hybrid organic-inorganic membrane material with properties that exceed the performance capabilities of current available polymeric membranes for desalination by pervaporation. To achieve this, comprehensive works have been carried out to establish a framework for the development of a new type of hybrid organic-inorganic membranes based on PVA, MA and TEOS.

By using this hybrid material, transport properties exceeded the properties obtainable by polymers alone. The development of this novel membrane system and characterisation of the material properties provided several important conclusions and highlighted the need for future research in some new areas. This chapter presents the primary conclusions drawn from the research objectives of this work and future work proposed for further development of this technology.

8.2   Conclusions

In this study, a new type of PVA/MA/silica hybrid membranes with inorganic silica nanoparticles uniformly dispersed in the polymer matrix has been synthesised via a sol-gel route and a solution casting method. Tetraethoxy-silane (TEOS) was used as the silica precursor for sol-gel reaction and MA was added as an additional crosslinking agent. Crosslinking among PVA, MA and TEOS led to a more compact structure with increasing amorphous membrane character with improved thermal properties and suppressed swelling. Pervaporation testing results on separating aqueous NaCl solution demonstrated a potential application of this type of hybrid membrane for desalination with improved water flux and high salt rejection. By adjusting MA and silica content, both water flux and salt rejection could be improved.

Heat treatment of membranes strongly affected the microstructure and pervaporation performance of membranes. Increasing heating temperature or time favoured the completion

of the crosslinking reaction among PVA, MA and TEOS, and also favoured the polycondensation reaction of TEOS. This resulted in a less hydrophilic membrane with reduced fractional free volume (FFV). Transport through hybrid PVA/MS/silica membranes was explained by the solution-diffusion mechansim and the free volume theory. The hydrophilic nature of hybrid membranes provides high water affinity and water sorption, and incorporation of silica particles into the polymer matrix at the nano-scale enhanced the free volume of the membrane and diffusion of water molecule through the membrane. The increased hydrophobicity upon heating led to less sorption of water at the membrane surface due to significantly decreased water solubility. Additionally, the reduced free volume upon heating led to less accommodation of water in the diffusion step. Combined together, the water flux decreased with either increaed heating temperature or heating time. The close correlation among pervaporation properties (e.g., global mass transfer coefficients, water flux and salt rejection), transport properties (e.g., NaCl/water diffusivity and permability) and FFV of the membrane confirmed that the diffusion through membrane was the controlling step of pervaporation separation of aqueous salt solution for this unsupported hybrid membrane. Both NaCl and water diffusivity increased exponential with decreasing $1/FFV$ and changing free volume had a more pronounced effect on NaCl diffusivity than water diffusivity.

Operating conditions have significant effect on water flux of hybrid PVA/MA/silica membrane. Salt rejection remained high (up to 99.9%) and was independent of the operating conditions mainly due to the non-volatile nature of NaCl. In the studied laminar flow region, feed velocity had little or negligible effect on the water flux and diffusion coefficients of water. This confirmed that the sorption of water onto the membrane surface was not the rate controlling step of desalination by pervaporation. High feed temperature and high vacuum had a significant enhancing effect on the water flux and diffusivity coefficients of water due to the increased driving force. A high water flux of 11.7 kg/m^2·hr could be achieved at a feed temperature of 65°C and a vacuum of 6 Torr. At low feed temperatures, the salt concentration in the feed solution had little or negligible effect on water flux and diffusion coefficients. However, at high feed temperature (50-60℃), feed flux and diffusivity of water decreased with increasing salt concentration due to the decreased water vapour pressure and consequently water concentration in the membrane surface.

A process engineering model was developed to assess the specific thermal energy and electrical power required for desalination by pervaporation. The thermal energy includes feed heating and permeate cooling/condensation, and the electrical energy includes the power required for feed circulation and maintaining vacuum. The thermal energy requirement is significant and the vacuum pump contributes to the majority of the electrical energy in the laminar flow regime. Thermal energy increases with the feed temperature and the electrical energy increases with decreasing permeate pressure. To reduce the process energy requirement, low-grate or waste heat resources and heat recovery could be used to provide efficient thermal heating and to recover the heat of condensation in the condenser. With the option of a free low grade waste heat source and heat recovery, the thermal energy needed for pervaporation (4-140 MJ/m^3) is significantly lower than distillation technologies such as MSF and MED and the electrical energy (0.9-2 kWh/m^3) is generally lower than RO. Assuming the fuel cost of 1.5 US$/GJ and electricity price of 0.03 US$/kWh, the energy related water production cost for pervaporation is 0.07-0.25 US$/m^3, which is comparable to RO (0.05-0.27 US$/m^3) .

The required specific membrane area for desalination by pervaporation was also assessd in this study. The membrane area decreases with increasing feed temperature and decreasing permeate pressure. To lower the membrane related capital and operating cost, it is advantageous for the pervaporation process to operate at high feed temperature and low permeate pressure to maximise the water productivity as the flux increases with high feed temperature and low permeate pressure. However, this needs to be balanced with the increased energy requirement. In general, the required specific membrane area for pervaporation is higher than RO due to current low water flux in pervaporation. This implies a higher membrane related capital cost. To make the process competitive, the water flux of pervaporation membrane needs to be further improved. In addition, pervaporation could be used to target niche markets where RO has limitation such as RO brine concentration.

8.3   Recommendations for Future Work

This study was based on experimental studies of using unsupported homogeneous and symmetric membranes with membrane thickness >5 µm as it is easy to cast and characterise. It is known that the permeate flux generally increase with decreasing membrane thickness by reducing the membrane resistance. It is, therefore, expected that the performance of this

type of membrane will be improved further by fabricating as a thin film composite membrane.

To improve the water flux achieved in this study and attain commercial viability, the membranes successful on the laboratory scale need to be prepared in an thin film composite or asymmetric form as shown in Figure 2-4. Morphologies of the thin film composite or asymmetric membranes offer a possibility of making a barrier with a thin effective separation layer, which enables high flux while maintaining desirable mechanical strength. It is recommended to extend findings from this work and develop technologies for making supported thin film composite membranes and gain theoretical understanding on the transport phenomena of the species in the complex composite membrane materials via a range of advanced characterisation technique such as an in-depth PALS, XPS and AFM study. In addition, fractional free volume (FFV) was found to directly affect membrane performance in terms of mass transfer and water/salt diffusion. To improve the water flux, it is important to develop fundamental understanding on the free volume of polymers which will assist in conducting molecular design of the polymers which gives ideally FFV.

The process engineering modelling work carried out in this study mainly focused on assessing the specific thermal and electrical energy required for pervaporation process. Further work on full cost estimation of desalination by pervaporation will be beneficial to understand the process economics including process capital set-up requirements and ongoing operating costs. This will help to identify competitiveness of this technology compared with other desalination processes.

As membrane fouling is an inevitable phenomenon during membrane filtration process, it is also recommended to study the fouling (inorganic and organic) of hybrid membranes in the future work. The present study has not considered fouling problems which may arise over the long periods of use and also from dealing with feeds with different quality. The future work could study factors that affecting membrane fouling, e.g. (1) membrane properties such as free volume, hydrophobicity, pore size distribution and membrane material; (2) solution properties such as concentration, the nature of the components and particle size distribution; (3) operating conditions such as pH, temperature, flow rate and pressure. Along with this, autopsy studies of fouled membranes would help to gain fundamental understanding of fouling mechanism. This will help to develop strategies for minimising fouling such as appropriate membrane design and choice of operating conditions.

References

Adham, S. (2007). Desalination. Proc. Membrane Specialty Conf. II, Australian Water Assoc., Paper 12.

Ahmad, Z., I. Sarwar, M. and Mark, J.E. (1997) Chemically bonded silica-polymer composites from linear and branched polyamides in a sol-gel process. Journal of Materials Chemistry 7(2), 259-263.

Alklaibi, A.M. (2008a) The potential of membrane distillation as a stand-alone desalination process. Desalination 223, 375-385.

Alklaibi, A.M. (2008b) The potential of membrane distillation as a stand-alone desalination process. Desalination 223(1-3), 375-385.

Aptel, P., Cuny, J., Jozefonvicz, J., Morel, G. and Neel, J. (1974) Liquid transport through membranes prepared by grafting of polar monomers onto poly(tetrafluoroethylene) films. II. Some factors determining pervaporation rate and selectivity. Journal of Applied Polymer Science 18(2), 351-364.

Baker, R.W. (2004) Membrane Technology and Applications, pp. 355-392, John Wiley & Sons, Ltd.

Balazs, A.C., Emrick, T. and Russell, T.P. (2006) Nanoparticle Polymer Composites: Where Two Small Worlds Meet. Science 314(5802), 1107-1110.

Bandyopadhyay, A., Sarkar, M. and Bhowmick, A.K. (2005) Poly(vinyl alcohol)/silica hybrid nanocomposites by sol-gel technique: Synthesis and properties. Journal of Materials Science 40(19), 5233-5241.

Binning, R.C., Lee, R.J., Jenning, J.F. and Martin, E.C. (1961) Separation of liquid mixtures by permeation. Industrial & Engineering Chemistry 53(45), 45-50.

Bird, B.R., Stewart, E. and Lightfoot, E.N. (2002) Transport Phenomena, John Wiley & Sons, New York.

Bolto, B., Hoang, M. and Xie, Z. (2010) Pervaporation - a further low energy desalination optoin? Water AWA 37(4), 77-81.

Bolto, B., Hoang, M. and Xie, Z. (2011) A review of membrane selection for the dehydration of aqueous ethanol by pervaporation. Chemical Engineering and Processing: Process Intensification 50(3), 227-235.

Bolto, B., Tran, T., Hoang, M. and Xie, Z. (2009) Crosslinked poly(vinyl alcohol) membranes. Progress in Polymer Science 34(9), 969-981.

Bowen, T.C., H.Kalipcilar, J.L.Falconer and R.D.Noble (2003) Pervaporation of organic/water mixtures through B-ZSM-5 zeolite membranes on monolith supports. Journal of Membrane Science 215, 235-247.

Brun, J.P., Bulvestre, G., Kergreis, A. and Guillou, M. (1974) Journal of Applied Polymer Science 18, 1663-1669.

Bruschke, H. (1995) Industrial application of membrane separation processes. Pure & Applied Chemistry 67(6), 993-1002.

Burshe, M.C., Sawant, S.B., Joshi, J.B. and Pangarkar, V.G. (1997) Sorption and permeation of binary water-alcohol systems through PVA membranes crosslinked with multifunctional crosslinking agents. Separation and Purification Technology 12(2), 145-156.

Cabasso, I., Korngold, E. and Liu, Z-Z. (1985). On the separation of alcohol/water mixtures by polyethylene ion exchange membranes. Polym. Sci.: Polym. Letters 23, 577-581.

Cabassud, C. And Wirth, D. (2003) Membrane distillation for water desalination: how to choose an appropriate membrane, Desalination, 157, 307-314.

Chang, J.-H., Yoo, J.-K., Ahn, S.-H., Lee, K.-H. and Ko, S.-M. (1998) Simulation of pervaporation process for ethanol dehydration by using pilot test results. Korean Journal of Chemical Engineering 15(1), 28-36.

Chapman, P.D., Oliveira, T., Livingston, A.G. and Li, K. (2008) Membranes for the dehydration of solvents by pervaporation. Journal of Membrane Science 318(1-2), 5-37.

Chen, M.S.K., Eng, R.M., Glazer, J.L. and Wensley, C.G. (1988) Pervaporation process for spearting alcohols from ethers, US Patent 4777365.

Choedkiatsakul, I., Charojrochkul, S., Kiatkittipong, W., Wiyaratn, W., Soottitantawat, A., Arpornwichanop, A., Laosiripojana, N. and Assabumrungrat, S. (2011) Performance improvement of bioethanol-fuelled solid oxide fuel cell system by using pervaporation. International Journal of Hydrogen Energy 36(8), 5067-5075.

Cohen, M.H. and Turnbull, D. (1959) Molecular Transport in Liquids and Glasses. The Journal of Chemical Physics 31(5), 1164-1169.

Cornelius, C., Hibshman, C. and Marand, E. (2001) Hybrid organic-inorganic membranes. Separation and Purification Technology 25(1-3), 181-193.

Cox, G. and Baker, R.W. (1998) Pervaporation fro teh treatmetn of small volume VOC-contaminated waste water streams. Industrial Wastewater 6, 35-41.

Crank, J. and Park, G.S. (1968) Diffusion in Polymers, Academic Press, New York.

Criscuoli, A., Carnevale, M.C. and Drioli, E. (2008) Evaluation of energy requirements in membrane distillation. Chemical Engineering and Processing: Process Intensification 47(7), 1098-1105.

Dong, A.W., Pascual-Izarra, C., Pas, S.J., Hill, A.J., Boyd, B.J. and Drummond, C.J. (2008) Positron Annihilation Lifetime Spectroscopy (PALS) as a Characterization Technique for Nanostructured Self-Assembled Amphiphile Systems. The Journal of Physical Chemistry B 113(1), 84-91.

Eckert, H. and Ward, M. (2001) Chemistry of Materials 13, 3059-3060.

Franks, F. (2000) Water: A Matrix of Life, Royal Society of Chemistry, Cambridge, UK

Freeman, B.D. (1999) Basis of Permeability/Selectivity Trade-off Relations in Polymeric Gas Separation Membranes. Macromolecules 32(2), 375-380.

George, S.C. and Thomas, S. (2001) Transport phenomena through polymeric systems. Prog. Polym. Sci. 26, 985-1017.

Giménez, V., Mantecón, A. and Cádiz, V. (1996) Crosslinking of poly(vinyl alcohol) using dianhydrides as hardeners. Journal of Applied Polymer Science 59(3), 425-431.

Gohil, J.M., Bhattacharya, A. and Ray, P. (2006) Studies On The Crosslinking Of Poly (Vinyl Alcohol). Journal of Polymer Research 13(2), 161-169.

Graham, T. (1866) Philos. Mag. 32, 401-405.

Greenlaw, F.W., Shelden, R.A. and Thompson, E.V. (1977) Dependence of diffusive permeation rates on upstream and downstream pressures : II. Two component permeant. Journal of Membrane Science 2(0), 333-348.

Gronda, A.M., Buechel, S. and Cussler, E.L. (2000) Mass transfer in corrugated membranes. Journal of Membrane Science 165(2), 177-187.

Guizard, C., Bac, A., Barboiu, M. and Hovnanian, N. (2001) Hybrid organic-inorganic membranes with specific transport properties: Applications in separation and sensors technologies. Separation and Purification Technology 25(1-3), 167-180.

Guo, R., Ma, X., Hu, C. and Jiang, Z. (2006) PVA-GPTMS/TEOS hybrid pervaporation membrane for dehydration of ethylene glycol aqueous solution. Journal of Membrane Science 281, 454-462.

Guo, R., Ma, X., Hu, C. and Jiang, Z. (2007) Novel PVA-silica nanocomposite membrane for pervaporative dehydration of ethylene glycol aqueous solution. Polymer 48(10), 2939-2945.

Heintz, A. and Stephan, W. (1994) A generalized solution--diffusion model of the pervaporation process through composite membranes Part I. Prediction of mixture solubilities in the dense active layer using the UNIQUAC model. Journal of Membrane Science 89(1-2), 143-151.

Hoang, M., Bolto, B., Haskard C., Barron, O., Gray, S. and Leslie, G. (2009) Desalination in Australia, CSIRO Water for a Healthy Country Flagship Report, ISSN: 1835-095X.

Hollein, M.E., Hammond, M. and Slater, C.S. (1993) Concentration of dilute acetone-water solutions using pervaporation. Separation Science and Technology 28, 1043-1049.

Honda, M., Shiba, N., Kuramoto, Y., Marushita, K. and Okada, M. (1998). Seawater desalination on pervaporation process. Nippon Kagakkai Koen Yokoshu 75, 36.

Howell, J.A. (ed) (1990) The membrane alternative: energy implications for industry, Elsevier Science Publishers Ltd.

Huang, R.Y.M. and Rhim, J.W. (1993) Modification of poly(vinyl alcohol) using maleic acid and its application to the separation of acetic acid-water mixtures by the pervaporation technique. Polymer International 30(1), 129-135.

Huang, R.Y.M. and Yeom, C.K. (1990) Pervaporation separation of aqueous mixtures using crosslinked poly(vinyl alcohol)(pva). II. Permeation of ethanol-water mixtures. Journal of Membrane Science 51(3), 273-292.

Huang, Z., Shi, Y., Wen, R., Guo, Y.-H., Su, J.-F. and Matsuura, T. (2006) Multilayer poly(vinyl alcohol)-zeolite 4A composite membranes for ethanol dehydration by means of pervaporation. Separation and Purification Technology 51(2), 126-136.

I. Koyuncu, D. Topacik, M. Turan, Celik, M.S. and Sarikaya, H.Z. (2001) Application of the membrane technology to control ammonia in surface water. Water Science and Technology: Water Supply 1(1), 117-124.

Isklan, N. and Sanl, O. (2005) Separation characteristics of acetic acid-water mixtures by pervaporation using poly(vinyl alcohol) membranes modified with malic acid. Chemical Engineering & Processing 44(9), 1019-1027.

Jonquieres, J., Clemnt, R., Lochon, P., Neel, J., Dresch, M.and Chrtien, B. (2002) Industrial state-of-the-art of pervaporation and vapour permeation in the western countries. Journal of Membrane Science 206, 87-117.

Jardón-Valadez, E. and Costas, M.a.E. (2004) Solvation properties of a polarizable water model in a NaCl solution: Monte Carlo isothermal–isobaric ensamble simulations. Journal of Molecular Structure: THEOCHEM 677(1–3), 227-236.

Ji, W., Hilaly, A., Sikdar, S.K. and Hwang, S.-T. (1994) Optimization of multicomponent pervaporation for removal of volatile organic compounds from water. Journal of Membrane Science 97(0), 109-125.

Jiraratananon, R., Chanachai, A., Huang, R.Y.M. and Uttapap, D. (2002) Pervaporation dehydration of ethanol-water mixtures with chitosan/hydroxyethylcellulose (CS/HEC) composite membranes: I. Effect of operating conditions. Journal of Membrane Science 195(2), 143-151.

Ju, H., Sagle, A.C., Freeman, B.D., Mardel, J.I. and Hill, A.J. (2010) Characterization of sodium chloride and water transport in crosslinked poly(ethylene oxide) hydrogels. Journal of Membrane Science 358(1-2), 131-141.

Kanti, P., Srigowri, K., Madhuri, J., Smitha, B. and Sridhar, S. (2004) Dehydration of ethanol through blend membranes of chitosan and sodium alginate by pervaporation. Separation and Purification Technology 40(3), 259-266.

Khalifa, A.J.N. (2010) Unit water cost for various desalination technologies, retrieved March 26, 2012 from

http://www.scitopics.com/Unit_Water_Cost_for_various_Desalination_Technologies.html

Khayet, M., Cojocaru, C. and Zakrzewska-Trznadel, G. (2008) Studies on pervaporation separation of acetone, acetonitrile and ethanol from aqueous solutions. Separation and Purification Technology 63(2), 303-310.

Kickelbick, G. (2003) Concepts for the incorporation of inorganic building blocks into organic polymers on a nanoscale. Progress in Polymer Science 28, 83-114.

Kim, K.-J., Park, S.-H., So, W.-W. and Moon, S.-J. (2001) Pervaporation separation of aqueous organic mixtures through sulfated zirconia-poly(vinyl alcohol) membrane. Journal of Applied Polymer Science 79(8), 1450-1455.

Kittur, A.A., Kariduraganavar, M.Y., Toti, U.S., Ramesh, K. and Aminabhavi, T.M. (2003) Pervaporation separation of water–isopropanol mixtures using ZSM-5 zeolite incorporated poly(vinyl alcohol) membranes. Journal of Applied Polymer Science 90(9), 2441-2448.

Koops, G.H., Nolten, J.A.M., Mulder, M.H.V. and Smolders, C.A. (1994) Selectivity as a function of membrane thickness: Gas separation and pervaporation. Journal of Applied Polymer Science 53(12), 1639-1651.

Korin, E., Ladizhensky, I. and Korngold, E. (1996) Hydrophilic hollow fiber membranes for water desalination by the pervaporation method. Chemical Engineering and Processing 35(6), 451-457.

Korngold, E. and Korin, E. (1993) Air sweep water pervaporation with hollow fiber membranes. Desalination 91(2), 187-197.

Korngold, E., Korin, E. and Ladizhensky, I. (1996) Water desalination by pervaporation with hollow fiber membranes. Desalination 107(2), 121-129.

Kotoky, T. and Dolui, S.K. (2004) Synthesis and Characterisation of Polyvinyl alcohol (PVA)/Silica Hybrid Composites Derived Through the Sol-Gel Method in Aqueous Medium: Effect of Acid Content, Silica Content and Viscosity of PVA on the Dispersion Characteristics of Silica and the Physical Properties of the Composites. Journal of Sol-Gel Science and Technology 29(2), 107-114.

Kulkarni, S.S., Kittur, A.A., Aralaguppi, M.I. and Kariduraganavar, M.Y. (2004) Synthesis and characterization of hybrid membranes using poly(vinyl alcohol) and tetraethylorthosilicate for the pervaporation separation of water-isopropanol mixtures. Journal of Applied Polymer Science 94(3), 1304-1315.

Kulkarni, S.S., Tambe, S.M., Kittur, A.A. and Kariduraganavar, M.Y. (2006) Modification of tetraorthosilicate crosslinked poly(vinyl alcohol) membrane using chitosan and its application to the pervaporation separation of water-isopropanol mixtures. Journal of Applied Polymer Science 99, 1380-1389.

Kusakabe, K., Yoneshige, S. and Morooka, S. (1998) Separation of benzene/cyclohexane mixtures using polyurethane–silica hybrid membranes. Journal of Membrane Science 149(1), 29-37.

Kuznetsov, Y.P., Kruchinina, E.V., Baklagina, Y.G., Khripunov, A.K. and Tulupova, O.A. (2007) Deep desalination of water by evaporation through polymeric membranes. Russian Journal of Applied Chemistry 80(5), 790-798.

Ladewig, B.P., Tan, Y.H. and Diniz da Costa, J.C. (2010) Preparation, characterisation and performance of templated silica membranes in non-osmotic desalination. Water Research submitted.

Lee, K.-H., Kim, H.-K. and Rhim, J.-W. (2003) Pervaporaiton separation of binary organic-aqueous liquid mixture using crosslinked PVA membranes. III. Ethanol-water mixtures. Journal of Applied Polymer Science 58, 1707-1712.

Lee, K.P., Arnot, T.C. and Mattia, D. (2011) A review of reverse osmosis membrane materials for desalination—Development to date and future potential. Journal of Membrane Science 370(1–2), 1-22.

Li, R. and Barbari, T. (1995) Performance of poly(vinyl alcohol) thin-gel composite ultrafiltration membranes. Journal of Membrane Science 105, 71-78.

Lonsdale, H.K. (1982) The growth of membrane and tehcnology. Journal of Membrane Science 10, 81-87.

Lonsdale, H.K., Merten, U. and Riley, R.L. (1965) Transport properties of cellulose acetate osmotic membranes. Journal of Applied Polymer Science 9, 1341-1362.

Macho, V., Fabíni, M., Rusina, M., Bobula, S. and Harustiak, M. (1994) Modified poly(vinyl alcohol) as a dispersant in suspension polymerization of vinyl chloride: 3. Acetalized poly(vinyl alcohol). Polymer 35(26), 5773-5777.

Marin, M., Kalantzi, K. and Gibert, H. (1992) Pervaporation process: membrane conditioning and experimental mass transfer analysis. Journal of Membrane Science 74(1-2), 105-114.

McGinnis, R.L. and Elimelech, M. (2007) Energy requirements of ammonia–carbon dioxide forward osmosis desalination. Desalination 207(1–3), 370-382.

McKenna, G.B. and Horkay, F. (1994) Effect of crosslinks on the thermodynamics of poly(vinyl alcohol) hydrogels. Polymer 35(26), 5737-5742.

Merkel, T.C., Freeman, B.D., Spontak, R.J., He, Z., Pinnau, I., Meakin, P. and Hill, A.J. (2002) Ultrapermeable, Reverse-Selective Nanocomposite Membranes. Science 296(5567), 519-522.

Moore, T.T. and Koros, W.J. (2005) Non-ideal effects in organic–inorganic materials for gas separation membranes. Journal of Molecular Structure 739(1-3), 87-98.

Munson, B.R., Young, D.F. and Qkiishi, T.H. (2002) Fundamentals of fluid mechanics, John Wiley & Sons, Iowa.

Nguyen, T.Q., Essamri, A., Pierre, S. and Neel, J. (1993) Synthesis of membranes for the dehydration of water/acetic acid mixtures by pervaporation, 2 poly(vinyl alcohol) membranes containing covalently bonded carboxylic groups. Makromol. Chem. 194, 1157-1168.

Orgaz-Orgaz, F. (1988) Gel to glass conversion: Densification kinetics and controlling mechanisms. Journal of Non-Crystalline Solids 100(1-3), 115-141.

Peivasti, M., Madandar, A. and Mohammadi, T. (2008) Effect of operating conditions on pervaporation of methanol/methyl tert-butyl ether mixtures. Chemical Engineering and Processing: Process Intensification 47(7), 1069-1074.

Peng, F., Lu, L., Hu, C., Wu, H. and Jiang, Z. (2005b) Significant increase of permeation flux and selectivity of poly(vinyl alcohol) membranes by incorporation of crystalline flake graphite. Journal of Membrane Science 259(1-2), 65-73.

Peng, F., Lu, L., Sun, H. and Jiang, Z. (2006b) Analysis of annealing effect on pervaporation properties of PVA-GPTMS hybrid membranes through PALS. Journal of Membrane Science 281(1-2), 600-608.

Peng, F., Lu, L., Sun, H., Wang, Y., Liu, J. and Jiang, Z. (2005a) Hybrid Organic–Inorganic Membrane:Solving the Trade-off between Permeability and Selectivity. Chemistry of Materials 17(26), 6790-6796.

Peng, F., Lu, L., Sun, H., Wang, Y., Wu, H. and Jiang, Z. (2006a) Correlations between free volume characteristics and pervaporation permeability of novel PVA-GPTMS hybrid membranes. Journal of Membrane Science 275(1-2), 97-104.

Ping, Z.H., Nguyen, Q.T., Clément, R. and Néel, J. (1990) Pervaporation of water-ethanol mixtures through a poly(acrylic acid) grafted polyethylene membrane. Influence of temperature and nature of counter-ions. Journal of Membrane Science 48(2-3), 297-308.

Praptowidodo, V.S. (2005) Influence of swelling on water transport through PVA-based membrane. Journal of Molecular Structure 739, 207-212.

Quiñones-Bolaños, E., Zhou, H., Soundararajan, R. and Otten, L. (2005) Water and solute transport in pervaporation hydrophilic membranes to reclaim contaminated water for micro-irrigation. Journal of Membrane Science 252(1-2), 19-28.

Qunhui, G., Ohya, H. and Negishi, Y. (1995) Investigation of the permselectivity of chitosan membrane used in pervaporation separation II. Influences of temperature and membrane thickness. Journal of Membrane Science 98(3), 223-232.

Reis, E.F.d., Campos, F.S., Lage, A.P., Leite, R.C., Heneine, L.G., Vasconcelos, W.L., Lobato, Z.I.P. and Mansur, H.S. (2006) Synthesis and characterization of poly (vinyl alcohol) hydrogels and hybrids for rMPB70 protein adsorption. Materials Research 9, 185-191.

Robeson, L.M., Borgoyne, W.F., Langsam, M., Savoca, A.C. and Tien, C.F. (1994) High performance polymers for membrane separation Polymer 35(23), 4970-4978.

Sagle, A.C., Ju, H., Freeman, B.D. and Sharma, M.M. (2009) PEG-based hydrogel membrane coatings. Polymer 50(3), 756-766.

Sander, U. and Soukup, P. (1988) Design and operation of a pervaporation plant for ethanol dehydration. Journal of Membrane Science 36, 463-475.

Shakhashiri, B.Z. (1992) Chemical Demonstrations: A handbook for Teachers in Chemistry, Madison: The University of Wisconsin Press.

Shao, P. and Huang, R.Y.M. (2007) Polymeric membrane pervaporation. Journal of Membrane Science 287(2), 162-179.

Shao, P. and Kumar, A. (2011) Process energy efficiency in pervaporative and vacuum membrane distillation separation of 2,3-butanediol. The Canadian Journal of Chemical Engineering 89(5), 1255-1265.

Smitha, B., Suhanya, D., Sridhar, S. and Ramakrishna, M. (2004) Separation of organic–organic mixtures by pervaporation—a review. Journal of Membrane Science 241(1), 1-21.

Song, K.M. and Hong, W.H. (1997) Dehydration of ethanol and isopropanol using tubular type cellulose acetate membrane with ceramic support in pervaporation process. Journal of Membrane Science 123(1), 27-33.

Sperling, L.H. (1994) Interpenetrating polymer networks. Advances in Chemistry Series 239, 3-12.

Staudt-Bickel, C. and Lichtenthaler, R.N. (1994) Pervaporation thermodynamic properties and selection of membrane polymers. Polymer Science 36(11), 1628-1646.

Suggala, S.V. and Bhattacharya, P.K. (2003) Real Coded Genetic Algorithm for Optimization of Pervaporation Process Parameters for Removal of Volatile Organics from Water. Industrial & Engineering Chemistry Research 42(13), 3118-3128.

Sunkara, H.B. (2005) Polyether ester elastomers comprising a poly(trimethylene-ethylene ether) ester soft segment and an alkylene ester hard segment US Patent 6,905,765.

Tamaki, R. and Chujo, Y. (1998) Synthesis of poly(vinyl alcohol) / silica gel polymer hybrids by in-situ hydrolysis method. Applied Organometallic Chemistry 12(10-11), 755-762.

Tung, K.-L., Jean, Y.-C., Nanda, D., Lee, K.-R., Hung, W.-S., Lo, C.-H. and Lai, J.-Y. (2009) Characterization of multilayer nanofiltration membranes using positron annihilation spectroscopy. Journal of Membrane Science 343(1-2), 147-156.

Ulbricht, M. (2006) Advanced functional polymer membranes. Polymer 47(7), 2217-2262.

Uragami, T., Matsugi, H. and Miyata, T. (2005) Pervaporation Characteristics of Organic−Inorganic Hybrid Membranes Composed of Poly(vinyl alcohol-co-acrylic acid) and Tetraethoxysilane for Water/Ethanol Separation. Macromolecules 38(20), 8440-8446.

Uragami, T., Okazaki, K., Matsugi, H. and Miyata, T. (2002) Structure and Permeation Characteristics of an Aqueous Ethanol Solution of Organic-Inorganic Hybrid Membranes Composed of Poly(vinyl alcohol) and Tetraethoxysilane. Macromolecules 35(24), 9156-9163.

Vallieres, C. and Favre, E. (2004) Vacuum versus sweeping gas operation for binary mixtures separation by dense membrane processes. Journal of Membrane Science 244(1-2), 17-23.

Van Andel, E. (2001) Pervaporation device and irrigation mat, US Patent 6,679,991.

Villaluenga, J.P.G., Godino, P., Khayet, M., Seoane, B. and Mengual, J.I. (2004) Pervaporation of Alcohols and Methyl tert-Butyl Ether through a Dense Poly(2,6-dimethyl-1,4-phenylene oxide) Membrane. Industrial & Engineering Chemistry Research 43(10), 2548-2555.

Villaluenga, J.P.G., Khayet, M., Godino, P., Seoane, B. and Mengual, J.I. (2005) Analysis of the membrane thickness effect on the pervaporation separation of methanol/methyl tertiary butyl ether mixtures. Separation and Purification Technology 47(1-2), 80-87.

Wade, N.M. (2001) Distillation plant development and cost update. Desalination 136(1–3), 3-12.

Walcarius, A. (2001) Electrochemical Applications of Silica-Based Organic−Inorganic Hybrid Materials. Chemistry of Materials 13(10), 3351-3372.

Wen, J. and Wilkes, G.L. (1996) Chemistry of Materials 8, 1667.

Xie, Z., Ng, D., Hoang, M., Duong, T. and Gray, S. (2010) Separation of aqueous salt solution by pervaporation through hybrid organic-inorganic membrane: effect of operating conditions. Desalination 273, 220-225.

Yasuda, H., Ikenberry, L.D. and Riley, R.L. (1968b) Permeability of solutes through hydrated polymer membranes. I. Diffusion of sodium chloride. Makromolekulare Chemie 118, 19-35.

Yasuda, H., Lamaze, C.E. and Ikenberry, L.D. (1968a) Permeability of solutes through hydrated polymer membranes. Part I. Diffusion of sodium chloride. Die Makromolekulare Chemie 118(1), 19-35.

Ye, L.Y., Liu, Q.L., Zhang, Q.G., Zhu, A.M. and Zhou, G.B. (2007) Pervaporation characteristics and structure of poly(vinyl alcohol)/poly(ethylene glycol)/tetraethoxysilane hybrid membranes. Journal of Applied Polymer Science 105(6), 3640-3648.

Yeom, C.-K. and Lee, K.-H. (1996) Pervaporation separation of water-acetic acid mixtures through poly(vinyl alcohol) membranes crosslinked with glutaraldehyde. Journal of Membrane Science 109(2), 257-265.

Zhang, Q.G., Liu, Q.L., Jiang, Z.Y. and Chen, Y. (2007) Anti-trade-off in dehydration of ethanol by novel PVA/APTEOS hybrid membranes. Journal of Membrane Science 287(2), 237-245.

Zwijnenberg, H.J., Koops, G.H. and Wessling, M. (2005) Solar driven membrane pervaporation for desalination processes. Journal of Membrane Science 250(1-2), 235-246.